

LEIBNIZ UNIVERSITÄT HANNOVER

DOCTORAL THESIS

**Geometric construction of Yang–Mills
fields in maximally symmetric spacetimes**

Von der Fakultät für Mathematik und Physik
der Gottfried Wilhelm Leibniz Universität Hannover

zur Erlangung des akademischen Grades
Doktor der Naturwissenschaften
- Dr. rer. nat. -

vorgelegte Dissertation von

M.Sc. Gabriel Picanço Costa

2024

Referent: **Prof. Dr. Olaf Lechtenfeld**
(Leibniz Universität Hannover)

Korreferent: **Prof. Dr. Domenico Giulini**
(Leibniz Universität Hannover)

Korreferent: **Prof. Dr. Mikhail Volkov**
(University of Tours, France)

Tag der Promotion: 29.04.2024

*“Mas é claro que o Sol
Vai voltar amanhã
Mais uma vez, eu sei.
Escuridão já vi pior,
De endoidecer gente sã.
Espera que o Sol já vem.”*

Legião Urbana

Resources

This thesis is based on the following research papers published by the author (with author names in alphabetical order by surname):

- (A) K. Kumar, O. Lechtenfeld, and G. Picanço Costa,
Instability of cosmic Yang–Mills fields,
Nuclear Physics B **973** (2021) 115583.
- (B) L. Hantzko, K. Kumar, and G. Picanço Costa
Conserved charges for rational electromagnetic knots,
European Physical Journal Plus **137** (2022) 407.
- (C) K. Kumar, O. Lechtenfeld, and G. Picanço Costa,
Trajectories of charged particles in knotted electromagnetic fields,
Journal of Physics A: Mathematical & Theoretical **55** (2022) 315401.
- (D) K. Kumar, O. Lechtenfeld, G. Picanço Costa, and J. Röhrig,
Yang–Mills solutions on Minkowski space via non-compact coset spaces,
Physics Letters B **835** (2022) 137564.
- (E) K. Kumar, O. Lechtenfeld, and G. Picanço Costa,
Exact gauge fields from anti-de Sitter space,
submitted to *Journal of Mathematical Physics* (2023) arXiv:2301.03606.
- (F) M. Ertürk and G. Picanço Costa,
Coset space dimensional reduction of Yang–Mills theory on non-compact
symmetric spaces,
submitted to *Physics Letters B* (2023) arXiv:2304.13645.

In particular, there is significant overlap between:

- References (B) and (C) and Chapter 5,
- references (D) and (E) and Chapter 6, and
- references (A) and (F) and Chapter 7.

Zusammenfassung

In dieser Arbeit behandeln wir geometrische Konstruktionsmethoden von Yang-Mills-Feldern in maximal symmetrischen Raumzeiten, einschließlich kosmologischer Anwendungen und verschiedene Fälle abelscher Reduktionen. Bemühungen dieser Art wurden inspiriert durch die Entwicklung einer neuen Konstruktionsmethode für elektromagnetische Knoten im Minkowski-Raum, bei welcher die abelsche Reduktion einer $SU(2)$ Yang—Mills-Theorie auf einem Lorentz-Zylinder über der Dreisphäre $S^3 \simeq SU(2)$ konform in den $\mathbb{R}^{1,3}$ überführt wird. Meine Untersuchungen und Ergebnisse werden in drei Teilen präsentiert, von denen jeder seine eigenen teils unabhängigen Motivationen, Schlussfolgerungen und Aussichten auf Fortschritte hat.

Der erste Satz von Ergebnissen behandelt die Basis aus elektromagnetischen Knoten im Minkowski-Raum. Wir untersuchten erhaltene Ladungen, die mit der konformen Invarianz der Lösungen verbunden sind, was uns dabei half, einige ihrer physikalischen Eigenschaften besser zu verstehen und sie mit anderen bekannten elektromagnetischen Knoten zu vergleichen, die mit verschiedenen etablierten Methoden konstruiert wurden. Insbesondere fanden wir spezifische Parameterauswahlen, die es uns ermöglichten, Verallgemeinerungen des Rañada-Hopf-Knotens wie rotierte Hopfionen und Torusknoten aus Batemans Konstruktion zu reproduzieren. Darüber hinaus führten wir im Zuge der Weiterentwicklung der Studien zur Reproduktion solcher verknoteten Lösungen im Labor eine numerische Untersuchung durch und dokumentierten die Auswirkungen der elektromagnetischen Knoten aus unserer Basis auf geladene Teilchen, was relevante Daten für mögliche experimentelle Anwendungen in der Zukunft darstellt.

Motiviert durch die oben genannten Ergebnisse aus dem $SU(2)$ Yang-Mills-Feld auf dS_4 , erforschten wir, welche weiteren Ergebnisse aus Yang-Mills-Theorien erzielt werden können, die sich durch ähnliche Konstruktionen mittels geometrischer Strukturen anderer maximal symmetrischer Raumzeiten ergeben. Zunächst verwendeten wir eine stückweise Blätterung der Minkowski-Raumzeit durch Orbits der Lorentz-Gruppe, um eine $SO(1,3)$ Eichtheorie in den verschiedenen Regionen zu konstruieren, die nach einer Regularisierung auf dem Lichtkegel ein Yang-Mills-Feld erzeugte, dessen Energie-Impuls-Tensor global in $\mathbb{R}^{1,3}$ ist und durch einen Verbesserungsterm gegeben ist. Dann erforschten wir eine $SU(1,1)$ Eichtheorie auf einer Blätterung des AdS_4 mit AdS_3 als Blätter und bildeten diese anschließend konform in den $\mathbb{R}^{1,3}$ ab. Die abelsche Reduktion einer solch generierten Lösung erzeugte das hyperbolische Äquivalent des Rañada-Hopf-Knotens, der sich in einer Projektion in 1+2-Dimensionen als bekannter magnetischer Vortex herausstellte. Abschließend diskutierten wir die Aussichten einer Methode zur Erzeugung einer überabzählbaren Basis von hyperbolischen Äquivalenten der zuvor diskutierten elektromagnetischen Knoten.

Der letzte Satz von Ergebnissen betrifft die Kopplung der Yang-Mills-Theorie an die Allgemeine Relativitätstheorie in Friedmann-Universen. Wir zeigten, dass in jeder Raumzeitdimension der äquivariante Ansatz jeder Yang-Mills-Theorie auf einem Zylinder über einem symmetrischen Raum seine Dynamik auf die eines Newtonschen skalaren Freiheitsgrades reduziert, der einem quartischen Potential unterliegt.

Der Effekt solcher Eichfelder auf die Raumzeitdynamik wird hierbei auf die Wheeler-DeWitt-Einschränkung reduziert, die die Anfangsbedingungen im Einstein-Yang-Mills-System verknüpft. Darüber hinaus zeigten wir, dass in Raumzeitdimensionen verschieden von vier ein dynamischer Skalenfaktor, welcher in konformer Zeit parametrisiert ist, einen Hubble-reibungsähnlichen Term in den reduzierten Bewegungsgleichungen des Eichsektors induziert. Schließlich untersuchten wir ein Modell, bei dem ein $SO(4)$ -symmetrisches $SU(2)$ Yang-Mills-Feld das symmetrische Higgs-Vakuum in einem geschlossenen Friedmann-Universum in der elektroschwachen Epoche thermodynamisch stabilisiert. Wir prüften generische Fluktuationen des Eichfeldes und zeigten, dass es unter jeder Störung außer dem Singulett instabil ist, von dem wir nach exakter Lösung fanden, dass es marginal stabil ist.

Abstract

In this thesis, we explore results from geometric construction methods of Yang–Mills fields in maximally symmetric spacetimes, including cosmological applications and abelian reductions in different settings. Such efforts were inspired by the development of a new construction method for electromagnetic knots in Minkowski space from an abelian reduction of an $SU(2)$ Yang–Mills theory in a Lorentzian cylinder over the three-sphere $S^3 \simeq SU(2)$, which is then conformally mapped into $\mathbb{R}^{1,3}$. My investigations and results will be presented in three parts, each with partially independent motivations, conclusions, and prospects for advancement.

The first set of results concerns the previously constructed basis of electromagnetic knots in Minkowski space. We investigated conserved charges associated with the conformal invariance of the solutions, which helped us better understand some of their physical properties and to compare them with other known electromagnetic knots constructed from different established methods. In particular, we found specific parameter choices that allowed us to reproduce generalisations of the Rañada-Hopf knot, such as rotated Hopfions, and torus knots from Bateman’s construction. Moreover, as studies on the reproduction of such knotted solutions in the lab advance, we performed a numerical investigation and documented the effects of the electromagnetic knots from our basis on charged particles, which is relevant data for possible experimental applications in the future.

Motivated by the aforementioned results from the $SU(2)$ Yang–Mills field on dS_4 , we explored what further results can be obtained from Yang–Mills theories constructed with similar use of the geometric structure of other maximally symmetric spacetimes. We first used a piecewise foliation of the Minkowski spacetime by orbits of the Lorentz group to construct an $SO(1,3)$ gauge theory in the different regions, which, after a regularisation on the lightcone, produced a Yang–Mills field whose energy-momentum tensor is global in $\mathbb{R}^{1,3}$ and is given by an improvement term. Then, we explored an $SU(1,1)$ gauge theory on AdS_4 foliated with AdS_3 sheets and conformally mapped it into $\mathbb{R}^{1,3}$. The abelian reduction of the non-abelian gauge theory generated the hyperbolic equivalent of the Rañada-Hopf knot. We showed that one of its projections into a plane was a known magnetic vortex in 1+2 dimensions. We finalised by discussing the prospects of a method to generate an uncountable basis of hyperbolic equivalents of the previously discussed electromagnetic knots.

The last set of results concerns the coupling of the Yang–Mills theory to General Relativity in Friedmann universes. We showed that, in any spacetime dimension, the equivariant Ansatz of any Yang–Mills theory on a cylinder over a symmetric space has its dynamics reduced to that of a Newtonian scalar degree of freedom subjected to a quartic potential. The effect of such gauge fields on the spacetime dynamics is simply reduced to the Wheeler-DeWitt constraint, which relates the initial conditions in the Einstein–Yang–Mills system. Moreover, we showed that, in spacetime dimensions other than four, a dynamical scale factor induces a Hubble friction-like term in conformal time in the reduced equation of motion for the gauge sector. Lastly, we investigated a model where an $SO(4)$ -symmetric $SU(2)$ Yang–Mills field thermodynamically stabilises the symmetric Higgs vacuum in a closed Friedmann universe in the electroweak epoch. We probed generic fluctuations of the gauge field and showed that it is unstable under any perturbation other than the singlet, which we solved exactly and found is marginally stable.

Acknowledgements

Firstly, I would like to thank my supervisor, Olaf Lechtenfeld, for the opportunity of doing this Ph.D., guiding me through my research projects while I cultivated my independence, incentivising me to frequently join conferences and Ph.D. summer schools, and unconditionally supporting my career decisions.

I must thank Leibniz Universität Hannover, its staff - especially Tanja Weißner -, and the Niedersachsen government for the position as wissenschaftliche Mitarbeiter and all related financial and administrative aid.

I want to thank my recent collaborators, Daniel Litim and Gustavo de Brito, for the very enlightening discussions as I ventured in new areas of physics and for warmly welcoming me into your cities and groups during periods as a visiting researcher.

In the same vein, I want to thank my colleagues in LUH, especially Kaushlendra Kumar and Mahir Ertürk, for great physics discussions and equally great company over the years.

In addition, I extend my thanks to the Professors from different institutions in Rio de Janeiro who were part of my academic trajectory and contributed in their own way to my accomplishments.

Last but not least, a special thanks to my family - especially my wife, Hellen Fortes da Silva Sales - and my special friends from Rio de Janeiro, without whom I would not be able to finish my Ph.D. through difficult times.

Contents

Zusammenfassung	iv
Abstract	vi
Acknowledgements	vii
Contents	viii
List of Figures	x
1 Introduction, motivation, and structure	1
2 Review on selected topics of differential geometry	4
2.1 Group action	4
2.2 Killing form	6
2.3 Homogeneous, reductive, and symmetric spaces	8
2.4 Locally orthonormal coframes	9
3 Maximally symmetric spacetimes	12
3.1 Maximally symmetric spacetimes and their properties	12
3.2 Hyperbolic spaces	15
3.3 DeSitter spaces	16
3.4 Anti-deSitter spaces	18
4 Fibre Bundles and Gauge Theory	22
4.1 Fibre bundles	22
4.2 Principal bundles	24
4.3 Connections on principal bundles	26
4.4 Local representatives: Yang–Mills field and field strength	29
4.5 Maxwell and Yang–Mills theories	32
4.6 Spacetime symmetries of Yang–Mills fields	34
5 The abelian case: electromagnetic knots	37
5.1 Hyperspherical harmonics and electromagnetic fields on $\mathcal{I} \times S^3$	37
5.2 Map to Minkowski	42
5.3 Conformal group and conserved Noether charges	45
5.4 Trajectories of charged particles	49
6 The non-abelian case I: non-compact gauge groups	55
6.1 $SO(1, 3)$ gauge theory on Minkowski space	55
6.1.1 General setting	56
6.1.2 Interior of the lightcone \mathcal{T}	56
6.1.3 Exterior of the lightcone \mathcal{S}	59
6.1.4 Lightcone surface \mathcal{L}	61

6.1.5	Energy-momentum tensor	62
6.2	SU(1, 1) gauge theory on AdS ₄	63
6.2.1	AdS ₄ , coframe, and map to Minkowski	63
6.2.2	Equivariant Yang–Mills fields	67
6.2.3	Abelian reduction	69
7	The non-abelian case II: cosmic Yang–Mills fields	75
7.1	Coset space dimensional reduction of the Yang–Mills theory and its coupling to general relativity	75
7.1.1	CSDR on cylinders over symmetric spaces	76
7.1.2	Application to H^n , dS _{n} , and AdS _{n} sheets	78
7.1.3	Effect of the Yang–Mills field on the spacetime dynamics	81
7.1.4	Effect of a general warping on the gauge field in arbitrary dimension	83
7.2	Instability of cosmic Yang–Mills fields	85
7.2.1	Preliminaries	85
7.2.2	Linear fluctuations of Yang–Mills fields and their natural frequencies	86
7.2.3	Stability analysis with Floquet theory	92
8	Conclusion and outlook	100
	Bibliography	102

List of Figures

3.1	Illustration of the hyperbolic space H^2	15
3.2	Illustration of the deSitter space dS_2	17
3.3	Illustration of the anti-deSitter space AdS_2	19
4.1	Illustration of the fibre bundle's fiber over a point of the base space	26
5.1	Map between cylinder over S^3 and the Minkowski space $R^{1,3}$	43
5.2	Electric and magnetic field lines of the RH knot, a $j = 0$ solution.	45
5.3	Electric and magnetic field lines of a time-translated Hopfion	50
5.4	Electric and magnetic field lines of $j = \frac{1}{2}$ and $j = 1$ EM knots	51
5.5	Evolution of energy densities for $j = 0$ and $j = \frac{1}{2}$ EM knots	51
5.6	Trajectory of charge particle from rest to ultra-relativistic speeds	54
5.7	Trajectories of charged particles illustrating the splitting for different solid-angle regions	54
6.1	Illustration of the cover of Minkowski space by two copies of AdS_4	66
6.2	Energy density of the equivariant $SU(1,1)$ gauge field mapped into Minkowski space.	70
6.3	Illustration on the Minkowskian energy density largely concentrated on the hyperboloid $\kappa=0$	70
6.4	Illustration of the field lines for the abelian reduction on Minkowski space.	72
6.5	Energy density of the abelian reduction on Minkowski space.	73
7.1	Cosmological potential $W(a)$ for different values of k and cosmological constant Λ	82
7.2	Frequency-squares $\Omega_{(0,v,\beta)}^2(\tau)$ over their respective periods, for different values of k^2	92
7.3	Frequency-squares $\Omega_{(2,v,\beta)}^2(\tau)$ over their respective periods, for different values of k^2	93
7.4	$SO(4)$ singlet fluctuation modes Φ_1 and Φ_2 over eight periods, for $k^2=0.81$	95
7.5	Exact perturbation $\eta(\tau)$ illustrating marginally-stable initial behaviour and long-time beat-wave behaviour	96
7.6	Plots of the trace of the stroboscopic map for $(j, v) = (2, 0)$	97
7.7	Plots of the trace of the stroboscopic map for the different modes with $(j, v) = (2, 2)$	98
7.8	Long-term numerical integration of $\Phi(\tau)$ for $(j, v, \beta) = (2, 2, 1)$ but different k illustrating the change in behaviour from unstable to stable.	98
7.9	Universal limiting natural frequency-squares $\tilde{\Omega}_{(j,v,\beta)}^2$ over one period in Z for $v=j$	99

Chapter 1

Introduction, motivation, and structure

Since its introduction by Yang and Mills in 1954 [1], non-abelian gauge theories, or simply Yang–Mills theories, have become essential for particle physics, and in particular for the establishment of the standard model of particle physics. Not only they very successfully describe the strong and weak interactions, leading to many predictions, but they are also explored in attempts of finding a grand unification theory for particle physics, or even a theory for quantum gravity, framing general relativity as a low-energy limit of a gauge theory for the gravitational field. In particular, the classical version of the Yang–Mills theory holds great importance by itself. The immediate first reason for that is that the path integral for the quantum theory is dominated by saddle-point contributions, which come from solutions to the classical equations of motion. Beyond that, classical Yang–Mills theories have direct applications not only in particle physics, like for QCD confinement models [2], but also in non-related fields such as condensed matter physics, for example in an adequate description of spin-orbit interactions [3].

Despite its continued relevance for the past 50 years, there is a relatively small number of explicitly known analytic Yang–Mills fields. One reason is that the Yang–Mills equations are quite difficult to solve, as a non-linear system of partial differential equations for matrix-valued fields. The lack of more analytic Yang–Mills fields in general hinders our capacity of getting a better grasp on phenomena related to non-abelian gauge fields. In this context, topological and geometrical methods which enable an explicit construction of solutions to the Yang–Mills equations are very valuable and should be investigated.

In this thesis, we will mainly explore how the Yang–Mills equations can be solved in Lorentzian n -dimensional maximally symmetric spacetimes when one employs geometrical descriptions of such spacetimes structures in terms of Lie groups or cosets thereof. In most cases, we will also make use of equivariant Ansätze for the gauge fields [4]. Additionally, in four-dimensional manifolds, the conformal invariance of Yang–Mills theory allows one to map non-abelian gauge fields between different conformally flat spacetimes, which further expands the solutions we can explicitly construct and analyse in different spacetimes. An example of application of the new non-abelian gauge fields is in their abelian reductions, allowing for a straightforward construction of electromagnetic fields with particular characteristics in different spacetimes. We will also be interested in the coupling of such Yang–Mills theories to the classical gravitational field in Friedmann universes, which may be relevant for applications of non-abelian gauge theories in cosmology, such as in gauge-fflation scenarios [5].

This text can be separated into two parts. The first one, consisting of Chapters 2, 3, and 4, is a non-comprehensive review on selected mathematical and theoretical

structures and results that will be more relevant to the discussions later on. The second part, with Chapters 5, 6, and 7, contains a pedagogical and slightly summarised version of the investigations and results from my research publications.

From the review part, Chapter 2 consists in a brief overview on particular topics of differential geometry which are of special interest for our analyses. We assume that the reader is familiar with the basics, such as (pseudo-)Riemannian geometry and Lie groups and algebras. Then, we discuss group actions on differentiable manifolds, the Killing form of a Lie group, homogeneous, reductive, and symmetric spaces, and locally orthonormal coframes and their construction from the Maurer–Cartan one-form. Chapter 3 starts from a definition of maximally symmetric spacetimes and a revision on their most relevant properties, to then discuss all Riemannian and Lorentzian examples, with the exception of the sphere, for which we assume that the reader is sufficiently familiar with. Specifically, we discuss n -dimensional hyperbolic spaces, deSitter spaces, and anti-deSitter spaces, including some of their parametrisations and foliations. Following the focus of the thesis on geometrical aspects, in Chapter 4, we briefly review the classical Yang–Mills theory in its geometrical construction, as a dynamical theory for a connection one-form on a principal bundle. For that, we first construct the more relevant aspects of the theory of fibre bundles, of principal bundles, and of connections on principal bundles.

The second part starts with Chapter 5, where we review a recently-developed construction method for a new (infinite) basis of electromagnetic knotted fields in Minkowski space $\mathbb{R}^{1,3}$ constructed as the abelian reduction of a $SU(2)$ Yang–Mills theory on a cylinder over the three-sphere S^3 . As one of the simplest basis elements, it was shown that the method reproduces the celebrated Rañada-Hopf knot. We will further investigate the fields generated by this basis focusing on their physical properties, how they compare to other electromagnetic knots obtained from alternative construction methods, and which kinds of experimental applications could apply to them based on their effects on charged particles.

The next chapter, Chapter 6, consists in further explorations of Yang–Mills theories reduced by the equivariant Ansatz on maximally symmetric spacetimes. After motivating the physical relevance of gauge theories with non-compact gauge groups, we investigate an $SO(1,3)$ gauge theory on Minkowski space, then an $SU(1,1)$ gauge theory on anti-deSitter AdS_4 , which is later conformally mapped into the Minkowski space. The abelian reduction of the latter is the hyperbolic equivalent of the Rañada-Hopf knot.

After that, in Chapter 7, we will consider the dynamics of the spacetime in Friedmann–Lemaître–Robertson–Walker (FLRW) universes, taking into account the coupled Einstein–Yang–Mills system before reducing it. Therefore, we will be looking into the possibility of cosmological applications of non-abelian gauge theories in different FLRW universes. In the first section, we will compute general results for a Yang–Mills field reduced with the equivariant Ansatz on any (pseudo-)Riemannian spacetime that can be foliated by symmetric spaces. Hence, we will couple it to the scale factor of the universe and discuss the effects of such a coupling in both fields. In the second section, we consider a Yang–Mills theory on a cylinder over the three-sphere S^3 which is reduced by the equivariant Ansatz. This approach was recently employed by Friedan [6] in a model where it stabilises the symmetric Higgs vacuum before the electroweak transition. However, only the singlet perturbation of such a gauge field was previously discussed in the literature [7]. Therefore, we will treat general perturbations in order to block-diagonalise the linear fluctuation operator of the gauge field while keeping the spacetime fixed, which will enable us to fully probe

the stability of the physical normal modes with respect to any of the background solutions. In particular, we will also specifically consider the very-high-energy limit, which is the one adequate for the discussion on a cosmological application in the electroweak epoch.

Chapter 2

Review on selected topics of differential geometry

In this thesis, we will assume familiarity with the basics of the differential geometry framework, including manifolds, tensor fields, differential forms, (pseudo)-Riemannian geometry, Lie groups, Lie algebras and their representations. For materials covering those subjects, we refer the reader to celebrated books such as [8–11] or to theses in similar subjects, as [12]. Analogously, standard quantum field theory and general relativity are not going to be revised. For those, we refer to [13, 14] and [15, 16], respectively. In this section, we will recall selected topics that are more central to the work presented in the thesis, namely aspects of group actions, the Killing form, homogeneous, reductive, and symmetric spaces, and locally orthonormal coframes.

2.1 Group action

The study of the action of a (continuous) group on a manifold is key not only to gauge theory in general, as we will discuss in Chapter 4, but also to the geometric methods that we will employ in the construction of new solutions to the Yang–Mills equations throughout this thesis. Let us start from the first definitions.

Definition 1. (Group action) Let M be a differentiable manifold and G a Lie group with identity element e . A **group action** α of G on M is a map

$$\begin{aligned} \alpha : G \times M &\rightarrow M \\ (g, p) &\mapsto \alpha_g(p) \end{aligned} \quad (2.1)$$

where α_e is the identity map on M and the map $g \mapsto \alpha_g(\cdot)$ is a group homomorphism from G into $S(M)$, the symmetric group of automorphisms of M . Then, M is called a G -space. If

$$\alpha_g(\alpha_h(p)) = \alpha_{gh}(p), \quad (2.2)$$

α is called a **left group action** and we denote $\alpha_g(p) \equiv L_g p \equiv g p$. Otherwise, if

$$\alpha_g(\alpha_h(p)) = \alpha_{hg}(p), \quad (2.3)$$

α is called a **right group action** and we denote $\alpha_g(p) \equiv R_g p \equiv p g$.

Definition 2. If M and N are two G -spaces with actions

$$\alpha : G \times M \rightarrow M \quad \text{and} \quad \beta : G \times N \rightarrow N, \quad (2.4)$$

a map $f : M \rightarrow N$ is called **G -equivariant** if

$$f \circ \alpha_g(p) = \beta_g \circ f(p), \quad \forall p \in M \text{ and } g \in G. \quad (2.5)$$

Assuming that α and β are left actions, the condition above is often simply written as $f(gp) = gf(p)$.

Given an action α and some point $p \in M$, it is useful to look into the image and the kernel of $\alpha_{(\cdot)}(p) : G \rightarrow M$. Let us define:

Definition 3. (Orbit of a point) The **orbit of p** is defined as

$$\text{Orb}_p := \alpha_G(p) := \{\alpha_g(p) \mid g \in G\}. \quad (2.6)$$

Theorem 1. If M is a G -space, two orbits Orb_p and Orb_q of $p, q \in M$ are either disjoint or identical.

This implies that orbits on M can be used to define an equivalence relation in which $p \sim q$ if $\text{Orb}_p = \text{Orb}_q$, thus partitioning M as the disjoint union of orbits of G .

Definition 4. (Quotient space of a G -space) If M is a G -space, the **quotient space** of the action of G on M is defined as

$$M/G := \{\text{Orb}_p \mid p \in M\}. \quad (2.7)$$

The quotient space can also be called the space of orbits or simply the coset space.

Definition 5. (Stabiliser of a point) We define the **stabiliser of p** as

$$\text{Stab}_p := \{g \in G \mid \alpha_g(p) = p\}. \quad (2.8)$$

Theorem 2. (Any stabiliser is a subgroup) If M is a G -set, the stabiliser Stab_p of any point $p \in M$ is a subgroup of G .

Stab_p is also called the **little group** or the **isotropy group** of p .

With the concepts above at hand, we can announce the **orbit-stabiliser theorem**:

Theorem 3. (Orbit-stabiliser) Let M be a G -space with action α . For any $p \in M$, $\alpha_{(\cdot)}(p) : G \rightarrow M$ establishes a bijection between Orb_p and the coset G/Stab_p .

This result is going to be used in later sections to map groups or cosets thereof into foliations of suitable spacetimes.

Some important classes of actions are:

Definition 6. (Transitive, faithful, and free actions) An action α is called

- (i) **transitive** if, $\forall p \in M, \text{Orb}_p = M$.
- (ii) **faithful** if $\alpha_g(p) = p \quad \forall p \Rightarrow g = e$. That is, the induced homomorphism $G \rightarrow S(M)$ is injective.
- (iii) **free** if, $\forall p \in M, \text{Stab}_p = \{e\}$. In other words, $\alpha_{(\cdot)}(p)$ is injective for all p .

A free action is always faithful, but the converse is not true.

Corollary 4. (of the orbit-stabiliser theorem)

- (i) If the action is transitive, the orbit-stabiliser theorem trivially implies that, $\forall p \in M$, the action establishes a bijection between M and G/Stab_p , further implying that all stabiliser subgroups for different points p are isomorphic. Then the action is a G -equivariant diffeomorphism.
- (ii) If the action is free, it establishes a bijection between G and Orb_p for all p , hence implying that all orbits are isomorphic.

2.2 Killing form

A Lie group is a differentiable manifold by definition. In the context of (pseudo-)Riemannian geometry, one benefits from defining a metric on it. In particular, we will be interested in metrics that are invariant under the action of translations by the group's own action:

Definition 7. (Left-, right-, bi-invariant metrics) A metric $s : G \times G \rightarrow \mathbb{R}$ is said to be:

- (i) **left-invariant** if, $\forall g \in G$, $L_g^*s = s$,
- (ii) **right-invariant** if, $\forall g \in G$, $R_g^*s = s$,
- (iii) and **bi-invariant** if it is both left- and right-invariant.

Remark 5. Every metric on G induces an inner product on the associated Lie algebra \mathfrak{g} . Conversely, any inner product $\langle \cdot, \cdot \rangle$ on \mathfrak{g} can be used to construct a left-invariant metric on G via

$$s(g_1, g_2) := \langle L_{g_1^{-1}*}(g_1), L_{g_1^{-1}*}(g_2) \rangle \quad (2.9)$$

or a right-invariant metric via

$$s(g_1, g_2) := \langle R_{g_1^{-1}*}(g_1), R_{g_1^{-1}*}(g_2) \rangle. \quad (2.10)$$

In order to characterise bi-invariant metrics on Lie groups, we need to define the adjoining actions:

Definition 8. (Adjoint actions)

- (i) The **adjoint action AD of a Lie group G on itself** is given by

$$\begin{aligned} \text{AD} : G \times G &\rightarrow G \\ (g, h) &\mapsto \text{AD}_g h := g h g^{-1}. \end{aligned} \quad (2.11)$$

- (ii) The **adjoint action Ad of a Lie group G on its Lie algebra \mathfrak{g}** is given by

$$\begin{aligned} \text{Ad} : G \times \mathfrak{g} &\rightarrow \mathfrak{g} \\ (g, x) &\mapsto \text{Ad}_g x := \text{AD}(g)_*(x). \end{aligned} \quad (2.12)$$

With a slight abuse of notation, the Ad action can also be expressed as $\text{Ad}_g(x) = g x g^{-1}$.

- (iii) The **adjoining action ad of a Lie algebra \mathfrak{g} on itself** is the differentiation of Ad with respect to the first argument and is given by

$$\begin{aligned} \text{ad} : \mathfrak{g} \times \mathfrak{g} &\rightarrow \mathfrak{g} \\ (x, y) &\mapsto \text{ad}_x y := [x, y], \end{aligned} \quad (2.13)$$

which is simply the Lie bracket of \mathfrak{g} .

Theorem 6. Let s be a left-invariant metric on a Lie group G . The metric s is bi-invariant if and only if the inner product on \mathfrak{g} defined by s is Ad-invariant, *i.e.*, for all $g \in G$ and $x, y \in \mathfrak{g}$,

$$\langle \text{Ad}_g x, \text{Ad}_g y \rangle = \langle x, y \rangle. \quad (2.14)$$

In particle physics theories, it is key to ensure gauge invariance of the Lagrangian, and, for compact gauge groups, the positivity of the kinetic energy of the gauge bosons. For that, the following theorem is essential:

Theorem 7. If G is a compact Lie group with Lie algebra \mathfrak{g} , there exists an Ad-invariant and positive-definite inner product on \mathfrak{g} . The adjoint representation is orthogonal with respect to this inner product.

It is useful to consider a particular Ad-invariant inner product on a Lie algebra \mathfrak{g} which can always be constructed:

Definition 9. (Killing form) The **Killing form** K on a Lie algebra \mathfrak{g} over the field $\mathbb{F} = \mathbb{R}, \mathbb{C}$ is the symmetric and bilinear form defined as

$$\begin{aligned} K : \mathfrak{g} \times \mathfrak{g} &\rightarrow \mathbb{F} \\ (x, y) &\mapsto \text{tr}(\text{ad}_x \circ \text{ad}_y). \end{aligned} \quad (2.15)$$

Remark 8. An immediate consequence of the Jacobi identity and the cyclicity of the trace is that ad is skew-symmetric with respect to the Killing form, that is,

$$K(\text{ad}_x y, z) = -K(y, \text{ad}_x z). \quad (2.16)$$

The Killing form as defined is invariant under automorphisms on \mathfrak{g} . Furthermore, it also characterises semisimple Lie algebras, according to the following results:

Theorem 9. (Cartan's Criterion for Semisimplicity) The Lie algebra \mathfrak{g} is semisimple if and only if the Killing form K is non-degenerate.

Theorem 10. A semisimple Lie algebra \mathfrak{g} can be decomposed as the direct sum

$$\mathfrak{g} = \bigoplus_{i=1}^s \mathfrak{g}_i \quad (2.17)$$

of ideals \mathfrak{g}_i which are simple Lie algebras and pairwise orthogonal with respect to the Killing form K .

The previous results related to the Killing form apply to both compact and non-compact algebras. If the algebra is compact, we have:

Theorem 11. If \mathfrak{g} is a compact real Lie algebra, its Killing form K is negative semidefinite, with

$$\begin{aligned} K(x, x) &= 0 \quad \forall x \in Z(\mathfrak{g}), \\ K(x, x) &< 0 \quad \forall x \in \mathfrak{g} \setminus Z(\mathfrak{g}), \end{aligned} \quad (2.18)$$

with $Z(\mathfrak{g})$ being the centre of \mathfrak{g} .

Corollary 12. If the compact Lie algebra \mathfrak{g} has trivial centre, $Z(\mathfrak{g}) = 0$, its Killing form K is negative definite.

The converse of the corollary above can also be proven:

Theorem 13. If the Killing form K of a real Lie algebra \mathfrak{g} is negative definite, \mathfrak{g} is compact and has trivial centre.

Theorem 14. If \mathfrak{g} is a compact Lie algebra with centre $Z(\mathfrak{g})$, \mathfrak{g} can be decomposed as

$$\mathfrak{g} = Z(\mathfrak{g}) \oplus \mathfrak{h} \quad (2.19)$$

with \mathfrak{h} being an ideal which is a compact semisimple Lie algebra.

Now take $\{T_i\}$ to be a basis of the Lie algebra \mathfrak{g} . It is useful to explicitly write the relation between the components of the Killing form and the structure constants f_{jk}^i in this basis. From the definition of the Killing form,

$$K_{ij} = \text{tr}(\text{ad}_{T_i} \circ \text{ad}_{T_j}). \quad (2.20)$$

Letting the adjoint actions inside the trace act on a basis element T_k , we have

$$\text{ad}_{T_i} \circ \text{ad}_{T_j} T_k = [T_i, [T_j, T_k]] = [T_i, f_{jk}^m T_m] = f_{jk}^m f_{im}^n T_n. \quad (2.21)$$

Finally, taking the trace of such linear map, we obtain

$$K_{ij} = f_{im}^k f_{jk}^m. \quad (2.22)$$

These are the components of the Killing form in a basis $\{T_i\}$ of the Lie algebra \mathfrak{g} . Exploring the identification between the Lie algebra and the set $\text{Lie}(G)$ of left-invariant vector fields on G , we can take the associated basis of left-invariant one-forms $\{e^i\} \subset \text{Lie}(G)^*$ and explicitly write the corresponding bi-invariant metric on G as

$$K = K_{ij} e^i \otimes e^j. \quad (2.23)$$

2.3 Homogeneous, reductive, and symmetric spaces

For the results covered in this thesis, we will be mainly interested in transitive actions of a Lie group G on a differentiable manifold M . In such cases, we define:

Definition 10. (Homogeneous space) A **homogeneous space** is a G -space M where the action is transitive.

As seen in Corollary 4, transitive action ensures that the stabiliser subgroups of all points are isomorphic, consisting in a Lie subgroup $H \subset G$ with $\dim(H) = \dim(G) - \dim(M)$. Note that M may be a manifold unrelated to G , G itself, or a coset space G/H , which is automatically a homogeneous space with respect to the natural action of G . If M is a coset space G/H of G , two important cases are:

Definition 11. (Reductive space) Let G be a Lie group with Lie algebra \mathfrak{g} and $H \subset G$ a closed Lie subgroup with Lie algebra \mathfrak{h} . Consider the coset space G/H , which is trivially a homogeneous space under the action of G . If there exists a vector subspace $\mathfrak{m} \subset \mathfrak{g}$ respecting

$$\mathfrak{g} = \mathfrak{h} \oplus \mathfrak{m} \quad \text{such that} \quad \text{Ad}_H \mathfrak{m} \subset \mathfrak{m}, \quad (2.24)$$

that is, \mathfrak{m} is invariant under the adjoint action of H , then G/H is called a **reductive space**. Notice that \mathfrak{m} need not be a subalgebra.

Definition 12. (Symmetric space) Let G be a Lie group with Lie algebra \mathfrak{g} and $H \subset G$ a closed Lie subgroup with Lie algebra \mathfrak{h} . Then G/H is a **symmetric space** if there exists an involution $\sigma \in \text{Aut}(G)$ which preserves H , that is,

$$\sigma : G \rightarrow G, \quad \sigma^2 = \text{Id}_G, \quad \text{and} \quad \sigma(h) = h, \forall h \in H. \quad (2.25)$$

When differentiating σ at the identity one obtains an induced automorphism on the Lie algebra \mathfrak{g} which is also an involution. Hence, its two eigenvalues are ± 1 . As H is preserved by σ , the eigenspace associated with the eigenvalue $+1$ is \mathfrak{h} . We can then denote the eigenspace associated with -1 as \mathfrak{m} . Since σ is an automorphism, we have a direct sum decomposition of the Lie algebra as

$$\mathfrak{g} = \mathfrak{h} \oplus \mathfrak{m} \quad (2.26)$$

with

$$[\mathfrak{h}, \mathfrak{h}] \subset \mathfrak{h}, \quad [\mathfrak{h}, \mathfrak{m}] \subset \mathfrak{m}, \quad \text{and} \quad [\mathfrak{m}, \mathfrak{m}] \subset \mathfrak{h}. \quad (2.27)$$

The second term of (2.27) implies that every symmetric space is a reductive space.

In the context of the decomposition $\mathfrak{g} = \mathfrak{h} \oplus \mathfrak{m}$, let us denote the basis of each of the three vector spaces with different sets of indices $\{A, B, C, D, \dots\}$, $\{i, j, k, l, \dots\}$, and $\{a, b, c, d, \dots\}$, respectively, such that

$$\mathfrak{g} = \text{span}\{T_A\}, \quad \mathfrak{h} = \text{span}\{T_i\}, \quad \text{and} \quad \mathfrak{m} = \text{span}\{T_a\}. \quad (2.28)$$

This convention will be kept throughout the thesis in the context of symmetric spaces. In terms of those indices, we can break the Lie brackets $[T_A, T_B]$ of \mathfrak{g} in three expressions:

$$\begin{cases} [T_a, T_b] = f_{ab}^c T_c + f_{ab}^i T_i, \\ [T_i, T_a] = f_{ia}^c T_c + f_{ia}^j T_j, \\ [T_i, T_j] = f_{ij}^k T_k, \end{cases} \quad (2.29)$$

where the absence of f_{ij}^a components in $[T_i, T_j]$ is a consequence of \mathfrak{h} being a Lie subalgebra. Analogously, \mathfrak{m} would also be a subalgebra if and only if $f_{ab}^i = 0$. Moreover, the Ad-invariance condition on \mathfrak{m} for the coset space G/H to be reductive is simply rewritten as $f_{ia}^j = 0$, while the further condition $[\mathfrak{m}, \mathfrak{m}] \subset \mathfrak{h}$ for G/H to be a symmetric space reduces to $f_{ab}^c = 0$.

2.4 Locally orthonormal coframes

Before reviewing the spacetimes to be used in our analysis, we will briefly discuss how we will use the Maurer–Cartan one-form to find locally orthonormal basis of left-invariant one-forms for manifolds isomorphic to groups or cosets thereof.

Definition 13. (Locally orthonormal basis) Let M be a (pseudo-)Riemannian manifold of signature (p, q) . A **locally orthonormal basis** of one-forms $\{e^\mu\}$ is a basis of (non-coordinate) one-forms satisfying, for all $x \in M$,

$$g_x = \eta_{\mu\nu} e_x^\mu \otimes e_x^\nu, \quad (2.30)$$

where η is the Minkowski metric of signature (p, q) .

Definition 14. (Maurer–Cartan frame and coframe) Let $\{T_a\}$ be a basis of \mathfrak{g} , the tangent space $T_e G$ at the identity of the Lie group G . Let $\{E_a\}$ be the corresponding

basis of $\text{Lie}(G)$, the set of left-invariant vector fields on G . Take $\{e^a\}$ as the dual basis of $\text{Lie}(G)^*$, that is, such that

$$e^a(E_b) = \delta_b^a. \quad (2.31)$$

Then, $\{E_a\}$ is called a **Maurer–Cartan frame** and $\{e^a\}$ a **Maurer–Cartan coframe**.

Theorem 15. A Maurer–Cartan coframe $\{e^a\}$ respects the **Maurer–Cartan equation**:

$$de^c = -\frac{1}{2}f_{ab}^c e^a \wedge e^b, \quad (2.32)$$

where f_{ab}^c are the structure constants associated with the basis $\{T_a\}$ of \mathfrak{g} .

Definition 15. (Maurer–Cartan form) The **Maurer–Cartan form** θ is a \mathfrak{g} -valued one-form field on G defined on each point $g \in G$ as

$$\begin{aligned} \theta_g : T_g G &\rightarrow T_e G \\ v_g &\mapsto (L_{g^{-1}})_* v_g. \end{aligned} \quad (2.33)$$

Its action is made explicit by the use of the coframe, in which it is written as

$$\theta_g(\cdot) = T_a e^a(\cdot), \quad (2.34)$$

or simply

$$\theta = T_a e^a. \quad (2.35)$$

The Maurer–Cartan equation (2.32) can be recast in terms of the Maurer–Cartan form, reading

$$d\theta = -\frac{1}{2}[\theta, \theta], \quad (2.36)$$

where

$$[T_a e^b, T_c e^d] := [T_a, T_c] e^b \wedge e^d. \quad (2.37)$$

Moreover, in matrix Lie groups, the Maurer–Cartan one-form reads

$$\theta_g^{ij} = (g^{-1})^{ik} dg^{kj}. \quad (2.38)$$

In (2.34) it becomes clear that, from the Lie algebra generated by $\{T_a\}$ and the Maurer–Cartan one-form, we can easily obtain the associated basis of left-invariant one-forms $\{e_a\}$. This procedure will be used in different cases in the following chapters to straightforwardly obtain local orthonormal bases for G -sets, with the Maurer–Cartan form being computed directly from (2.38), since we will always work with matrix Lie groups, for example, $\text{SU}(1,1) \simeq \text{AdS}_3$ and $\text{SU}(2) \simeq S^3$.

Let us now consider the case of $M := G/H$ being a symmetric space under the action of the matrix Lie group G . Recall the index convention for \mathfrak{g} , \mathfrak{h} , and \mathfrak{m} used in (2.28). We will now equip M with a G -invariant metric. First, one obtains the Maurer–Cartan form on G and a basis of left-invariant one-forms $\{\tilde{e}^A\}$ in it, as described above. Now, take a (section) smooth map $\sigma : G/H \rightarrow G$ that chooses particular representatives for each orbit. Then, one can use σ to pull back the one-forms on G to one-forms on M :

$$e^A := \sigma^* \tilde{e}^A. \quad (2.39)$$

The set $\{e^A\}$ is comprised of $\dim(G)$ one-forms in G/H , hence, it cannot be linear independent. We have $\dim(G/H)$ linearly independent one-forms $\{e^a\}$ (corresponding to \mathfrak{m}), such that the remaining forms $\{e^i\}$ (corresponding to \mathfrak{h}) can be decomposed in terms of the former as

$$e^i = \chi_a^i e^a, \quad (2.40)$$

where χ_a^i are smooth scalar functions on G/H . Finally, to obtain a G -invariant metric on G/H , simply take the Killing form K on G and pull it back with σ , restricting it to the one-forms $\{e^a\}$:

$$K_{G/H} = (\sigma^* K)|_{G/H} = K_{ab} e^a \otimes e^b. \quad (2.41)$$

To express the exterior derivative of the pulled-back one-forms, one can simply consider the splitting of the Maurer–Cartan equation in terms of the decomposition $\mathfrak{g} = \mathfrak{h} \oplus \mathfrak{m}$. For the one-forms corresponding to \mathfrak{h} , we have

$$de^i = \frac{1}{2} f_{jk}^i e^j \wedge e^k + \frac{1}{2} f_{ab}^i e^a \wedge e^b, \quad (2.42)$$

while, for the ones corresponding to \mathfrak{m} ,

$$de^a = \frac{1}{2} f_{ib}^a e^i \wedge e^b. \quad (2.43)$$

Now that we reviewed the preliminary geometrical elements, in the next chapter we will define the spacetimes in which we are going to work on.

Chapter 3

Maximally symmetric spacetimes

Maximally symmetric spacetimes are of great importance in theoretical physics. To name a few examples, the anti-deSitter space is required for some holography and string theory settings and the deSitter space is key to Cosmology, since our universe seems to be homogeneous and isotropic in large scales and have a positive cosmological constant, even if very small. In this chapter, we are going to define and characterise the spacetimes in which we are going to work on along this thesis, including some of their foliations. Before delving into the specific cases, let us start by discussing general properties of maximally symmetric spacetimes.

3.1 Maximally symmetric spacetimes and their properties

Two very important and physically intuitive concepts should precede the definition of maximally symmetric spaces for a complete discussion, namely homogeneity and isotropy of spaces. Homogeneity encodes the idea of all points in space being pairwise indistinguishable, while isotropy around a point encodes the idea of all directions around this point being indistinguishable. Let us first formalise such concepts.

Definition 16. (Homogeneous spacetime) A (pseudo-)Riemannian spacetime is said to be **homogeneous** if, for any two points $p, q \in M$, there exists an isometry ϕ such that $\phi(p) = q$.

Definition 17. (Isotropic space) A (pseudo-)Riemannian manifold (M, g) is said to be **isotropic at a point** p if, for any two vectors $X, Y \in T_p M$ with $g(X, X) = g(Y, Y)$, there exists an isometry ϕ such that $\phi(p) = p$ and $\phi_*(X) = Y$. If it is isotropic at any point, one may simply say that the manifold is **isotropic**.

The two concepts above are closely related, as shown by the two results below:

Theorem 16. If a manifold is homogeneous and isotropic around a single point, then it is isotropic at any point.

Theorem 17. If a manifold is isotropic at any point, then it is homogeneous.

With those concepts at hand, we can characterise maximally symmetric spacetimes.

Definition 18. (Maximally symmetric spacetime) A n -dimensional (pseudo-)Riemannian manifold is said to be **maximally symmetric** if it possesses $n(n + 1)/2$ independent Killing vectors.

Theorem 18. A (pseudo-)Riemannian manifold is maximally symmetric if and only if it is homogeneous and isotropic.

An easy way to interpret the above result is to realise that homogeneity implies the existence of n independent translational isometries and isotropy implies the existence of $n(n-1)/2$ independent (hyperbolic or regular) rotational isometries, which add to $n(n+1)/2$.

In such highly symmetrical manifolds, the tensor structure of the Riemann and the Ricci tensors are greatly simplified. They should be written only in terms of the metric g , the Levi-Civita symbol ϵ and the Kronecker delta δ . Hence, one can use the symmetry properties of the Riemann tensor to show that it necessary reduces to the following:

Theorem 19. In a n -dimensional maximally symmetric spacetime with metric g , the Riemann tensor reduces to

$$R_{\alpha\mu\nu\beta} = \frac{R}{n(n-1)}(g_{\mu\nu}g_{\alpha\beta} - g_{\alpha\nu}g_{\beta\mu}) \quad (3.1)$$

and the Ricci tensor reduces to

$$R_{\mu\nu} = \frac{R}{n}g_{\mu\nu}, \quad (3.2)$$

where R is the Ricci scalar.

Theorem 20. In a n -dimensional maximally symmetric spacetime, if $n > 2$, the Ricci scalar is a constant.

The results above show that, for $n > 2$, the curvature information on maximally symmetric spacetimes is completely encoded in one constant real value R . Moreover, we will see below that what will fundamentally distinguish maximally symmetric spacetimes is the sign of the Ricci scalar. We say that the geometry is **spherical**, **flat**, or **hyperbolic** if R is positive, zero, or negative, respectively. Let us now consider the metric structure on such spaces for Lorentzian manifolds.

Theorem 21. If M is a maximally symmetric Lorentzian manifold, the metric can always be written as

$$ds^2 = -dt^2 + a(t)^2 [d\tilde{r}^2 + f(\tilde{r})^2 d\Omega_{n-2}^2], \quad (3.3)$$

where t is a timelike coordinate, \tilde{r} is a radial coordinate on the spatial slices, and $d\Omega_{n-2}^2$ is the metric on the unit sphere S^{n-2} . Moreover,

$$f(\tilde{r}) = \begin{cases} \sin(\tilde{r}) & \text{in spherical geometry} \\ \tilde{r} & \text{in flat geometry} \\ \sinh(\tilde{r}) & \text{in hyperbolic geometry} \end{cases} \quad (3.4)$$

and the function $a : \mathbb{R} \rightarrow \mathbb{R}$ is called the **scale factor**.

Performing the change of variable $\tilde{r} \mapsto r := f(\tilde{r})$, the metric then reads

$$ds^2 = -dt^2 + a(t)^2 \left[\frac{dr^2}{1 - kr^2} + r^2 d\Omega_{n-2}^2 \right], \quad (3.5)$$

where

$$k = \begin{cases} +1 & \text{in spherical geometry} \\ 0 & \text{in flat geometry} \\ -1 & \text{in hyperbolic geometry} \end{cases}. \quad (3.6)$$

Such metrics are called **Friedmann–Lemaître–Robertson–Walker** (FLRW) metrics. Furthermore, it is also useful to perform a second change of variables to the so-called **conformal time** τ , defined as

$$\tau(t) = \int^t \frac{dt'}{a(t')}, \quad (3.7)$$

such that the metric reads

$$ds^2 = a(t(\tau))^2 \left[-d\tau^2 + \frac{dr^2}{1 - kr^2} + r^2 d\Omega_{n-2}^2 \right]. \quad (3.8)$$

The discussion above is a kinematic consequence of requiring homogeneity and isotropy on the manifold and is independent of general relativity. To discuss the dynamics of such spaces, we now employ the Einstein equation,

$$R_{\mu\nu} - \frac{1}{2}Rg_{\mu\nu} + \Lambda g_{\mu\nu} = \frac{8\pi G}{c^4} T_{\mu\nu}, \quad (3.9)$$

where T is the energy-momentum tensor from matter fields and Λ is the cosmological constant. Let us define $\kappa := \frac{8\pi G}{c^4}$ as the Einstein gravitational constant. In FLRW universes, the energy-momentum tensor can be greatly simplified. In the absence of matter or in the presence of conformally invariant matter, we have $\text{tr } T = 0$, and the Einstein equation can be used to fix the cosmological constant. Taking the trace of (3.9), we obtain

$$R - \frac{n}{2}R + n\Lambda = 0 \quad \Rightarrow \quad \Lambda = \frac{(n-2)R}{2n}, \quad (3.10)$$

determining the cosmological constant in terms of the Ricci scalar. Moreover, compatibility with homogeneity and isotropy reduces T to the perfect-fluid type, in which it is diagonal and with non-zero components

$$T_{\mu\mu} = p_{\mu}g_{\mu\mu} \quad (3.11)$$

(no sum in μ intended), with $p_0 = \rho(t)$ being the energy density and $p_i = p(t)$ being the pressure. In particular, for Yang–Mills matter in four-dimensional spacetimes we have conformal invariance, which further imposes tracelessness of the energy-momentum tensor, translating to $p = \rho/3$.

Coming back to the general discussion, it can be shown that, in FLRW universes, there are only two independent components of the Einstein equation, which we can take as the $(0,0)$ and the trace components. From them, we obtain the celebrated **Friedmann equations**,

$$\begin{aligned} H(t)^2 &:= \left(\frac{\dot{a}}{a}\right)^2 = \frac{\kappa\rho + \Lambda}{3} - \frac{k}{a^2}, \\ \left(\frac{\ddot{a}}{a}\right) &= -\frac{\kappa}{6}(\rho + 3p) + \frac{\Lambda}{3}, \end{aligned} \quad (3.12)$$

where $H(t)$ is called the Hubble parameter. The above system is underdetermined, so we usually impose the so-called **equation of state**

$$p = w\rho, \quad (3.13)$$

where w is not necessarily constant, and depends on the kind of matter being discussed. As mentioned above, for Maxwell or Yang–Mills (radiation) fields the energy-momentum tensor is traceless, which is equivalent to $w = 1/3$.

3.2 Hyperbolic spaces

Having established some general characteristics of maximally symmetric spacetimes, from now on we will discuss specific examples of Riemannian and Lorentzian signatures. The flat examples are simpler, consisting respectively of the Euclidean and the Minkowski spaces, so we will aim on the positively and negatively curved cases. Their Lorentzian versions are respectively the deSitter and the anti-deSitter spaces, and their characterisation is the final objective of this chapter. For both pedagogical and practical reasons, we will however start from the Riemannian version. The practical aspect comes from the Riemannian version being used to foliate the Lorentzian ones, as we will see in the coming sections. The positively curved Riemannian case, the sphere, is again too standard and will be skipped, hence, in this section we will start by discussing the negatively-curved maximally symmetric Riemannian manifold, the hyperbolic space. The two-dimensional version is illustrated in Figure 3.1.

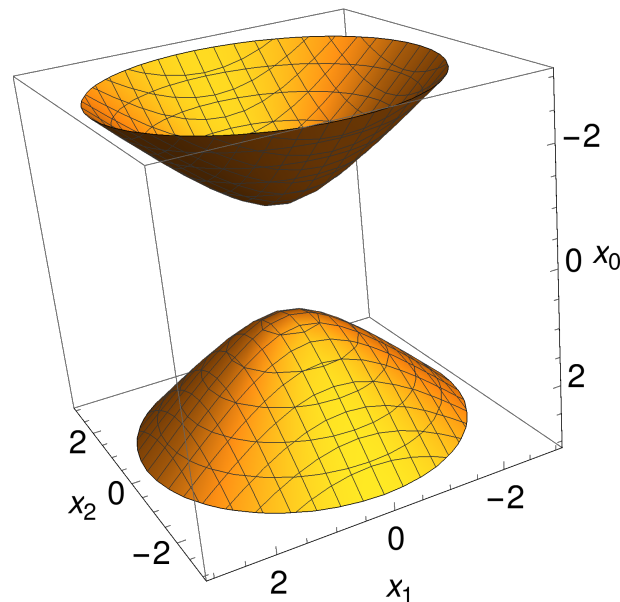


FIGURE 3.1: Illustration of the two sheets of the unit-radius two-dimensional hyperbolic space H^2 embedded in $\mathbb{R}^{1,2}$.

Definition 19. (Hyperbolic space) Consider the Minkowskian spacetime $\mathbb{R}^{1,n}$ with metric

$$ds_{\mathbb{R}^{1,n}} = -dx_0 dx_0 + dx_i dx_i. \quad (3.14)$$

The n -dimensional hyperbolic space H^n is defined as one of the two simply connected components of the two-sheeted hyperboloid determined by

$$-x_0^2 + x_i x_i = -R^2, \quad (3.15)$$

where R here is called the *radius of the hyperbolic space*.

Following the discussion in Section 2.1, the hyperbolic space H^n could equivalently be defined as the coset space $O(1, n)/O(n)$, where $O(1, n)$ are the (hyperbolic or not) rotational isometries of $\mathbb{R}^{1,n}$ acting transitively on each hyperboloid level set (3.15) and $O(n)$ is the stabiliser group of a point on it. Moreover, the hyperbolic space

is a symmetric space with constant negative curvature, and it will be topologically equivalent to \mathbb{R}^n .

To obtain the H^n metric explicitly we can parametrise the hyperboloid with

$$x_0 = \pm R \cosh(r) \quad \text{and} \quad x_i = R w_i \sinh(r), \quad (3.16)$$

where $r \in [0, +\infty)$ will be a radial coordinate in the hyperbolic space, w_i will parametrise the sphere S^{n-1} , and the signal of x_0 only defines which of the two connected components was chosen. As an explicit example, let us take $n = 4$ such that

$$\begin{aligned} w_1 &= \cos(\chi) \\ w_2 &= \sin(\chi) \cos(\theta) \\ w_3 &= \sin(\chi) \sin(\theta) \cos(\phi) \\ w_4 &= \sin(\chi) \sin(\theta) \sin(\phi) \end{aligned} \quad (3.17)$$

parametrise S^3 in terms of angular coordinates (χ, θ, ϕ) , with

$$\chi, \theta \in [0, \pi] \quad \text{and} \quad \phi \in [0, 2\pi). \quad (3.18)$$

In such coordinates, the metric induced on the submanifold by the standard Minkowskian metric on $\mathbb{R}^{1,4}$ reads

$$\begin{aligned} ds_{H^4}^2 &= R^2 [dr^2 + \sinh(r)^2 (d\chi^2 + \sin(\chi)^2 (d\theta^2 + \sin(\theta)^2 d\phi^2))] \\ &= R^2 [dr^2 + \sinh(r)^2 d\Omega_3^2]. \end{aligned} \quad (3.19)$$

Taking $r \mapsto \tilde{r} = \sinh(r)$, we obtain

$$ds_{H^4}^2 = R^2 \left[\frac{d\tilde{r}^2}{1 + \tilde{r}^2} + \tilde{r}^2 d\Omega_3^2 \right], \quad (3.20)$$

evidencing the negative curvature of H^4 (and, with a more general but almost identical procedure, for H^n).

3.3 DeSitter spaces

Now, let us start discussing Lorentzian maximally symmetric spacetimes. In this section, we will begin with the positively curved case (positive cosmological constant), namely the deSitter spacetime, and some of its foliations. The two-dimensional example is illustrated in Figure 3.2. The n -dimensional deSitter space can be defined as follows:

Definition 20. (deSitter spacetime) Consider the Minkowskian spacetime $\mathbb{R}^{1,n}$ with metric

$$ds_{\mathbb{R}^{1,n}} = -dx_0 dx_0 + dx_i dx_i. \quad (3.21)$$

The n -dimensional deSitter spacetime dS_n is defined as the submanifold consisting in the one-sheeted hyperboloid determined by

$$-x_0^2 + x_i x_i = R^2, \quad (3.22)$$

where R here is the *deSitter radius*.

Similarly as for hyperbolic spaces, the deSitter spacetime dS_n could equivalently be defined as the coset space $O(1, n)/O(1, n-1)$, where $O(1, n)$ are the rotational

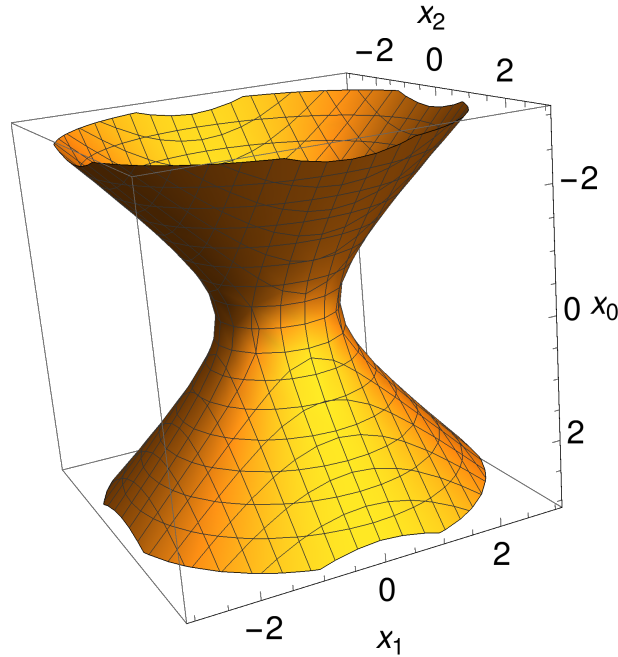


FIGURE 3.2: Illustration of the unit-radius two-dimensional deSitter space dS^2 embedded in $\mathbb{R}^{1,2}$.

isometries of $\mathbb{R}^{1,n}$ acting transitively on each hyperboloid level set (3.22) and $O(1, n - 1)$ is the stabiliser group of a point in it. The deSitter space is a symmetric space and it is topologically equivalent to $\mathbb{R} \times S^{n-1}$.

To obtain the dS_n metric, we can parametrise the hyperboloid as

$$x_0 = R \sinh(t) \quad \text{and} \quad x_i = R w_i \cosh(t), \quad (3.23)$$

where t will be the new timelike coordinate and w_i will parametrise S^{n-1} . To compute an explicit example, let us take $n = 4$. The same $\{w_i\}$ from (3.17) subjected to (3.18) will parametrise the three-sphere S^3 in terms of the angular coordinates (χ, θ, ϕ) . Then, the metric induced by the standard Minkowskian metric on $\mathbb{R}^{1,4}$ reduces to

$$\begin{aligned} ds_{dS_4}^2 &= R^2 \left[-dt^2 + \cosh(t)^2 (d\chi^2 + \sin(\chi)^2 (d\theta^2 + \sin(\theta)^2 d\phi^2)) \right] \\ &= R^2 \left[-dt^2 + \cosh(t)^2 (d\chi^2 + \sin(\chi)^2 d\Omega_2^2) \right]. \end{aligned} \quad (3.24)$$

Taking $\chi \mapsto r = \sin(\chi)$, we go to the usual form of FLRW metrics,

$$ds_{dS_4}^2 = R^2 \left[-dt^2 + \cosh(t)^2 \left(\frac{dr^2}{1-r^2} + r^2 d\Omega_2^2 \right) \right], \quad (3.25)$$

with scale factor $a(t) = \cosh(t)$. The conformal time in this case will be

$$\tau = \int^t \frac{dt'}{\cosh(t')} = 2 \tan^{-1} \left(\tanh \left(\frac{t}{2} \right) \right), \quad (3.26)$$

obeying

$$\tan \left(\frac{\tau}{2} \right) = \tanh \left(\frac{t}{2} \right). \quad (3.27)$$

In terms of the the conformal time, the metric (3.24) reads

$$ds_{dS_4}^2 = R^2 \sec(\tau)^2 [-d\tau^2 + d\chi^2 + \sin(\chi)^2 d\Omega_2^2]. \quad (3.28)$$

These coordinates will be particularly useful ahead since here dS_4 is written as a Lorentzian cylinder over $S^3 \simeq \text{SU}(2)$. Another useful parametrisation is the Euclidean slicing of dS_n by dS_{n-1} , where we can take

$$\begin{aligned} x_0 &= R \sin\left(\frac{\chi}{R}\right) \sinh\left(\frac{t}{R}\right) \cosh \zeta, \\ x_1 &= R \cos\left(\frac{\chi}{R}\right), \\ x_2 &= R \sin\left(\frac{\chi}{R}\right) \cosh\left(\frac{t}{R}\right), \\ x_i &= R w_i \sin\left(\frac{\chi}{R}\right) \sinh\left(\frac{t}{R}\right) \sinh \zeta, \quad \text{for } 3 \leq i \leq n, \end{aligned} \quad (3.29)$$

with w_i parametrising S^{n-3} , χ being the foliation parameter, t being the timelike coordinate, and ζ being the radial coordinate in dS_{n-1} . They respect

$$\chi, \zeta \in [0, +\infty) \quad \text{and} \quad t \in \mathbb{R}. \quad (3.30)$$

With this foliation, the induced metric will be

$$ds_{dS_n}^2 = d\chi^2 + \sin\left(\frac{\chi}{R}\right)^2 ds_{dS_{n-1}}^2, \quad (3.31)$$

with

$$ds_{dS_{n-1}}^2 = -dt^2 + R^2 \sinh\left(\frac{t}{R}\right)^2 dH_{n-2}^2, \quad (3.32)$$

and dH_{n-2}^2 being the same hyperbolic space metric from (3.19), here written as

$$dH_{n-2}^2 = d\zeta^2 + \sinh(\zeta)^2 d\Omega_{n-3}^2. \quad (3.33)$$

3.4 Anti-deSitter spaces

Finally, let us conclude the discussion on the maximally symmetric Lorentzian spacetimes by considering the negatively curved case (negative cosmological constant), namely the anti-deSitter spacetime, and some of its foliations. The two-dimensional example is illustrated in Figure 3.3. The construction in this section will be similar to the previous cases, but in this case we have to fix a timelike direction while still maintaining a Lorentzian manifold. For that reason, we will start from $\mathbb{R}^{2,n-1}$ instead of $\mathbb{R}^{1,n}$:

Definition 21. (anti-deSitter spacetime) Consider the Minkowskian spacetime $\mathbb{R}^{2,n-1}$ with metric

$$ds_{\mathbb{R}^{2,n-1}} = -dx_0 dx_0 + dx_i dx_i - dx_n dx_n. \quad (3.34)$$

The n -dimensional anti-deSitter spacetime AdS_n is defined as the submanifold consisting in the hyperboloid determined by

$$-x_0^2 + x_i x_i - x_n^2 = -R^2, \quad (3.35)$$

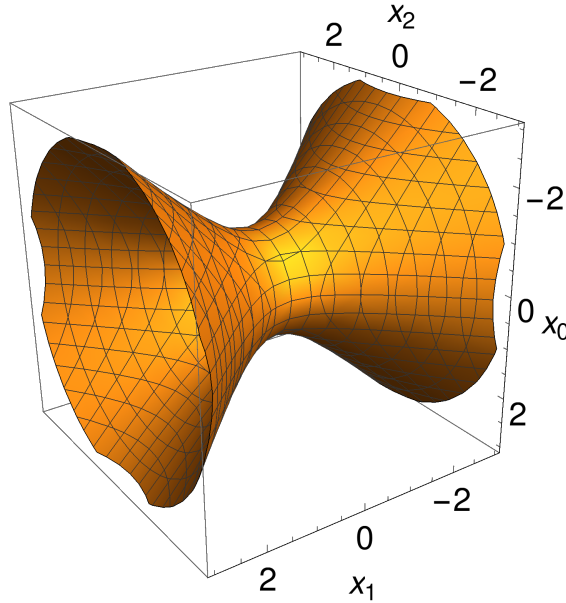


FIGURE 3.3: Illustration of the unit-radius two-dimensional anti-deSitter space AdS^2 embedded in $\mathbb{R}^{2,1}$.

where R here is the *anti-deSitter radius*.

Once again, the anti-deSitter spacetime AdS_n is equivalently defined as the coset space $\text{O}(2, n-1)/\text{O}(1, n-1)$, where $\text{O}(2, n-1)$ are the rotational isometries of $\mathbb{R}^{2, n-1}$ acting transitively on each hyperboloid level set (3.35) and $\text{O}(1, n-1)$ is the stabiliser group of a point in it. The anti-deSitter space is a symmetric space and it is topologically equivalent to $S^1 \times \mathbb{R}^{n-1}$.

To obtain the AdS_n metric explicitly, we can parametrise the hyperboloid as

$$x_0 = R \cos(t) \quad \text{and} \quad x_i = R w_i \sin(t), \quad (3.36)$$

where t is the timelike coordinate and the w_i parametrise the unit-radius hyperbolic space H^3 with

$$\begin{aligned} w_1 &= \sinh(\rho) \cos(\theta) \\ w_2 &= \sinh(\rho) \sin(\theta) \cos(\phi) \\ w_3 &= \sinh(\rho) \sin(\theta) \sin(\phi) \\ w_4 &= \cosh(\rho) \end{aligned} \quad (3.37)$$

in terms of the radial coordinate ρ and the angular coordinates (θ, ϕ) . The coordinates respect

$$t \in [-\pi, +\pi], \quad \rho \in [0, +\infty), \quad \theta \in [0, \pi], \quad \text{and} \quad \phi \in [0, 2\pi). \quad (3.38)$$

Notice that the time coordinate is periodic. In such parametrisation, the metric induced by the standard Minkowskian metric on $\mathbb{R}^{2,3}$ reads

$$\begin{aligned} ds_{\text{AdS}_4}^2 &= R^2 [-dt^2 + \sin^2(t) (d\rho^2 + \sinh(\rho)^2 (d\theta^2 + \sin(\theta)^2 d\phi^2))] \\ &= R^2 [-dt^2 + \sin^2(t) (d\rho^2 + \sinh(\rho)^2 d\Omega_2^2)], \end{aligned} \quad (3.39)$$

which is simply the metric of a Lorentzian cylinder over the hyperbolic space H^3 . Taking $\rho \mapsto r = \sinh(\rho)$, we go to the usual form of FLRW metrics,

$$ds_{\text{AdS}_4}^2 = R^2 \left[-dt^2 + \sin(t)^2 \left(\frac{dr^2}{1+r^2} + r^2 d\Omega_2^2 \right) \right], \quad (3.40)$$

again evidencing the fact that the curvature is negative. The scale factor here is $a(t) = \sin(t)$, so we can compute the conformal time as

$$\tau = \int^t \frac{dt'}{\sin(t')} = \log \left(\tan \left(\frac{t}{2} \right) \right). \quad (3.41)$$

In terms of the conformal time, the metric reads

$$ds_{\text{AdS}_4}^2 = \frac{R^2}{\cosh(\tau)^2} \left[-d\tau^2 + \frac{dr^2}{1+r^2} + r^2 d\Omega_2^2 \right]. \quad (3.42)$$

Now, let us see some other relevant foliations for AdS_4 which are easily adaptable to AdS_n . Take

$$x_0 = R \cosh(\rho) \cos(t), \quad x_n = R \cosh(\rho) \sin(t) \quad \text{and} \quad x_i = R w_i \sinh(\rho), \quad (3.43)$$

where again $\rho \in [0, +\infty)$ is the radial coordinate, $t \in [-\pi, +\pi)$ is the periodic time coordinate, and

$$\begin{aligned} w_1 &= \cos(\theta) \\ w_2 &= \sin(\theta) \cos(\phi) \\ w_3 &= \sin(\theta) \sin(\phi) \end{aligned} \quad (3.44)$$

parametrise the 2-sphere in the usual way. The metric in such coordinates read

$$\begin{aligned} ds_{\text{AdS}_4}^2 &= R^2 [d\rho^2 - \cosh(\rho)^2 dt^2 + \sinh(\rho)^2 (d\theta^2 + \sin(\theta)^2 d\phi^2)] \\ &= R^2 [d\rho^2 - \cosh(\rho)^2 dt^2 + \sinh(\rho)^2 d\Omega_2^2], \end{aligned} \quad (3.45)$$

which shows that, in these coordinates, constant- t slices are also hyperbolic spaces H^3 despite the twist provided by the $\cosh(\rho)^2$ factor. Taking $\rho \mapsto \chi = \tan^{-1}(\sinh(\rho))$, we obtain

$$\begin{aligned} ds_{\text{AdS}_4}^2 &= R^2 \sec(\chi)^2 [-dt^2 + d\chi^2 + \sin(\chi)^2 d\Omega_2^2] \\ &= R^2 \sec(\chi)^2 [-dt^2 + d\Omega_3^2], \end{aligned} \quad (3.46)$$

where $\chi \in [0, \pi/2)$. Since χ only takes values in half the usual interval of $[0, \pi]$, only the upper half of the 3-sphere is being considered. Hence, we see again that AdS_4 is topologically equivalent to $S^1 \times S_+^3$, which in turn is topologically equivalent to $S^1 \times \mathbb{R}^3$.

As in the deSitter case, we can also write the anti-deSitter space AdS_n as an Euclidean cylinder over AdS_{n-1} . For that, let us go back to (3.45) and change coordinates $(\chi, \theta) \mapsto (z, r)$ according to

$$\sinh(z) = \cos(\theta) \sinh(\chi) \quad \text{and} \quad \tanh(r) = \sin(\theta) \tanh(\chi). \quad (3.47)$$

The new coordinates are defined for $z \in \mathbb{R}$ and $r \in \mathbb{R}_+$. In terms of (z, t, r, ϕ) , the metric then reads

$$\begin{aligned} ds_{\text{AdS}_4}^2 &= R^2 [dz^2 + \cosh(z)^2 (-\cosh(r)^2 dt^2 + dr^2 + \sinh(r)^2 d\phi^2)] \\ &= R^2 [dz^2 + \cosh(z)^2 d\Omega_{1,2}^2], \end{aligned} \quad (3.48)$$

where $d\Omega_{1,2}^2$ is the metric on the unit-radius AdS_3 . We can define a conformal foliation parameter Z to get rid of the warping factor $\cosh(z)$. Since the factor is identical to the one in (3.26), we can directly use

$$\tan\left(\frac{Z}{2}\right) = \tanh\left(\frac{z}{2}\right), \quad (3.49)$$

where $Z \in (-\pi/2, +\pi/2)$. Then, the metric reads

$$ds_{\text{AdS}_4}^2 = \frac{R^2}{\cos(Z)^2} [dZ^2 + d\Omega_{1,2}^2]. \quad (3.50)$$

Chapter 4

Fibre Bundles and Gauge Theory

Since its introduction in the seminal paper by Yang and Mills [1], the Yang–Mills theory was greatly developed and shown to be essential for the foundations of Particle Physics. In addition, it also plays important roles in many other areas, such as Condensed Matter physics, Cosmology, and Quantum Gravity. This chapter is a brief review on the classical Yang–Mills theory. Moreover, following the geometrical root of this thesis, we will discuss gauge theory in its more geometrical setting, as a theory for the connection one-form of a principal bundle. For the more pragmatism approach, we refer the reader to [13, 17]. Even in the geometrical setting, we are not aiming on a comprehensive discussion; for that, we refer to [11, 18]. More specifically, in this chapter we introduce fibre bundles, principal bundles, connections in principal bundles, the Yang–Mills field as a local representative of a connection one-form, and, finally, the dynamics of classical Maxwell and Yang–Mills theories.

4.1 Fibre bundles

Before we properly define a fibre bundle, let us briefly recall how the concept of a bundle already appears naturally in the study of differentiable manifolds. In such context, it is clear that it is important to distinguish the tangent space T_pM of each point $p \in M$, even if they are all isomorphic as vector spaces to some \mathbb{F}^n , where \mathbb{F} is a field and n is the dimension of the manifold. Hence, it becomes useful to define the so-called *tangent bundle*

$$TM = \{(p, v) \mid p \in M \text{ and } v \in T_pM\}. \quad (4.1)$$

The notion of a *bundle* is going to generalise this structure. Notice that topologically and geometrically TM is not simply $M \times \mathbb{F}^n$, which is what makes such a notion essential. We now define:

Definition 22. ((Differentiable) Bundle) A **bundle** is a triple $\xi = (E, \pi, M)$, often represented as

$$E \xrightarrow{\pi} M, \quad (4.2)$$

composed of two differentiable manifolds E and M , named respectively **total space** and **base space**, and a smooth surjective projection map $\pi : E \rightarrow M$. The pre-image $\pi^{-1}(p) =: F_p$ of a point $p \in M$ is called the **fiber over p**.

Definition 23. (Fibre bundle) A **fibre bundle** is a bundle (E, π, M) where all fibers F_p are isomorphic, in the adequate sense¹, to the same set F , named the **standard** or

¹for example, for topological bundles, they have to be homeomorphic. For differentiable bundles, they have to be diffeomorphic.

typical fiber. Fibre bundles can also be represented as (E, π, M, F) or as

$$F \rightarrow E \xrightarrow{\pi} M. \quad (4.3)$$

As previously mentioned, the total space E of a bundle (E, π, M, F) is in general topologically not equivalent from the product space $M \times F$. However, for fibre bundles, we can always establish such a relation locally in M , which is a corollary of theorem 22 below, in addition to the fact that every manifold is locally contractible. This relation is established through a *local trivialisation*:

Definition 24. (Local trivialisation) Let $\zeta = (E, \pi, M, F)$ be a fibre bundle. Let $\{U_i\}$ be an open covering of M . A **local trivialisation** of ζ is a map

$$\phi_i : U_i \times F \rightarrow \pi^{-1}(U_i) \quad \text{such that} \quad \pi \circ \phi_i(p, f) = p. \quad (4.4)$$

Fixing p , the map

$$\begin{aligned} \phi_{i,p} : F &\rightarrow \pi^{-1}(p) \\ f &\mapsto \phi_i(p, f) \end{aligned} \quad (4.5)$$

is an isomorphism.

Naturally, we can use relations between charts in M to do the same in E :

Definition 25. (Transition function and structure group) Let (E, π, M, F) be a fibre bundle, U_i and U_j two non-disjoint elements of an open cover of M , and ϕ_i and ϕ_j local trivialisations on them. A **transition function** on a point $p \in U_i \cap U_j$ is a function

$$t_{ij}(p) : F \rightarrow F \quad \text{where} \quad t_{ij}(p) := \phi_{i,p}^{-1} \circ \phi_{j,p}. \quad (4.6)$$

Then, we can relate the two trivialisations via

$$\phi_j(p, f) = \phi_i(p, t_{ij}(p)f). \quad (4.7)$$

If $p \in U_i \cap U_j \cap U_k$, the transition functions satisfy the following consistency conditions:

- (i) $t_{ii}(p) = \text{Id}_F$,
- (ii) $t_{ij}(p) = t_{ji}^{-1}(p)$, and
- (iii) $t_{ij}(p) \cdot t_{jk}(p) = t_{ik}(p)$.

The transition functions of a fibre bundle are then elements of some group G which acts on F from the left and is called the **structure group**. Fibre bundles can also be denoted as (E, π, M, F, G) , where the transition functions in G contain the global information of the non-trivial topology of E . However, we will usually omit G from the tuple. If the standard fiber is not explicitly relevant in the context, we may also omit F .

Definition 26. (Section) Let (E, π, M) be a fibre bundle. A **section** $s : M \rightarrow E$ is a smooth map satisfying

$$\pi \circ s = \text{Id}_M, \quad (4.8)$$

which implies that, $\forall p \in M$, $s(p) \in \pi^{-1}(p)$.

Now let us consider maps between bundles:

Definition 27. ((M-)Morphism on fibre bundles) Let $\xi = (E, \pi, M)$ and $\xi' = (E', \pi', M')$ be fibre bundles. $u : E \rightarrow E'$ is a **fibre-bundle morphism** if it defines an unique function $f : M \rightarrow M'$ such that

$$\pi' \circ u = f \circ \pi, \quad (4.9)$$

that is, the diagram

$$\begin{array}{ccc} E & \xrightarrow{u} & E' \\ \pi \downarrow & & \downarrow \pi' \\ M & \xrightarrow{f} & M' \end{array} \quad (4.10)$$

commutes. If both bundles have the same base space, that is, $M' = M$, we say that u is a **M-morphism**.

Definition 28. (Isomorphism of differential bundles) A differential bundle morphism u is an **isomorphism** if it is a diffeomorphism.

The notion of isomorphism can also be made local:

Definition 29. (Local isomorphism) Two bundles $\xi = (E, \pi, M)$ and $\xi' = (E', \pi', M)$ are **locally isomorphic** if, $\forall p \in M, \exists U \ni p$ such that the restrictions of the bundles to U , $\xi|_U$ and $\xi'|_U$, are U -isomorphic.

Local triviality implies that all fibre bundles (E, π, M, F) are locally isomorphic to $(M \times F, \pi, M, F)$.

Definition 30. (Trivial bundle) A fibre bundle $\xi = (E, \pi, M, F)$ is said be **trivial** if it is M -isomorphic to $(M \times F, \pi, M, F)$.

An alternative definition of a trivial bundle would be a bundle where all transition functions could be taken to be the identity element.

Theorem 22. (Sufficient condition for triviality of fibre bundles) A fibre bundle (E, π, M) is trivial if its base space M is contractible.

4.2 Principal bundles

After establishing the basics of fibre bundles, we can focus on *principal bundles*, the class of bundles in which Yang–Mills theory is properly constructed. Moreover, they are key for many further developments of the theory, for example for the addition of matter fields and their couplings with the gauge fields in the context of *associated bundles*, which we will not cover in this work. Geometrically, a gauge theory with gauge group G is constructed on a fibre bundle where the standard fiber is the group G itself. More precisely, a *principal G -bundle* is defined as:

Definition 31. (Principal G -bundle) Let G be a Lie group and $\xi = (E, \pi, M, F, G)$ be a fibre bundle. ξ is called a **principal G -bundle** when there is an extra action by the right of G on E such that:

- (i) it is a free action, and
- (ii) $\forall p \in M, G$ acts transitively on $\pi^{-1}(p)$.

With those assumptions, the orbit-stabiliser theorem can be evoked to conclude that, $\forall p \in M, F_p$ and G are isomorphic, that is, G can be taken as the standard fiber.

Another trivial consequence is that (E, π, M) and $(E, \pi, E/G)$ are isomorphic as fibre bundles.

The fact that G acts by the right is important such that it commutes with the left action from the transition functions, implying that the principal bundle action is the same regardless of charts. Moreover, one can assume that the structure group of a principal G -bundle is some other group G' , but it is possible to show that there is a correspondence between the two groups, so we will just take them to be the same from the start.

Some examples of principal G -bundles are homogeneous spaces such as

$$\mathrm{SO}(n) \rightarrow \mathrm{SO}(n+1) \rightarrow S^n, \quad (4.11)$$

where S^n is diffeomorphic to $\mathrm{SO}(n+1)/\mathrm{SO}(n)$, or, analogously,

$$\mathrm{SU}(n) \rightarrow \mathrm{SU}(n+1) \rightarrow S^{2n+1}. \quad (4.12)$$

In general, whenever G is a Lie group and H is a closed Lie subgroup,

$$H \rightarrow G \rightarrow G/H \quad (4.13)$$

is a principal H -bundle. Another example is the so-called *frame bundle*, that is, the tuple

$$(B(M), \pi, M, \mathrm{GL}(n, \mathbb{F})) \quad (4.14)$$

where M is the base space, $\pi^{-1}(p) = B_p(M)$ is the set of all frames of $T_p M$, π is the natural projection on p , and the standard fiber is $\mathrm{GL}(n, \mathbb{F})$.

Naturally, morphisms between principal bundles should also respect the right G -action:

Definition 32. (Principal map) A **principal bundle morphism** or **principal map** between two G -bundles (E, π, M) and (E', π', M') is a bundle morphism (u, f) such that $u : E \rightarrow E'$ is G -equivariant, that is,

$$\forall g \in G \text{ and } \forall e \in E, \quad u(eg) = u(e)g. \quad (4.15)$$

The above can be generalised to bundles with different groups G and G' if there is an homomorphism $\Lambda : G \rightarrow G'$. Then, the condition above becomes

$$u(eg) = u(e)\Lambda(g). \quad (4.16)$$

Concepts as trivial principal bundle and local triviality of a principal bundle are the same as before, but now requiring principal maps as morphisms. Furthermore, for principal bundles we can establish a necessary and sufficient condition for triviality:

Theorem 23. (Triviality of principal bundle) A principal bundle is trivial if and only if there is a global section.

Theorem 24. Let $\xi = (E, \pi, M)$ and $\xi' = (E', \pi', M')$ be two principal bundles and (u, f) be a principal map between them. If f is an isomorphism between M and M' , then u is an isomorphism between E and E' and the principal map is a principal bundle isomorphism between ξ and ξ' .

Corollary 25. If there is a principal bundle map (u, Id_M) between $\xi = (E, \pi, M)$ and $\xi' = (E', \pi', M)$, then ξ and ξ' are isomorphic.

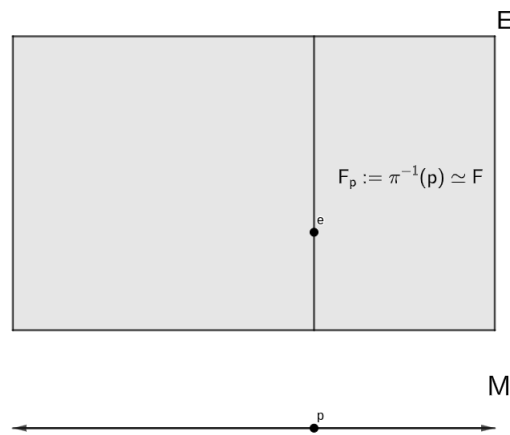


FIGURE 4.1: Fibre bundle (E, π, M, F) with $\pi(e) = p$ illustrating the picture of the fibers $F_p \subset E$ vertically above the points $p \in M$.

From the corollary above, every G -equivariant endomorphism $u : E \rightarrow E$ defines an automorphism (u, Id_M) on (E, π, M, G) . Hence, we can define

$$\text{Aut}(\xi) = \{(u, \text{Id}_M) \mid u \text{ is } G\text{-equivariant}\} \quad (4.17)$$

as the **group of automorphisms of ξ** . This is a particularly important for gauge theory, as $\text{Aut}(\xi)$ will be the group of gauge transformations of a G gauge theory over M .

Before we are able to see how the Yang–Mills field shows up in this setting, we have to define connections on principal bundles, as they are a key ingredient in the discussion.

4.3 Connections on principal bundles

On principal G -bundles, the action of the group G , transitive within each fiber, allows one to connect any two elements of the same fiber. As illustrated in Figure 4.1, if we think of the fibers as located above the corresponding points in the base space, the action of G allows us to move “vertically” in E . However, we do not have a way of relating elements in different fibers, that is, moving “horizontally” in E in such a picture. This is going to be the role of the connection on principal bundles. Before its definition, let us recall the standard connection on manifolds, which we will see that is just a particular example of the connections to be discussed in this chapter.

Let M be a n -dimensional differentiable manifold over the field \mathbb{F} . In the aforementioned picture, the fibers $T_p M$ are “above” each point $p \in M$ and elements of $\text{GL}(n, \mathbb{F})$ allow us to connect different vectors in $T_p M$, inside each fiber, moving “vertically” in E . To be able to connect vectors from different tangent spaces, we define *parallel transport*, which requires a *covariant derivative* coming from a *connection*. In differentiable manifolds, the connection is defined as follows:

Definition 33. (Connection on differential manifold) Let M be a manifold and $V(M)$ the set of smooth vector fields over M . A **connection** D is a map

$$D : V(M) \times V(M) \rightarrow V(M), \quad (4.18)$$

often denoted $D(X, Y) =: D_X Y$, satisfying:

- (i) $D_{X+Y}Z = D_X Z + D_Y Z$,
- (ii) $D_X(Y+Z) = D_X Y + D_X Z$,
- (iii) $D_{fX}Y = fD_X Y$, and
- (iv) $D_X(fY) = X(f)Y + fD_X Y =: (D_X f)Y + f(D_X Y)$.

The connection is then used to define a **covariant derivative**:

Definition 34. (Covariant derivative) Let D be a connection, X, Y be vector fields on M and ω be an one-form on it. The **covariant derivative** DY of Y is defined as the $(1, 1)$ -tensor field such that

$$DY(\omega, X) := \omega(D_X Y). \quad (4.19)$$

In terms of a coordinate basis $\{\partial_\mu\}$, and using the shorthand $D_\mu := D_{\partial_\mu}$, we can decompose the connection as

$$D_\nu \partial_\rho = D(\partial_\nu, \partial_\rho) =: \Gamma_{\nu\rho}^\mu \partial_\mu, \quad (4.20)$$

which defines the components $\Gamma_{\nu\rho}^\mu$ of the connection on this coordinate basis. With it, we can finally define the parallel transport:

Definition 35. (Parallel transport) Let $I \subset \mathbb{R}$ be an interval containing 0, $\gamma : I \rightarrow M$ be a curve in M with $\gamma(0) = p$, and $Y_p \in T_p M$. The **parallel transport** of Y_p along γ is the solution $Y(t)$ of the equation

$$\frac{DY(t)}{dt} = D_{\dot{\gamma}(t)} Y(t) = 0 \Rightarrow \frac{dY^\mu(t)}{dt} + \Gamma_{\nu\rho}^\mu Y^\nu(t) \frac{dx^\rho(t)}{dt} = 0 \quad (4.21)$$

with $Y(0) = Y_p$. Then, $Y(t) \in T_{\gamma(t)} M$.

Definition 36. (Geodesic) A curve is said to be a geodesic if its tangent vector is everywhere parallel along the curve, that is, if

$$D_{\dot{\gamma}} \dot{\gamma} = 0. \quad (4.22)$$

It is clear that, in the picture of the fibers above the base space, the parallel transport is allowing us to “move horizontally”, relating elements of different fibers. Let us see how those concepts are generalised to principal bundles, where they are essential to the definition of a Yang–Mills field. Starting from some preliminar concepts:

Definition 37. (Vertical vector and vertical space in principal bundles) Let (E, π, M, G) be a principal G -bundle. A tangent vector $X \in T_e E$ is called **vertical** if $\pi_* X = 0$. Vertical vectors form a vector subspace $V_e E \subset T_e E$ called **vertical space on e** and defined by

$$V_e E := \ker(\pi_*|_{T_e E}). \quad (4.23)$$

One can show that the structure of vertical spaces $V_e E \subset T_e E$ is given by the Lie algebra \mathfrak{g} of the fiber G :

Theorem 26. Let $\zeta = (E, \pi, M, G)$ be a principal G -bundle. For any point $e \in E$, there exists an one-to-one correspondence f_e between the Lie algebra \mathfrak{g} of G and the vertical space $V_e E$:

$$\begin{aligned} f_e : \mathfrak{g} &\rightarrow V_e E \\ A &\mapsto X_V =: X_e^A \end{aligned} \quad (4.24)$$

Our next goal is to define a horizontal vector space $H_e E \subset T_e E$ respecting

- (i) $T_e E = V_e E \oplus H_e E$,
- (ii) any smooth vector field X in TE is decomposable in two smooth vector fields $X = X_V + X_H$ such that $X_V(e) \in V_e E$ and $X_H(e) \in H_e E$, and
- (iii) If $\tilde{X} \in H_{e_g} E \Rightarrow \exists X \in H_e E$ such that $R_{g*} X = \tilde{X}$.

The third condition means that, to define the horizontal space in a fiber, it suffices to define it in a single point of the fiber, then we can move the horizontal vectors vertically through the pushforward of the right G -action. It is worth noticing that the function

$$\pi_*|_{H_e E} : H_e E \rightarrow T_{\pi(e)} M \quad (4.25)$$

is an isomorphism between the horizontal space in e and the tangent space in $\pi(e)$, since $V_e E$ is the kernel of $\pi_*|_{T_e E}$. We refer to $H_e E$ and $V_e E$ as the collection of horizontal and vertical spaces $H_e E$ and $V_e E$, respectively.

Defining a *connection* for a principal bundle will be equivalent to a smooth choice of $H_e E$ satisfying the three conditions above. A couple of simple examples of connections are the Maurer–Cartan form of G on a trivial bundle $G \rightarrow M \times G \rightarrow M$ and both the Maurer–Cartan forms of G or of H on the coset bundle $H \rightarrow G \rightarrow G/H$. An explicit construction of a connection on a principal bundle uses the so-called **Ehresmann connection**, known simply as the **(Lie algebra-valued) connection one-form**, defined as follows:

Definition 38. (Connection one-form) Let $\xi = (E, \pi, M, G)$ be a principal G -bundle and \mathfrak{g} be the Lie algebra of G . Let $X \in T_e E$ be decomposed as $X = X_V + X_H$ such that $X_V = X_e^A$, according to theorem 26. The (Lie algebra-valued) **connection one-form** in ξ is defined as

$$\omega \in \mathfrak{g} \otimes T^* E, \quad \text{with} \quad \begin{cases} \omega_e : T_e E & \rightarrow \mathfrak{g} \\ X & \mapsto \omega(X) = A \end{cases}. \quad (4.26)$$

We can then employ the connection one-form to simply define the horizontal space on any point $e \in E$ as

$$H_e E := \ker \omega_e. \quad (4.27)$$

It is straightforward to check that such a definition satisfies the requirements for a horizontal space. Moreover, the connection one-form also satisfies

$$\forall e \in E \text{ and } A \in \mathfrak{g}, \quad \omega(X_e^A) = A, \quad (4.28)$$

and

$$\forall X \in T_e E, \quad [R_g^* \omega_{eg}](X) = (\text{AD}_{g^{-1}})_*(\omega_e(X)). \quad (4.29)$$

As for differentiable manifolds, after defining a connection we can define the curvature of the manifold. For that, we first need to define an exterior covariant derivative with such a connection:

Definition 39. (External covariant derivative of forms on a principal bundle) Let (E, π, M, G) be a principal G -bundle with connection one-form ω . Let η be any k -form on E . The **exterior covariant derivative** of η with respect to ω is defined as

$$D\eta := d\eta \circ \text{hor}^{\otimes k+1}, \quad (4.30)$$

where hor is the horizontal projection of tangent vector fields from TE to HE . Explicitly,

$$D\eta(X_1, \dots, X_{k+1}) = d\eta(\text{hor}X_1, \dots, \text{hor}X_{k+1}). \quad (4.31)$$

The exterior covariant derivative can be defined to act on a Lie algebra-valued k -form $\theta \in \mathfrak{g} \otimes \Lambda^k(E)$ according to

$$\theta = A \otimes \eta \Rightarrow D\theta := A \otimes D\eta. \quad (4.32)$$

Definition 40. (Curvature two-form) Let (E, π, M, G) be a principal G -bundle with connection one-form ω . The (Lie algebra-valued) **curvature two-form** G of such a connection is defined as

$$G := D\omega. \quad (4.33)$$

The action of the curvature two-form on two vector fields X, Y on TE is given through

$$G(X, Y) = d\omega(X, Y) + [\omega(X), \omega(Y)], \quad (4.34)$$

where d is the standard exterior derivative bypassing the Lie algebra element, as in (4.32), and $[\cdot, \cdot]$ is the Lie bracket of the two Lie algebra elements resulting after the action of ω . If $\{T_a\}$ is a basis of the Lie algebra with structure constants f_{bc}^a , we can decompose $G = T_a G^a$ and $\omega = T_a \omega^a$ and take the a -component of the action of G , which then reads

$$G^a = d\omega^a + \frac{1}{2} f_{bc}^a \omega^b \wedge \omega^c. \quad (4.35)$$

Moreover, it is immediate to see that the curvature two-form satisfies the Bianchi identity, that is,

$$DG = D^2\omega = 0. \quad (4.36)$$

4.4 Local representatives: Yang–Mills field and field strength

With the connection one-form in hand, in this section we will be able to define the Yang–Mills field as a pullback of the connection one-form to the base space of the principal bundle. Then, we will briefly discuss the field strength and gauge transformations in this context.

It is natural to consider how the connection one-form ω on E can be used to define new structures on M . However, to be able to pull ω back from E to M , we need a section $\sigma : M \rightarrow E$. Unless the principal bundle is trivial, there is no global section, so we have to choose an open set U_i of some open cover of M and work with local sections $\sigma_i : U_i \rightarrow E$. Hence, we define:

Definition 41. (Local representative of the connection one-form) Let (E, π, M, G) be a principal G -bundle with connection one-form ω and $\sigma_i : U_i \rightarrow E$ a local section of the open set $U_i \subset M$. Then, the **local representative** A of the connection one-form is defined as the pullback

$$A^{(i)} := \sigma_i^* \omega, \quad (4.37)$$

where the pullback acts on a Lie-algebra valued k -form by bypassing the Lie algebra element and acting only on the k -form. The local representative is also denoted as **local Yang–Mills field**. When not explicitly needed, the index i will be omitted.

As the horizontal space in a fiber is completely defined by its definition in a single point of it, it is natural to expect that the local representative on $U \subset M$ may be used

to uniquely define a connection one-form on the principal bundle (E', π', U, G) given by the restriction of (E, π, M, G) to U . Indeed,

Theorem 27. Let (E, π, M, G) be a principal G -bundle, \mathfrak{g} be the Lie algebra of G , and $A \in \mathfrak{g} \otimes T^*U$, for $U \subset M$. Then,

$$\exists! \omega \in \mathfrak{g} \otimes T^*(E|_{\pi^{-1}(U)}) \quad \text{such that} \quad \sigma^* \omega = A. \quad (4.38)$$

Indeed, if $E \ni e = \sigma(p)g$, for $g \in G$, ω_e is given in terms of $\omega_{\sigma(p)}$ via

$$\omega_e(X_e) := \text{Ad}_{g^{-1}}(\omega_{\sigma(p)}(R_{g^{-1}*}X_e)). \quad (4.39)$$

As a local section is required to define the local representative from the connection one-form, it is important to establish the connection of local representatives defined from the same connection one-form but with different local sections. This is called a *passive gauge transformation*.

Definition 42. (Passive gauge transformation) Let (E, π, M, G) be a principal G -bundle with $U_1, U_2 \subset M$ such that $U_1 \cap U_2 \neq \emptyset$. Let $\sigma_1 : U_1 \rightarrow M$ and $\sigma_2 : U_2 \rightarrow M$ be two local sections related through $\Omega : U_1 \cap U_2 \rightarrow G$ such that $\sigma_2(p) = \sigma_1(p)\Omega(p)$. The local representatives defined through the two local sections are related via

$$A_p^{(2)}(X) = \text{Ad}_{\Omega(p)^{-1}}[A_p^{(1)}(X)] + (\Omega^*\theta)(X), \quad (4.40)$$

where $X \in T_pM$ and θ is the Maurer-Cartan form of G .

Equation (4.40) acts as a compatibility condition between local representative defined along different non-disjoint open sets of M . Notice that the passive gauge transformation defined above keeps ω fixed. On the other hand, an *active gauge transformation* is associated with a change on the connection one-form ω :

Definition 43. (Active gauge transformation) Let $\xi = (E, \pi, M, G)$ be a principal G -bundle. An **active gauge transformation** is an element (u, Id_M) of $\text{Aut}(\xi)$.

It is straightforward to show that $u^*\omega$ is also a valid connection one-form on E . Now, take a local section $\sigma : U \rightarrow E$ and define the two local representatives

$$A^{(1)} := \sigma^* \omega \quad \text{and} \quad A^{(2)} := \sigma^*(u^* \omega) = (u \circ \sigma)^* \omega \quad (4.41)$$

of the two connection one-forms. Then, let

$$\Omega : U \rightarrow G \quad \text{such that} \quad (u \circ \sigma)(p) = \sigma(p)\Omega(p). \quad (4.42)$$

For $X \in T_pM$, the two local representatives are then related by

$$A_p^{(2)}(X) = \text{Ad}_{\Omega(p)^{-1}}[A_p^{(1)}(X)] + (\Omega^*\theta)(X), \quad (4.43)$$

which is identical to (4.40).

In most cases, and in all cases on this thesis, the gauge group is a matrix Lie group, in which case the relation above simplifies a bit. Taking a coordinate basis $\{\partial_\mu\}$ for M and defining $A_\mu(p) := A_p(\partial_\mu)$, for matrix Lie groups equation (4.43) reduces to

$$A_\mu^{(2)}(p) = \Omega(p)^{-1}A_\mu^{(1)}(p)\Omega(p) + \Omega(p)^{-1}\partial_\mu\Omega(p). \quad (4.44)$$

For completeness, we now define the *group of gauge transformations*:

Definition 44. (Group of gauge transformations) Let $\zeta = (E, \pi, M, G)$ be a principal G -bundle. The **group of gauge transformations** of ζ is defined as

$$\mathcal{G} := \text{Aut}(\zeta). \quad (4.45)$$

Theorem 28. If a principal G -bundle $\zeta = (E, \pi, M, G)$ is a trivial bundle, then

$$\mathcal{G} \simeq G^M, \quad (4.46)$$

that is, the group of gauge transformations is isomorphic to the set of functions from the base space M into the gauge group G .

Notice that the group of gauge transformations is infinite dimensional, which begins to illustrate why fixing the ambiguity carried by A due to gauge transformations of non-abelian gauge theories is in general very hard or even impossible.

Finally, with the Yang–Mills field in hand, we can construct its field strength and discuss how it relates to the curvature two-form G .

Definition 45. (Local representative of the curvature two-form) Let (E, π, M, G) be a principal G -bundle with curvature two-form G and $\sigma_i : U_i \rightarrow E$ a local section of the open set $U_i \subset M$. Then, the **local representative** F of the curvature two-form is defined as the pullback

$$F^{(i)} := \sigma_i^* G. \quad (4.47)$$

We can show that the local representative of the curvature two-form $F^{(i)}$ is simply the field strength associated with the local representative of the connection one-form $A^{(i)}$. Omitting the index i , F can be constructed through

$$F = DA, \quad (4.48)$$

where here D is the exterior covariant derivative with respect to the connection A . Moreover, we can once more decompose the two-form curvature in components F^a regarding the Lie algebra \mathfrak{g} of G with some basis $\{T_a\}$ and structure constants f_{bc}^a . Then the relation between F and A can be opened as

$$F^a = dA^a + \frac{1}{2} f_{bc}^a A^b \wedge A^c. \quad (4.49)$$

As in (4.44), choosing a coordinate basis $\{\partial_\mu\}$ for M , we can further decompose the equation above as

$$F_{\mu\nu}^a = \partial_\mu A_\nu^a - \partial_\nu A_\mu^a + f_{bc}^a A_\mu^b A_\nu^c. \quad (4.50)$$

With the same conventions as in definitions 42 and 43, the expressions for both the passive and the active gauge transformations on F read

$$F_p^{(2)} = \text{Ad}_{\Omega(p)^{-1}} F_p^{(1)}, \quad (4.51)$$

which, for matrix Lie groups, reduce to

$$F_p^{(2)} = \Omega(p)^{-1} F_p^{(1)} \Omega(p). \quad (4.52)$$

Lastly, the Bianchi identity also translates from E to M as

$$DF = D^2 A = 0. \quad (4.53)$$

4.5 Maxwell and Yang–Mills theories

Now that we went through the mathematical background and the construction of the Yang–Mills field and its field strength, we can finally discuss the physics interpretation and its dynamics. The principal G -bundle (E, π, M, G) is a bundle over the spacetime M describing a gauge theory with gauge group G . In case one is also interested in adding matter fields to this description, associated bundles of the adequate representation of G would be constructed from the principal G -bundle. The local representative A of the connection one-form is the Yang–Mills field, a Lie algebra-valued one-form on M that can be decomposed as

$$A = A_\mu^a T_a dx^\mu, \quad (4.54)$$

where $\{T_a\}$ is a basis of the Lie algebra \mathfrak{g} of G and $\{dx^\mu\}$ is a coordinate basis of one-forms on M . Analogously, the local representative F of the curvature two-form, the field strength, is decomposed as

$$F = \frac{1}{2} F_{\mu\nu}^a T_a dx^\mu \wedge dx^\nu. \quad (4.55)$$

In four-dimensional spacetime, we can denote its spacetime components as

$$[F_{\mu\nu}]^a = \begin{pmatrix} 0 & E_1^a & E_2^a & E_3^a \\ -E_1^a & 0 & -B_3^a & B_2^a \\ -E_2^a & B_3^a & 0 & -B_1^a \\ -E_3^a & -B_2^a & B_1^a & 0 \end{pmatrix}, \quad (4.56)$$

where

$$E_i^a := F_{0i}^a \quad (4.57)$$

is called the *colour-electric field* and

$$B_i^a := -\frac{1}{2} \epsilon_{ijk} F_{jk}^a \quad (4.58)$$

is the *colour-magnetic* one.

We will now build a gauge invariant action functional to encode the dynamics of the gauge field on M . For that, we need a functional that depends quadratically on the derivatives $F = DA$ of the gauge field. Moreover, we need to generate a volume form to be integrated over while, in the Lie algebra side, also maintaining gauge invariance. For the forms, we will take the standard inner product of differential forms:

Definition 46. (Inner product of differential forms) Let M be a (pseudo-)Riemannian manifold M and let $*$ be the Hodge star operator in terms of its metric. The **inner product** $\langle \cdot, \cdot \rangle$ of two k -forms ω and η , for all natural $k \leq \dim(M)$, is defined by

$$\langle \omega, \eta \rangle := \int_M \omega \wedge * \eta. \quad (4.59)$$

Due to the form (4.51) of gauge transformations on F , it is clear that, to ensure gauge invariance, one only needs to choose an Ad-invariant inner product $\langle \cdot, \cdot \rangle_{\mathfrak{g}}$ on

the Lie algebra \mathfrak{g} . With it, we can extend the inner product on (4.59) to Lie algebra-valued forms $\omega = T_a \omega^a$ and $\eta = T_b \eta^b$ through

$$\langle \omega, \eta \rangle := \langle T_a, T_b \rangle_{\mathfrak{g}} \langle \omega^a, \eta^b \rangle, \quad (4.60)$$

where $\{T_a\}$ is a basis of \mathfrak{g} . In principle, any Ad-invariant inner product on \mathfrak{g} could be chosen to construct a mathematical gauge theory. In order to match the physical theories, the Killing form from Definition 9 will be used. With that, we can finally define:

Definition 47. (Yang–Mills action functional) Let M be a (pseudo-)Riemannian manifold. Let A be the Yang–Mills field of a G gauge theory, where \mathfrak{g} is the Lie algebra of G with basis $\{T_a\}$ and Killing form K . Let F be the field strength corresponding to A . The (gauge-invariant) **Yang–Mills action functional** of such a theory is defined as

$$S_{\text{YM}}[A] := -\frac{1}{4} \langle F, F \rangle = -\frac{1}{4} \langle T_a, T_b \rangle_K \int_M F^a \wedge *F^b, \quad (4.61)$$

which is often expressed as

$$S_{\text{YM}}[A] = -\frac{1}{4} \int_M \text{tr}(F \wedge *F). \quad (4.62)$$

The factor of $-1/4$ is just a useful convention for physics and will be discussed below.

It is important to notice that, as discussed in Section 2.2, the definiteness of the Killing form is only guaranteed if the Lie group is compact, in which case it is negative semidefinite. Then, the overall minus sign in (4.61) makes the action bounded from below instead of from above. If the Lie group is non-compact, it becomes harder (but not impossible) to interpret such theories as being physically relevant, as we will mention in Chapter 6.

Extremising the Yang–Mills action functional (4.61), one obtains the **Yang–Mills equation**

$$*D *F = 0, \quad (4.63)$$

which can be decomposed in a system of coupled second-order non-linear partial differential equations. However, such a system is underdetermined, which is to be expected since Yang–Mills fields are only determined up to gauge transformations. To deal with this redundancy, we impose a **gauge fixing** condition, which is an extra condition on A to (partially or completely) restrict the gauge field on each point of M to some representative of the gauge orbit respecting such a condition. How to completely and adequately gauge fix a non-abelian gauge theory is still an open problem, but this discussion is out of the scope of this work.

The Maxwell theory is a particular case of the Yang–Mills theory where the gauge group is $U(1)$, which is abelian. In this case, the Lie algebra is trivial and the covariant derivative simplifies, such that

$$F = dA. \quad (4.64)$$

The Bianchi identity in this case is simply $dF = d^2A = 0$. In four-dimensional Minkowski spacetime, it can be decomposed in terms of components of F as

$$\nabla \cdot \vec{B} = 0 \quad \text{and} \quad \nabla \times \vec{E} = -\frac{\partial \vec{E}}{\partial t}, \quad (4.65)$$

two of the four Maxwell's equations, which are then simply geometric, non-dynamical. The Yang–Mills action reduces to the Maxwell action, namely

$$S_{\text{Maxwell}}[A] = \int_M d^4x \frac{1}{2}(\vec{E}^2 - \vec{B}^2), \quad (4.66)$$

and the Yang–Mills equation reduces to

$$\nabla \cdot \vec{E} = 0 \quad \text{and} \quad \nabla \times \vec{B} = \frac{\partial \vec{E}}{\partial t}, \quad (4.67)$$

the remaining two Maxwell's equations which encode the dynamics of the theory. Here we can see a justification for the factor of $1/4$ in (4.61), such that the abelian case of the Yang–Mills action matches the Maxwell action.

To finalise this section, let us briefly mention two special aspects of gauge theories in four-dimensional spacetimes. The first one is an extra spacetime symmetry that is automatically fulfilled, namely:

Theorem 29. Vacuum Yang–Mills theories on a four-dimensional (pseudo-)Riemannian manifold M with metric g are conformally invariant. That is, the Yang–Mills action S_{YM} becomes invariant under a conformal change of the metric, namely,

$$g \mapsto g' = e^{2\lambda(x)}g, \quad (4.68)$$

for any smooth scalar function λ on M .

The second aspect only applies to Riemannian manifolds, in which we define:

Definition 48. (Instanton solutions of Yang–Mills theories) Let M be a four-dimensional Riemannian manifold. Then, Yang–Mills fields A for which the curvature F satisfies

$$*F = \pm F \quad (4.69)$$

are called **self-** or **anti-self-dual** Yang–Mills fields, respectively. In these cases, the Bianchi identity implies that the Yang–Mills equation is automatically satisfied. Such fields are **instanton solutions** of the Yang–Mills theory.

4.6 Spacetime symmetries of Yang–Mills fields

Lastly, it will be important for us to consider how do spacetime symmetries manifest in Yang–Mills theories. Even though we construct non-trivial gauge theories with more restrictive symmetry requirements in the results on the following chapters, it is important to consider a (brief and non-comprehensive) historical review of the subject in more generality. Such a discussion dates back to the 1970s, when, e.g., Romanov *et al* [19] and Jackiw [20] considered, in particular cases, gauge fields symmetric with respect to a specific spacetime transformation group when the transformation induced on the gauge field by such group could be compensated by a gauge transformation. Bergmann and Flaherty then generalised such discussion for a generic infinitesimal generator of a spacetime transformation [21], which was later expanded by Forgács and Manton to consider a spacetime symmetry group with more generators ζ_m and then further investigate the consequences [22]. In 1980, Harnad *et al* considered finite spacetime symmetries and showed that such symmetric gauge fields are invariant connections [23]. Later, Molelekoa showed that invariant

connections may be too restrictive for the definition of a symmetric Yang–Mills field, further generalising it and showing when the two definitions are equivalent [24].

In what follows, we will first recall the treatment of a symmetric Yang–Mills fields by Forgacs and Manton [22], which works on the level of the local representative. Hence, we will advance to the generalisation by Molelekoa [24], adequately considering lifts of the action of the spacetime transformation group on the principal bundle. Let us begin by considering spacetime transformation groups as symmetries of general tensors.

Definition 49. (Spacetime symmetries of tensors) Let M be a manifold and H a group of spacetime diffeomorphisms. A tensor $T \in TM^{\otimes p} \otimes T^*M^{\otimes q}$ of rank (p, q) is said to be symmetric with respect to H if

$$\mathcal{L}_\zeta T = 0, \quad (4.70)$$

where $\zeta \in TM$ is any generator of H and $\mathcal{L}_\zeta T$ is the Lie derivative of T with respect to ζ .

However, for the gauge field, the condition $\mathcal{L}_\zeta A_\mu = 0$ may be too restrictive. For gauge theories, it is enough that any change in the local representative induced by the group of spacetime transformations can be compensated by a gauge transformation. It is straightforward to show that this is equivalent to the Lie derivative of the gauge field A along ζ being proportional to the (gauge) covariant derivative of an element $W := W^a T_a$ of the Lie algebra. Therefore, we define:

Definition 50. (Spacetime symmetries of gauge fields acc. [22]) Let (E, π, M, G) be a principal G -bundle and A be a local representative (Yang–Mills field) of the connection one-form ω in a neighbourhood $U \subset M$. Let $\{\zeta_m\} \in TU$ be a set of infinitesimal generators of a group of spacetime diffeomorphisms H with $\dim(H) = \bar{d}$. The gauge field A is said to be **symmetric with respect to H** if

$$\mathcal{L}_{\zeta_m} A = DW_m, \quad \forall m \in \{1, \dots, \bar{d}\}, \quad (4.71)$$

where the W_m are Lie algebra-valued spacetime scalars that locally transform under a gauge transformation $g \in G^U$ as

$$W_m^{(g)} = g^{-1} W_m g + g^{-1} (\mathcal{L}_\zeta g). \quad (4.72)$$

For any ζ linear combination of the $\{\zeta_m\}$, let W be the same linear combination of the $\{W_m\}$, then equation (4.71) implies that the field strength F transforms according to

$$\mathcal{L}_\zeta F = -[F, W]. \quad (4.73)$$

It is straightforward to show that such a shift preserves the inner product from (4.60) for any inner product on \mathfrak{g} , and, in particular, preserves the Yang–Mills action.

Even though definition 50 is enough for a range of applications, Molelekoa showed that it may be too restrictive in some scenarios [24]. In particular, he also considered the case of a Yang–Mills field in $M = \mathbb{R}^n$, where it is expected that imposing translational symmetry with respect to all directions would imply that there exists a gauge choice in which F is constant; however, the use of (4.71) implies that $F = 0$. He instead proposes another definition which he shows reproduces a constant field strength in such a scenario. This property is denoted as *homogeneity with respect to H* and is defined as:

Definition 51. (Homogeneity of a gauge field acc. [24]) Let (E, π, M, G) be a principal G -bundle and H a Lie group acting smoothly on M such that each element $h \in H$ can be seen as a diffeomorphism of M . Let ω be the connection one-form giving rise to the Yang–Mills field A in M . The gauge field is said to be **homogeneous with respect to H** if the action of H on M lifts to a map

$$L : H \times E \rightarrow E \quad (4.74)$$

such that, $\forall h \in H$, $L(h, \cdot) : E \rightarrow E$ defines an automorphism of E covering h and satisfying

$$L(h, \cdot)^* \omega = \omega. \quad (4.75)$$

Further developments followed, both in the theoretical aspects (e.g. [25–27]) and in applications of such concepts in related areas, such as in Cosmology. One family of examples of the latter is in obtaining analytical solutions of the coupled Einstein–Yang–Mills system for highly symmetric gauge fields in Friedmann universes [26, 28], which is related to some of the results to be discussed in the following chapters.

Chapter 5

The abelian case: electromagnetic knots

In this chapter, we are going to discuss the construction and properties of a set of finite-action rational functions on the Minkowski coordinates which solve the Maxwell equations, the well-known electromagnetic knots. In the original reference [29], the deSitter space dS_4 not only motivated, but was used in the construction steps. For this reason, the procedure was labelled *the deSitter method*. However, in this chapter, we will directly construct a conformal map between a Lorentzian cylinder over S^3 and the Minkowski space. Furthermore, we will not discuss non-abelian gauge theories in this chapter and we will just use the Maxwell equations.

Electromagnetic knots were first discovered in their simplest form in [30]. Since then, numerous generalisations and construction methods were developed and investigated, from theoretical aspects to possible experimental applications. For a review, see [31]. In this chapter, we will review the construction method developed in [29]. We will start from the hyperspherical harmonics and their use on this procedure; then, we will construct the conformal map to Minkowski and use the conformal invariance of the Maxwell theory in four dimensions to pull the electromagnetic fields back to it; having the complete theories both on the cylinder and on the Minkowski space, we can discuss some of their properties, both to allow for a better understanding of the fields and to provide a more straightforward route of comparison with knotted electromagnetic fields from other construction methods [32]; finally, we will discuss how charged particles behave under the influence of such background fields [33], which is key for experimental applications.

5.1 Hyperspherical harmonics and electromagnetic fields on $\mathcal{I} \times S^3$

Consider a finite Lorentzian cylinder over the three-sphere, $\mathcal{I} \times S^3$, with $\tau \in (-\frac{\pi}{2}, \frac{\pi}{2}) =: \mathcal{I}$ and metric

$$ds_{\text{cyl}}^2 = -d\tau^2 + d\Omega_3^2, \quad (5.1)$$

which, up to the conformal factor of $R^2 \sec(\tau)^2$, is equivalent to the metric (3.28) on dS_4 . The three-sphere $S^3 \hookrightarrow \mathbb{R}^4$ is parametrised by $\omega := (\omega_1, \omega_2, \omega_3, \omega_4) \in \mathbb{R}^4$ subjected to $\omega_i \omega_i = 1$. As in (3.24), these coordinates can also be written in terms of three angular coordinates (χ, θ, ϕ) as

$$\omega_a = \sin \chi \hat{\omega}_a, \quad a \in \{1, 2, 3\}, \quad \text{and} \quad \omega_4 = \cos \chi, \quad (5.2)$$

where

$$\begin{cases} \hat{\omega}_1 = \sin \theta \cos \phi \\ \hat{\omega}_2 = \sin \theta \sin \phi \\ \hat{\omega}_3 = \cos \theta \end{cases} . \quad (5.3)$$

After we map $\mathcal{I} \times S^3$ to the Minkowski space $\mathbb{R}^{1,3}$, the $\hat{\omega}_a$ will also parametrise the two-sphere $S^2 \hookrightarrow \mathbb{R}^3$, the spatial hypersurfaces consisting of temporal slices of $\mathbb{R}^{1,3}$.

In this section, we will use the hyperspherical harmonics and explore the fact that S^3 is the group manifold of $SU(2)$ to solve Maxwell's equations more easily in $\mathcal{I} \times S^3$. Let us begin by expliciting the diffeomorphism

$$\begin{aligned} g : S^3 &\rightarrow SU(2) \\ \omega &\mapsto -i \begin{pmatrix} \beta & \alpha^* \\ \alpha & -\beta^* \end{pmatrix}, \end{aligned} \quad (5.4)$$

where

$$\alpha := \omega_1 + i\omega_2 \quad \text{and} \quad \beta := \omega_3 + i\omega_4. \quad (5.5)$$

Here, the north pole $(0,0,0,1)$ of $S^3 \hookrightarrow \mathbb{R}^4$ is mapped into the identity 1_2 of $SU(2)$. With this parametrisation, we can compute the Maurer–Cartan one-form θ explicitly in terms of ω , using the discussion from Section 2.4. Taking $T_a = -i\sigma_a$ as the $\mathfrak{su}(2)$ generators, with σ_a being the Pauli matrices, we have, for $g \in SU(2)$,

$$\Omega_g := g^{-1}dg = e^a T_a, \quad (5.6)$$

where e^a are the left-invariant one-forms on $SU(2)$. Using the so-called self-dual 't Hooft symbol η^a_{ij} constructed from the identity and the Levi-Civita symbol according to

$$\eta^a_{bc} = \epsilon_{abc} \quad \text{and} \quad \eta^a_{i4} = -\eta^a_{4i} = \delta^a_i, \quad (5.7)$$

for $a \in \{1,2,3\}$ and $i,j \in \{1,2,3,4\}$, we can express the elements e^a of the coframe in terms of ω in a more compact form, through

$$e^a = -\eta^a_{ij} \omega_i d\omega_j. \quad (5.8)$$

We will make use of the fact that they (locally) diagonalise the metric,

$$d\Omega_3^2 = \delta_{ab} e^a e^b. \quad (5.9)$$

The dual of the e^a , the left-invariant vector fields L_a , are also expressed in terms of ω using the 't Hooft symbol, as

$$L_a = -\eta^a_{ij} \omega_i \frac{\partial}{\partial \omega_j}, \quad (5.10)$$

or, directly in terms of the angular coordinates (χ, θ, ϕ) , as

$$\begin{aligned} L_1 &= \sin \theta \cos \phi \partial_\chi + (\cot \chi \cos \theta \cos \phi + \sin \phi) \partial_\theta - (\cot \chi \csc \theta \sin \phi - \cot \theta \cos \phi) \partial_\phi, \\ L_2 &= \sin \theta \sin \phi \partial_\chi + (\cot \chi \cos \theta \sin \phi - \cos \phi) \partial_\theta + (\cot \chi \csc \theta \cos \phi + \cot \theta \sin \phi) \partial_\phi, \\ L_3 &= \cos \theta \partial_\chi - \cot \chi \sin \theta \partial_\theta - \partial_\phi. \end{aligned} \quad (5.11)$$

It is straightforward to check that they obey the $\mathfrak{su}(2)$ commutation relation

$$[L_a, L_b] = 2\epsilon_{abc}L_c, \quad (5.12)$$

as expected. Hence, the differential of any function f on $\mathcal{I} \times S^3$ can be written as

$$df = \partial_\tau f d\tau + e^a L_a f. \quad (5.13)$$

Similarly, from the anti-self-dual 't Hooft symbol $\tilde{\eta}^a_{ij}$ with components

$$\tilde{\eta}^a_{bc} = \epsilon_{abc} \quad \text{and} \quad \tilde{\eta}^a_{i4} = -\tilde{\eta}^a_{4i} = -\delta_i^a, \quad (5.14)$$

we obtain the right-invariant vector fields R_a through

$$R_a = -\tilde{\eta}^a_{ij}\omega_i \frac{\partial}{\partial\omega_j}, \quad (5.15)$$

which also obey the $\mathfrak{su}(2)$ commutation relation shown in (5.12) and which commute with any of the L_a . Moreover, for the Minkowski space discussion coming on next sections, it will be important to consider the set $\{\mathcal{D}_a\}$ defined as

$$\mathcal{D}_a := L_a + R_a = -2\epsilon_{abc}\omega_b \frac{\partial}{\partial\omega_c}, \quad (5.16)$$

which trivially obey the same commutation relation as L_a and R_a and generate the stability subgroup $\text{SO}(3)$ of the two-sphere S^2 from (5.3).

We now have the key ingredients to build the hyperspherical harmonics on S^3 . For more detailed discussions on such functions and their properties, we refer the reader to [34, 35]. The space of functions on S^3 can be decomposed into irreducible representations of the $\mathfrak{so}(4) = \mathfrak{su}(2)_L \times \mathfrak{su}(2)_R$ algebra generated by the L_a and the R_a . Defining the “left- and right-angular momentum operators” as

$$I_a := \frac{i}{2}L_a \quad \text{and} \quad J_a := \frac{i}{2}R_a, \quad (5.17)$$

we can express the Laplacian operator Δ_3 on S^3 as

$$\Delta_3 = I^2 = J^2, \quad (5.18)$$

where $I^2 := I_a I_a$ and $J^2 = J_a J_a$. The eigenvalues of Δ_3 are of the form $j(j+1)$, where j is a non-negative half-integer, that is, $j \in \{0, \frac{1}{2}, 1, \frac{3}{2}, \dots\}$. For any such j , the hyperspherical harmonics can be fixed by the eigenvalues of, say, I_3 and J_3 . Summarising, functions from S^3 to \mathbb{C} can be decomposed in terms of the orthonormal basis

$$\{Y_{j;m,n}(\omega)\}, \quad \text{where} \quad 2j \in \mathbb{N} \quad \text{and} \quad m, n \in \{-j, -j+1, \dots, +j\}, \quad (5.19)$$

such that

$$\begin{aligned} I_3 Y_{j;m,n} &= m Y_{j;m,n}, & J_3 Y_{j;m,n} &= n Y_{j;m,n}, \\ \text{and} \quad I^2 Y_{j;m,n} &= J^2 Y_{j;m,n} = j(j+1) Y_{j;m,n}. \end{aligned} \quad (5.20)$$

The orthonormality condition reads, explicitly,

$$\int d^3\Omega_3 Y_{j';m',n'}^* Y_{j;m,n} = \delta_{jj'} \delta_{mm'} \delta_{nn'}, \quad (5.21)$$

where $d^3\Omega_3 = \sin(\chi)^2 \sin(\theta) d\chi d\theta d\phi$ on the angular (χ, θ, ϕ) coordinates.

As on the treatment of the standard spherical harmonics, we can employ the $\mathfrak{su}(2)$ structure to algorithmically construct the hyperspherical harmonics. Let us define the left- and right-ladder operators

$$I_{\pm} := \frac{I_1 \pm iI_2}{\sqrt{2}} \quad \text{and} \quad J_{\pm} := \frac{J_1 \pm iJ_2}{\sqrt{2}}. \quad (5.22)$$

Using the Laplacian operator, the normalisation condition on $Y_{j,m,n}$, and the $\mathfrak{su}(2)$ commutation relations, it is easy to show that they act on the harmonics according to

$$\begin{aligned} (I_{\pm}) Y_{j;m\mp 1,n} &= \sqrt{\frac{(j \pm m)(j \mp m + 1)}{2}} Y_{j;m,n} \\ (J_{\pm}) Y_{j;m,n\mp 1} &= \sqrt{\frac{(j \pm n)(j \mp n + 1)}{2}} Y_{j;m,n} \end{aligned} \quad (5.23)$$

The ladder operators I_a and J_a can be explicitly expressed in a more compact form in terms of the complex (α, β) coordinates from (5.5) as

$$\begin{aligned} I_+ &= \frac{\bar{\beta}\partial_{\bar{\alpha}} - \alpha\partial_{\beta}}{\sqrt{2}}, & J_+ &= \frac{\beta\partial_{\bar{\alpha}} - \alpha\partial_{\bar{\beta}}}{\sqrt{2}}, \\ I_- &= \frac{\bar{\alpha}\partial_{\bar{\beta}} - \beta\partial_{\alpha}}{\sqrt{2}}, & J_- &= \frac{\bar{\alpha}\partial_{\beta} - \bar{\beta}\partial_{\alpha}}{\sqrt{2}}, \\ I_3 &= \frac{\alpha\partial_{\alpha} + \bar{\beta}\partial_{\bar{\beta}} - \bar{\alpha}\partial_{\bar{\alpha}} - \beta\partial_{\beta}}{2}, & J_3 &= \frac{\alpha\partial_{\alpha} + \beta\partial_{\beta} - \bar{\alpha}\partial_{\bar{\alpha}} - \bar{\beta}\partial_{\bar{\beta}}}{2}, \end{aligned} \quad (5.24)$$

Then, a closed expression to compute $Y_{j,m,n}$ in such a parametrisation reads

$$Y_{j,m,n} = \sqrt{\frac{2j+1}{2\pi^2}} \sqrt{\frac{2^{j-m}(j+m)!}{(2j)!(j-m)!}} \sqrt{\frac{2^{j-n}(j+n)!}{(2j)!(j-n)!}} (I_-)^{j-m} (J_-)^{j-n} \alpha^{2j}. \quad (5.25)$$

The use of the hyperspherical harmonics allows us to encode all of the ω dependency into the orthonormal basis elements $Y_{j,m,n}$, that is, any function $f(\tau, \omega)$ on $\mathcal{I} \times S^3$ can be decomposed as

$$f(\tau, \omega) = f^{j;m,n}(\tau) Y_{j,m,n}(\omega), \quad (5.26)$$

where the sum over all valid j , m , and n is implicit. Notice that f does not need to be a scalar. If f is, for example, a (r, s) -tensor, so will be the components $f^{j;m,n}$. In particular, we will work with the Maxwell gauge potential

$$\mathcal{A} = X_{\tau}(\tau, \omega) e^{\tau} + X_a(\tau, \omega) e^a, \quad (5.27)$$

where $e^{\tau} := d\tau$. In the non-Abelian case, the X_a components of \mathcal{A} would carry the explicit Lie algebra dependency. However, in the Maxwell theory, the Lie algebra is trivial and the X_a can be considered scalar functions. Moreover, as we are working with vacuum theories, we can take both the temporal and the Coulomb gauges simultaneously, reading

$$X_{\tau} = 0 \quad \text{and} \quad J_a X_a = 0. \quad (5.28)$$

Hence, the Maxwell equations reduce to

$$-\frac{1}{4}\partial_\tau^2 X_a = (J^2 + 1)X_a + i\epsilon_{abc}J_b X_c. \quad (5.29)$$

With the use of (J_+, J_-) instead of (J_1, J_2) , it is convenient to define and work with

$$X_+ = \frac{X_1 + iX_2}{\sqrt{2}} \quad \text{and} \quad X_- = \frac{X_1 - iX_2}{\sqrt{2}}. \quad (5.30)$$

In terms of (X_+, X_-, X_3) , the Coulomb gauge condition becomes

$$J_+ X_- + J_- X_+ + J_3 X_3 = 0 \quad (5.31)$$

and the Maxwell equations read, for X_\pm ,

$$-\frac{1}{4}\partial_\tau^2 X_\pm = (J^2 \mp J_3 + 1)X_\pm + J_\pm X_3 \quad (5.32)$$

and, for X_3 ,

$$-\frac{1}{4}\partial_\tau^2 X_3 = (J^2 + 1)X_3 + J_+ X_- + J_- X_+. \quad (5.33)$$

Let us now factorise the ω dependence from the X components through

$$X_a(\tau, \omega) = X_a^{j;m,n}(\tau) Y_{j;m,n}(\omega) \quad (5.34)$$

such that the J operators only act on the harmonics. From (5.23), notice that the linear equations (5.31), (5.32), and (5.33) are diagonal in the quantum numbers j and m , such that they can be kept fixed while solving the system. Moreover, since the same ladder operator only acts once in each factor, the equations will only couple triplets $(X_+^{j;m,n+1}, X_-^{j;m,n-1}, X_3^{j;m,n})$, which implies that $X_\pm \propto J_\pm X_3$. After such considerations and exploring the orthonormality of the harmonics, we straightforwardly obtain that there are two types of solutions, both harmonic oscillator-like in terms of τ , with frequencies

$$\Omega_I^{j;m,n} = \pm 2(j+1) \quad \text{or} \quad \Omega_{II}^{j;m,n} = \pm 2j \quad (5.35)$$

and explicit expressions given by:

- type-I: $j \geq 0, \quad -j \leq m \leq j, \quad -j-1 \leq n \leq j+1,$

$$\begin{aligned} X_+ &= \sqrt{(j-n)(j-n+1)/2} e^{\pm 2i(j+1)\tau} Y_{j;m,n+1}(\omega), \\ X_3 &= \sqrt{(j+1)^2 - n^2} e^{\pm 2i(j+1)\tau} Y_{j;m,n}(\omega), \\ X_- &= -\sqrt{(j+n)(j+n+1)/2} e^{\pm 2i(j+1)\tau} Y_{j;m,n-1}(\omega), \end{aligned} \quad (5.36)$$

- type-II: $j > 0, \quad -j \leq m \leq j, \quad -j+1 \leq n \leq j-1,$

$$\begin{aligned} X_+ &= -\sqrt{(j+n)(j+n+1)/2} e^{\pm 2ij\tau} Y_{j;m,n+1}(\omega), \\ X_3 &= \sqrt{j^2 - n^2} e^{\pm 2i(j+1)\tau} Y_{j;m,n}(\omega), \\ X_- &= \sqrt{(j-n)(j-n+1)/2} e^{\pm 2ij\tau} Y_{j;m,n-1}(\omega). \end{aligned} \quad (5.37)$$

For simplicity, $Y_{j;m,n}$ is defined to be equal to zero when n lies outside the interval $[-j, j]$. In the rest of the text, we will restrict our discussion to type-I solutions since they can give rise to the type-II solutions through a parity transformation between the two $\mathfrak{su}(2)$ subalgebras [29]. For any choice of triple (j, m, n) , we refer to the corresponding type-I solution components as $X_a^{j;m,n}(\tau, \omega)$. Factoring out the τ dependence, we define

$$Z_a^{j;m,n}(\omega) := X_a^{j;m,n}(0, \omega) \quad \text{such that} \quad X_a^{j;m,n} = Z_a^{j;m,n} e^{\pm i\Omega_j \tau}. \quad (5.38)$$

As the Maxwell theory is linear, we will use a slight abuse of notation and define “spin- j solutions” as any linear combination of solutions labeled by (j, m, n) with the same j . Take

$$Z_a^j(\omega) := \sum_{m=-j}^j \sum_{n=-j-1}^{j+1} \Lambda_{j;m,n} Z_a^{j;m,n}(\omega), \quad (5.39)$$

for any set of complex coefficients $\Lambda_{j;m,n}$. Then,

$$\mathcal{A}^{(j)} = Z_a^j(\omega) e^{\pm i\Omega_j \tau} e^a \quad (5.40)$$

is a spin- j solution. Finally, with the gauge potential fully solved, we can construct the corresponding field strengths \mathcal{F} of the Maxwell solutions on the cylinder $\mathcal{I} \times S^3$ by taking the exterior derivative of \mathcal{A} . The exterior derivative of the left-invariant one-forms are obtained directly from the Maurer–Cartan equation,

$$de^a + \epsilon_{abc} e^b \wedge e^c = 0, \quad (5.41)$$

where we already substituted the structure constants $f_{bc}^a = 2\epsilon_{abc}$ of $\mathfrak{su}(2)$. The electric and magnetic fields are extracted from

$$\mathcal{F} = \frac{1}{2} \mathcal{F}_{AB} e^A \wedge e^B = d\mathcal{A} = \mathcal{E}_a e^a \wedge e^\tau + \frac{1}{2} \mathcal{B}_a \epsilon_{abc} e^b \wedge e^c, \quad (5.42)$$

where $A, B \in \{\tau, 1, 2, 3\}$. For spin- j solutions, the electric and magnetic fields on the cylinder are simply given by

$$\mathcal{E}_a^{(j)} = -\partial_\tau \mathcal{A}_a^{(j)} \quad \text{and} \quad \mathcal{B}_a^{(j)} = -\Omega_j \mathcal{A}_a^{(j)}. \quad (5.43)$$

5.2 Map to Minkowski

In the previous section, we used the hyperspherical harmonics on S^3 to derive a basis of solutions for the gauge potential and the electromagnetic fields of the vacuum Maxwell theory on a Lorentzian cylinder over the three-sphere. As previously discussed, due to the compactedness of the cylinder, such solutions have finite energy and action. We can now explore the conformal invariance of the Maxwell theory on four-dimensional spacetimes to conformally map such solutions back to $\mathbb{R}^{1,3}$, which will result in a basis of finite-energy and finite-action electromagnetic knots on the Minkowski spacetime. In the rest of this chapter, we will focus on the solutions’ properties that are relevant for the analyses in [32, 33]. For other discussions, we refer the reader to [36].

In this section, we will use both the polar (t, r, θ, ϕ) and the cartesian (t, x, y, z) coordinates for the Minkowski spacetime $\mathbb{R}^{1,3}$. The (piece-wise) map between $\mathcal{I} \times S^3$ and $\mathbb{R}^{1,3}$ will preserve the angular coordinates (θ, ϕ) from $S^2 \hookrightarrow S^3$ to parametrise

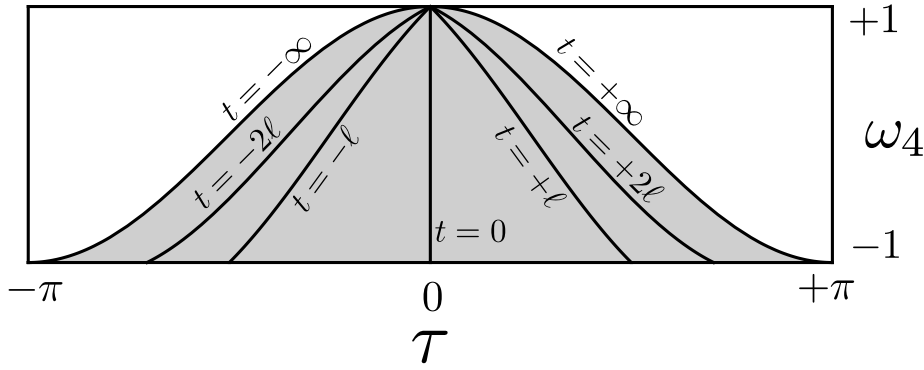


FIGURE 5.1: Illustration of the half of the $2\mathcal{I} \times S^3$ cylinder which is mapped into Minkowski space $\mathbb{R}^{1,3}$. In the vertical axis, $\omega_4 := \cos \chi$.

the unit-radius two-sphere $S^2 \hookrightarrow \mathbb{R}^{0,3} \hookrightarrow \mathbb{R}^{1,3}$, hence, we will use the same $\hat{\omega}_a$ from equation (5.3) in the Minkowski space. Moreover, two copies of $\mathcal{I} \times S^3$ are going to be glued together to cover the entirety of the Minkowski space, one covering the positive-time hyperplane $\mathbb{R}_+^{1,3}$ and one covering the negative-time hyperplane $\mathbb{R}_-^{1,3}$.

Let us start from the Minkowski metric

$$ds_{\text{Mink}}^2 = -dt^2 + dr^2 + r^2 d\Omega_2^2. \quad (5.44)$$

In terms of light-cone coordinates

$$u := t - r \quad \text{and} \quad v := t + r, \quad (5.45)$$

the metric reads

$$ds_{\text{Mink}}^2 = -dudv + \frac{1}{4}(v - u)^2 d\Omega_2^2. \quad (5.46)$$

We can then compactify the spacetime using

$$U := \tan^{-1}(u/\ell) \quad \text{and} \quad V := \tan^{-1}(v/\ell), \quad (5.47)$$

where $-\frac{\pi}{2} < U \leq V < \frac{\pi}{2}$ and ℓ sets a dimensionful scale for the compactification. Then, the metric becomes

$$ds_{\text{Mink}}^2 = \frac{1}{4 \cos(U)^2 \cos(V)^2} (-4dUdV + \sin(V - U)^2 d\Omega_2^2). \quad (5.48)$$

Finally, the conformal map from Minkowski space to the Lorentzian cylinder over S^3 is made explicit through

$$\tau := U + V \quad \text{and} \quad \chi := \pi + U - V, \quad (5.49)$$

such that $\chi \in (0, \pi]$ and $\tau \in (-\pi, \pi) =: 2\mathcal{I}$, with $|\tau| < \chi$. Notice that, in order to extend the interval of the τ variable, we glued together two cylinders at $\tau = 0$, otherwise we would only be reaching the $t > 0$ half of the Minkowski space. Moreover, the inequality between τ and χ shows that only the $|\tau| < \chi$ half of the $2\mathcal{I} \times S^3$ cylinder is mapped into the entire Minkowski space. Such map is illustrated in Figure 5.1. In terms of τ and χ , the metric now reads

$$\begin{aligned} ds_{\text{Mink}}^2 &= \gamma^{-2} (-d\tau^2 + d\chi^2 + \sin(\chi)^2 d\Omega_2^2) \\ &= \gamma^{-2} (-d\tau^2 + d\Omega_3^2) = \gamma^{-2} ds_{\text{cyl}}^2, \end{aligned} \quad (5.50)$$

where

$$\gamma = \frac{2\ell^2}{\sqrt{4\ell^2 t^2 + (r^2 - t^2 + \ell^2)^2}} = \frac{2\ell^2}{\sqrt{4\ell^2 r^2 + (t^2 - r^2 + \ell^2)^2}} = \cos \tau - \cos \chi. \quad (5.51)$$

As previously mentioned, the θ and ϕ coordinates are kept fixed from $2\mathcal{I} \times S^3$ to $\mathbb{R}^{1,3}$, so the map can be expressed simply in terms of a transformation from (τ, χ) to (t, r) , namely,

$$\sin \tau = \gamma t / \ell \quad \text{and} \quad \sin \chi = \gamma r / \ell. \quad (5.52)$$

Another useful relation will be

$$\exp(i\tau) = \gamma \frac{(\ell + it)^2 + r^2}{2\ell^2}. \quad (5.53)$$

The Jacobian of the transformation (5.52) reads

$$\frac{\partial(\tau, \chi)}{\partial(t, r)} = \frac{1}{\ell} \begin{pmatrix} p & -q \\ q & -p \end{pmatrix}, \quad (5.54)$$

where

$$p = \gamma^2 \frac{r^2 + t^2 + \ell^2}{2\ell^2} = 1 - \cos \tau \cos \chi \quad \text{and} \quad q = \gamma^2 \frac{tr}{\ell^2} = \sin \tau \sin \chi. \quad (5.55)$$

Alternatively, one can also express the map in terms of cartesian coordinates, in which we use the ω_a from equation (5.2) to parametrise the three-sphere S^3 . It then reads

$$\begin{aligned} \cot \tau &= \frac{r^2 - t^2 + \ell^2}{2\ell t}, & \omega_1 &= \gamma \frac{x}{\ell}, & \omega_2 &= \gamma \frac{y}{\ell}, & \omega_3 &= \gamma \frac{z}{\ell}, \\ \text{and} \quad \omega_4 &= \gamma \frac{r^2 - t^2 - \ell^2}{2\ell^2}. \end{aligned} \quad (5.56)$$

Using the conformal map, we can straightforwardly pull the left-invariant one-forms on the cylinder back to Minkowski space. In polar coordinates, and using the $\hat{\omega}^a$ from (5.3) instead of (θ, ϕ) to parametrise the two-sphere, they read

$$\begin{aligned} e^\tau &= \gamma^2 \frac{(t^2 + r^2 + \ell^2)dt - 2trdr}{2\ell^3}, \\ e^a &= \gamma^2 \frac{\hat{\omega}^a (2rtdt - (t^2 + r^2 + \ell^2)dr) - (t^2 - r^2 + \ell^2)rd\hat{\omega}^a - 2\ell r^2 \epsilon^{ajk} \hat{\omega}^j d\hat{\omega}^k}{2\ell^3}. \end{aligned} \quad (5.57)$$

From those expressions, we easily obtain functions χ_μ^A , where $A \in \{\tau, 1, 2, 3\}$, such that

$$e^A = \chi_\mu^A dx^\mu. \quad (5.58)$$

With the relation between the two sets of one-forms, we can directly obtain a set of finite-action and finite-energy Maxwell vacuum solutions on Minkowski from (5.27) (with $X_\tau = 0$) and components (5.36). For each solution on the Lorentzian cylinder, the cartesian components A_μ ¹ and $F_{\mu\nu}$ of the gauge potential and the field strength tensor in Minkowski space are simply obtained through

$$\mathcal{A} = \mathcal{A}_a e^a = A_\mu dx^\mu \quad \text{and} \quad \mathcal{F} = \frac{1}{2} \mathcal{F}_{AB} e^A \wedge e^B = \frac{1}{2} F_{\mu\nu} dx^\mu \wedge dx^\nu. \quad (5.59)$$

¹Notice that the temporal gauge condition on the cylinder does not imply $A_t = 0$ on the Minkowski space. Indeed, A_t will have a non-zero contribution from A_χ .

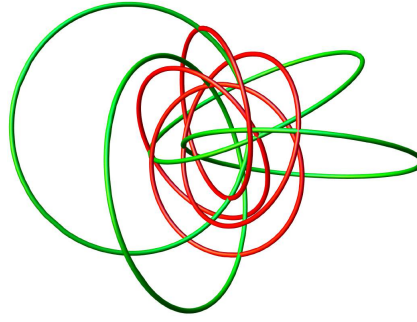


FIGURE 5.2: Illustration of some of the electric (red) and magnetic (green) field lines of the imaginary part of the $(j, m, n) = (0, 0, 1)$ solution, which turns out to be the Rañada-Hopf knot.

Moreover, using the hyperspherical harmonics and the relation (5.53), it is straightforward to show that the components of the electric and magnetic fields built from this method are always rational functions of the Minkowski coordinates (t, x, y, z) . Explicitly, for type-I spin- j solutions, they are always of the form

$$\frac{P_{2(2j+1)}(t, x, y, z)}{Q_{2(2j+3)}(t, x, y, z)}, \quad (5.60)$$

where P_n and Q_n here are polynomials of degree n . This implies that the energy and action of such solutions are indeed finite, as expected. For more details, see [36].

The fields increase in complexity with the “spin” of the solution. For an explicit example, let us take one of the simplest examples available to illustrate how such fields can behave. Consider the complex solution for $j = 0$, $m = 0$, and $n = 1$ and take its imaginary part, by linearity of the Maxwell equations. Such electromagnetic field turns out to be the celebrated Rañada-Hopf electromagnetic knot [30]. It is more simply expressed in terms of its Riemann-Silberstein vector $\vec{S} := \vec{E} + i\vec{B}$, as

$$\vec{S}_{\text{RH}} = \frac{1}{((t-i)^2 - r^2)^3} \begin{pmatrix} (x-iy)^2 - (t-i-z)^2 \\ i(x-iy)^2 + i(t-i-z)^2 \\ -2(x-iy)(t-i-z) \end{pmatrix}, \quad (5.61)$$

and some of its field lines are illustrated in Figure 5.2.

5.3 Conformal group and conserved Noether charges

Conformal transformations on an inner product space are defined as angle-preserving transformations and they form a group referred to as the conformal group of such space [37]. The conformal group of the Lorentzian space $\mathbb{R}^{p,q}$ is $\text{SO}(p+1, q+1)$. In particular, for the four-dimensional Minkowski spacetime it is $\text{SO}(2, 4)$, which include transformations from the Lorentz group $\text{SO}(1, 3)$, translations, dilatations, and the so-called special conformal transformations, as we will see below. By Noether’s theorem, the fact that Maxwell’s theory in four-dimensions is invariant with respect to such transformations implies the existence of conserved charges, which can then be used to better understand properties of these solutions and compare them to other known ones. Computing and analysing such quantities will be the objective of this

section. However, let us first briefly review the conformal group and how it acts on $\mathbb{R}^{1,3}$.

In a general pseudo-Riemannian manifold with metric $g_{\mu\nu}$, the local angle-preserving condition for a transformation $x \mapsto x'$ reads

$$g_{\rho\sigma}(x') \frac{\partial x'^{\rho}}{\partial x^{\mu}} \frac{\partial x'^{\sigma}}{\partial x^{\nu}} = \Omega(x)^2 g_{\mu\nu}(x), \quad (5.62)$$

for any real smooth function $\Omega(x)$. Considering infinitesimal coordinate transformations $x \mapsto x' = x + \epsilon(x) + \mathcal{O}(\epsilon^2)$ on a Minkowskian spacetime $\mathbb{R}^{p,q}$, with $p + q = d$, the condition reduces to

$$\eta_{\rho\sigma}(\delta_{\mu}^{\rho} + \partial_{\mu}\epsilon^{\rho})(\delta_{\nu}^{\sigma} + \partial_{\nu}\epsilon^{\sigma}) + \mathcal{O}(\epsilon^2) = \Omega(x)^2 \eta_{\mu\nu}. \quad (5.63)$$

If $\kappa(x) := \Omega(x)^2 - 1$, we have

$$\partial_{\mu}\epsilon_{\nu} + \partial_{\nu}\epsilon_{\mu} = \kappa(x)\eta_{\mu\nu}. \quad (5.64)$$

Taking the trace by contracting with $\eta^{\mu\nu}$, the expression above turns into

$$2(\partial \cdot \epsilon) := 2\partial_{\mu}\epsilon^{\mu}(x) = d\kappa(x) \quad \Rightarrow \quad \kappa(x) = \frac{2}{d}(\partial \cdot \epsilon), \quad (5.65)$$

allowing us to rewrite (5.64) as

$$\partial_{\mu}\epsilon_{\nu} + \partial_{\nu}\epsilon_{\mu} - \frac{2}{d}\eta_{\mu\nu}(\partial \cdot \epsilon) = 0. \quad (5.66)$$

This equation is called the **conformal Killing equation**. One can show that it is solved by

$$\epsilon^{\mu} = a^{\mu} + \theta^{\mu\nu}x_{\nu} + \alpha x^{\mu} + [2(b \cdot x)x^{\mu} - (x \cdot x)b^{\mu}], \quad (5.67)$$

where θ is anti-symmetric. Clearly, a^{μ} and $\theta^{\mu\nu}$ correspond to the $\mathbb{R}^d \times \text{SO}(p, q)$ isometry group of $\mathbb{R}^{p,q}$, which in $\mathbb{R}^{1,3}$ reduces to the Poincaré group. Moreover, there are two new transformations, the **dilatation** from the α parameter and the **special conformal transformations** (SCTs) from b^{μ} . As a consistency check, we can sum the number of independent transformations, respectively,

$$\left(d + \frac{d(d-1)}{2}\right) + 1 + d = \frac{(d+1)(d+2)}{2} = \dim(\text{SO}(p+1, q+1)). \quad (5.68)$$

One can show that the finite forms of the special conformal transformations are built from the composition of an inversion around the origin, a translation by $-b^{\mu}$, then a second inversion around the origin. Finally, the transformations discussed above are generated by

$$\begin{aligned} \text{Translations : } P_{\mu} &= i\partial_{\mu} \\ \text{Rotations : } M_{\mu\nu} &= i(x_{\mu}\partial_{\nu} - x_{\nu}\partial_{\mu}) \\ \text{Dilatation : } D &= -ix^{\mu}\partial_{\mu} \\ \text{SCTs : } K_{\mu} &= -i(2x_{\mu}x^{\nu}\partial_{\nu} - (x \cdot x)\partial_{\mu}) \end{aligned} \quad (5.69)$$

Let us now go back to the Maxwell theory in Minkowski space. In four dimensions, the free theory with action

$$S[A_{\mu}] = \int d^4x \mathcal{L} = - \int d^4x \frac{1}{4} F^{\mu\nu} F_{\mu\nu} \quad (5.70)$$

is invariant under the conformal group $\text{SO}(2,4)$. The variation of the gauge field A_μ with respect to a transformation $\zeta^\mu(x)$ is given by its Lie derivative \mathcal{L} with respect to ζ^μ , namely

$$\delta A_\mu := \mathcal{L}_\zeta A_\mu = -\zeta^\nu \partial_\nu A_\mu - A_\nu \partial_\mu \zeta^\nu = F_{\mu\nu} \zeta^\nu, \quad (5.71)$$

where an integration by parts was performed in the last step and the boundary term vanishes on the variation with fixed ends. With the variation of the gauge field, we can compute the conserved current J as

$$J^\mu = \frac{\partial \mathcal{L}}{\partial (\partial_\mu A_\nu)} \delta A_\nu + \zeta^\mu \mathcal{L} = (F^{\mu\rho} F_{\nu\rho} - \frac{1}{4} \delta_\nu^\mu F^2) \zeta^\nu, \quad (5.72)$$

where $F^2 = F_{\alpha\beta} F^{\alpha\beta}$. The current J satisfies the continuity equation $\partial_\mu J^\mu = 0$, implying that an associated conserved charge Q can be computed as

$$Q = \int_V d^3x J^0, \quad (5.73)$$

for any fixed time. Hence, we can choose to compute those with $t = 0$. For $t = \tau = 0$, some of the expressions on the previous section simplify, and we have

$$\begin{aligned} \chi_i^a &= \frac{\gamma \omega_4 \delta_i^a + \gamma \epsilon_{aib} \omega_b - \omega_a \omega_i}{\ell}, & \chi_i^a \chi_i^b &= \frac{\gamma^2}{\ell^2} \delta^{ab}, \\ \gamma &= 1 - \omega_4, & \text{and } d^3x &= \frac{\ell^3}{\gamma^3} d^3\Omega_3 = \frac{\ell^3}{\gamma^3} e^1 \wedge e^2 \wedge e^3. \end{aligned} \quad (5.74)$$

Moreover, the explicit relation between the electric and magnetic fields on the cylinder and on Minkowski space computed from (5.59) is also made simpler with $t = \tau = 0$ since then $\chi_i^\tau = \chi_0^a = 0$, which “decouple” the electric and magnetic parts. The relation becomes

$$E_i = \chi_0^\tau \chi_i^a \mathcal{E}_a \quad \text{and} \quad B_i = \frac{1}{2} \epsilon_{ijk} \epsilon_{abc} \chi_j^b \chi_k^c \mathcal{B}_a. \quad (5.75)$$

For spin- j solutions, equation (5.43) contains the electromagnetic fields on the cylinder of spin- j solutions in terms of the potential $\mathcal{A}^{(j)}$. For the rest of this section, let us take \mathcal{A} to be real with

$$\mathcal{A}_a^{(j)} = Z_a^j(\omega) e^{i\Omega_j \tau} + \bar{Z}_a^j(\omega) e^{i\Omega_j \tau}. \quad (5.76)$$

Equations (5.43), (5.75), and (5.76) will be used throughout the rest of the section to compute the charges associated with conformal symmetries of spin- j solutions.

The simplest charge is the one associated with translations, which is also used to define the energy-momentum tensor T . Namely, the current J associated with an ζ^μ translation is

$$(J_\mu)^\nu = T_\mu^\nu = F_{\mu\alpha} F^{\nu\alpha} - \frac{1}{4} \delta_\mu^\nu F^2. \quad (5.77)$$

The corresponding charges are the energy E for $\mu = 0$ and the three-momentum components P_i for $\mu = i$. Explicitly, the energy density $e := T^{00}$ reads

$$e := \frac{1}{2} (E_i^2 + B_i^2) = \left(\frac{\gamma}{\ell}\right)^4 \rho, \quad \text{where } \rho = \frac{1}{2} (\mathcal{E}_a^2 + \mathcal{B}_a^2) \quad (5.78)$$

is the energy density on the cylinder. Integrating the energy density e on the $t = 0$ slice of the Minkowski space results in the total energy

$$E = \frac{8}{\ell} (j+1)^3 (2j+1) \sum_{m,n} |\Lambda_{j;m,n}|^2. \quad (5.79)$$

For the momentum, it is useful to work with the momentum-density one-forms $p := p_i dx^i$ on the Minkowski space and $\mathcal{P} = \mathcal{P}_a e^a$ on the cylinder. Hence,

$$\mathcal{P}_a = \epsilon_{abc} \mathcal{E}_b \mathcal{B}_c \quad \text{and} \quad p = \left(\frac{\gamma}{\ell}\right)^3 \mathcal{P}. \quad (5.80)$$

Once more, the momentum components P_i are obtained from the integration of p_i on the $t = 0$ slice of Minkowski space. As an example, the expressions for $j = 0$ in terms of the $\Lambda_{j;m,n}$ components read

$$\begin{aligned} P_1^{(j=0)} &= -\frac{\sqrt{2}}{\ell} ((\bar{\Lambda}_{0,-1} + \bar{\Lambda}_{0,1}) \Lambda_{0,0} + \bar{\Lambda}_{0,0} (\Lambda_{0,-1} + \Lambda_{0,1})), \\ P_2^{(j=0)} &= \frac{i\sqrt{2}}{\ell} ((-\bar{\Lambda}_{0,-1} + \bar{\Lambda}_{0,1}) \Lambda_{0,0} + \bar{\Lambda}_{0,0} (\Lambda_{0,-1} - \Lambda_{0,1})), \\ P_3^{(j=0)} &= \frac{2}{\ell} (|\Lambda_{0,-1}|^2 - |\Lambda_{0,1}|^2), \end{aligned} \quad (5.81)$$

and they grow in complexity with increasing j . It is worth noticing that, after consistently defining the action of the \mathcal{D}_a on the Λ components (see [32] for the details), the P_i transform as vector components according to the $\mathfrak{so}(3)$ algebra generated by the \mathcal{D}_a . Explicitly,

$$\mathcal{D}_a P_i = 2\epsilon_{aij} P_j, \quad (5.82)$$

which allows us to obtain the $P_1^{(j)}$ and $P_2^{(j)}$ components from the $P_3^{(j)}$ one with an adequate action of \mathcal{D}_a . Moreover, if we take the momentum components (P_r, P_θ, P_ϕ) in spherical coordinates, P_θ vanishes identically for the cases we tested, for $j = 0, 1/2, 1$. Additionally, for $j = 0$, P_ϕ is proportional to P_z :

$$P_\phi^{(j=0)} = \ell P_3^{(j=0)} = 2 (|\Lambda_{0;0,-1}|^2 - |\Lambda_{0;0,1}|^2). \quad (5.83)$$

This matching does not hold for higher values of j .

Lorentz transformations come from

$$\zeta^\mu = M_\nu^\mu x^\nu \quad \text{where} \quad M_{\mu\nu} = -M_{\nu\mu}, \quad (5.84)$$

and they can be separated in standard rotations, associated with the M_{ij} , and hyperbolic rotations, or boosts, associated with the M_{0j} . For any j , the boost charges are going to vanish identically, which means that the "centre of momentum" of such solutions at $t = 0$ is in the origin of the chosen coordinate system. On the other hand, the charges associated with rotations are the components of the angular momentum L , and in general do not vanish. As with the momentum P in (5.82), we can check that the L_i components also transform as a $\text{SO}(3)$ vector with respect to the action of the \mathcal{D}_a . Once more, we can simplify our computations by defining the one-forms $l = l_i dx^i$ and $\mathcal{L} = \mathcal{L}_a e^a$, with $\mathcal{L}_a = \epsilon_{abc} \mathcal{P}_b \omega_c$, and using

$$l = \left(\frac{\gamma}{\ell}\right)^2 \mathcal{L} \quad (5.85)$$

to extract the components of the density l_i and integrate to obtain the charges L_j . For the spherical components of the angular momentum of spin-0 solutions, we find that L_r vanishes and that the θ and ϕ components are proportional to P_3 ,

$$L_\theta^{(j=0)} = \frac{4}{3}\ell^2 P_3^{(j=0)} \quad \text{and} \quad L_\phi^{(j=0)} = -\frac{1}{3}\ell^2 P_3^{(j=0)}. \quad (5.86)$$

This result does not hold for higher- j solutions.

For the dilatations, associated with transformations

$$\zeta^\mu = \lambda x^\mu, \quad (5.87)$$

it is straightforward to show that its charge D vanishes. That leaves us with the special conformal transformations, associated with

$$\zeta^\mu = 2x^\mu b_\nu x^\nu - x^\nu x_\nu b^\mu, \quad (5.88)$$

which have four charges V_μ . V_0 is said to be the charge of the ‘‘scalar SCT’’, and its density v_0 is, for all j , proportional to the energy density according to

$$v_0 = (x_\mu x^\mu) e. \quad (5.89)$$

Integrating the density, we get the charge

$$V_0^{(j)} = \ell^2 E^{(j)} = 8\ell(j+1)^3(2j+1) \sum_{m,n} |\Lambda_{j;m,n}|^2 \quad (5.90)$$

for spin- j solutions. Finally, for the three-vector components of V , we verified that, up to at least $j = 1$, they are proportional to the three-momentum P :

$$V_i = \ell^2 P_i. \quad (5.91)$$

As such, they have the same properties as the ones discussed for the P_i .

Such charges were used in [32] to more easily categorise our solutions and to find equivalences between (linear combinations of) them and electromagnetic knotted fields obtained from other constructions, as well as to easily find the correct correspondence of parameters to map the equivalent solutions into each other. One such example is the time-translated Hopfian from equations (3.16-3.17) of [38], obtained from the Bateman construction. For that, to match their parameter c , we have to choose $\ell = 1 - c$. Hence, it becomes clear that the time-translated Hopfian obtained from Bateman’s construction is proportional to one of our spin-0 basis solutions, namely with

$$(\Lambda_{0;0;1}, \Lambda_{0;0;0}, \Lambda_{0;0;-1}) = \left(0, 0, -i\frac{\pi}{2\ell^2}\right). \quad (5.92)$$

Some field lines of the electric and magnetic fields generated by this setting are shown in Figure 5.3. More examples of previously known knotted electromagnetic fields from the literature being generated by our basis of solutions are discussed in [32, 33] and will also be exemplified in the next section.

5.4 Trajectories of charged particles

In addition to construction methods and theoretical and mathematical properties of knotted electromagnetic fields, there are important advancements in discussions

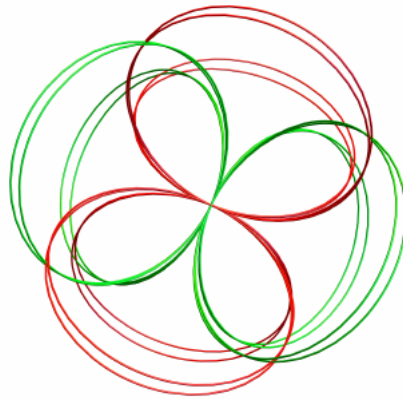


FIGURE 5.3: Illustration of some field lines of electric (green) and magnetic (red) fields of the time-translated Hopfian, described in [38] (for $t = 0$ and $c = 60$ in their conventions).

about experimental settings for generation and application of such fields. In [39], for example, the generation of knotted electromagnetic fields using Laguerre–Gaussian beams is discussed, as well as potential applications in atomic particle trapping, manipulation of cold atomic ensembles, helicity injection for plasma confinement, and generation of soliton-like fields in a nonlinear medium. More recently, some simple knotted field configurations, including the figure-8 knot, were produced in the laboratory using laser beams with knotted polarisation singularities [40]. In this scenario, in order to enable more in-depth discussions on experimental applications, it becomes essential to better understand the possible effects of such fields on a charged particle. As their complexity does not allow for analytical solutions of equations of motion of charged particles in such backgrounds, a numerical work on simulations of such trajectories was performed in [33] and will be discussed in this section.

Let us split the complex basis solutions into two real sets labeled $(j; m, n)_R$ and $(j; m, n)_I$ for the real and the imaginary parts, respectively, of the $(j; m, n)$ solution on (5.36), and consider the respective electric and magnetic fields. Characteristic features due to the particular construction method should and will be clearly illustrated in their behaviour and on trajectories of charged particles in them. Some characteristics are intrinsic to the type of solutions we are working with, such as the complexity of the field lines growing with j . In addition to the spin-0 example in Figure 5.2, see Figure 5.4 for instances of electric and magnetic field lines of a spin- $\frac{1}{2}$ and a spin-1 solution, illustrating their increasing complexity. Those fields correspond, respectively, to the $(1, 1)$, $(2, 1)$, and $(1, 3)$ examples of the (p, q) -torus knotted fields arising from Bateman’s construction [31], as mentioned in the previous section.

Other characteristics are a more straightforward consequence of one of our conventions. As an example, we can see that, due to the choice to diagonalise the J_3 action of the isometry subgroup $SO(3) \hookrightarrow SO(4)$, which also acts on the Minkowski unit-radius sphere $S^2 \hookrightarrow \mathbb{R}^{1,3}$, the z -direction is singled out. Both the electric and magnetic fields along the z -axis, that is,

$$\vec{E}(t, x = 0, y = 0, z) \quad \text{and} \quad \vec{B}(t, x = 0, y = 0, z), \quad (5.93)$$

are either contained in the xy -plane or in the z -axis, for all (j, m, n) , for both the real and the imaginary parts. The singling out of the z -direction is illustrated in Figure 5.5.

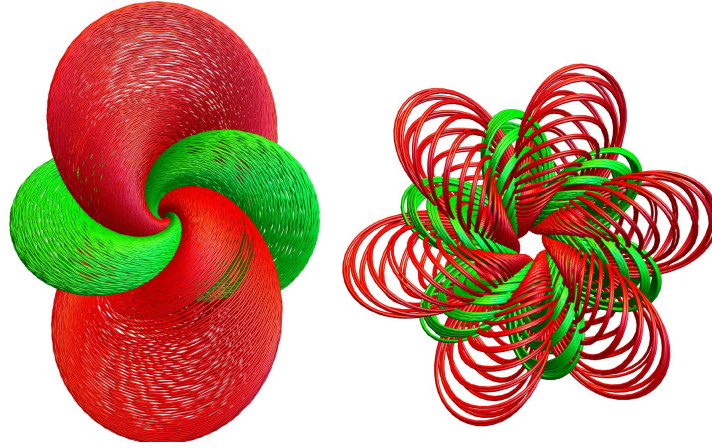


FIGURE 5.4: Illustration of field lines of the electric (red) and magnetic (green) fields from the $(\frac{1}{2}, -\frac{1}{2}, \frac{3}{2})_R$ and $(1, 1, 2)_I$ solutions, respectively, with $t = 0$.

To try to better understand the basis solutions and for future use on the trajectories simulations, for each configuration K we computed the maximum $E_{\max}^K(t)$ of the energy density $E := \frac{1}{2}(\vec{E}^2 + \vec{B}^2)$ along the space for each time t . Moreover, we defined $R_{\max}^K(t)$ such that

$$E^K(t, \vec{x}_{\max}(t)) = E_{\max}^K(t) \quad \Rightarrow \quad R_{\max}^K(t) := |\vec{x}_{\max}(t)|. \quad (5.94)$$

When the configuration being considered is clear from the context, we will omit K from the notation. The three-vectors $\vec{x}_{\max}(t)$ which maximise the energy density of a field configuration at the time t will generally not be unique, however, the multiple vectors will always be equidistant to the origin, hence $R_{\max}(t)$ is unique and well-defined for all configurations and time t . In Figure 5.5, for example, we use $E_{\max}(t)$ to set a scale for the contour plot of energy densities. It will also be used in what follows to establish more adequate initial conditions for the simulations of particle trajectories.

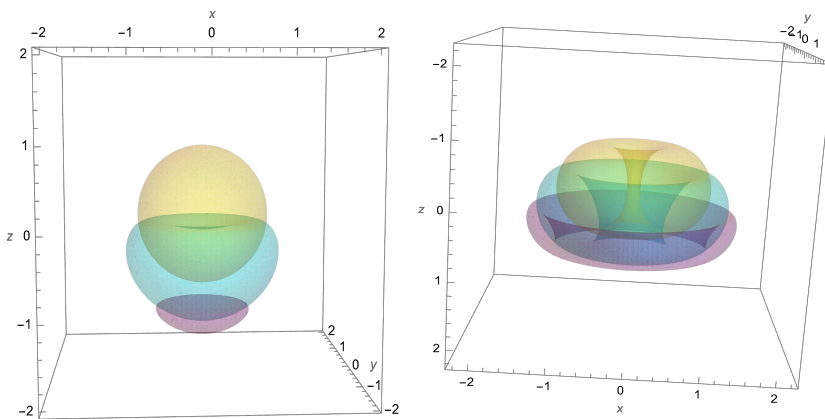


FIGURE 5.5: Contour plots for energy densities at $T=0$ (yellow), $T=1$ (cyan) and $T=1.5$ (purple) with contour value $0.9E_{\max}(1.5)$. Left: $(0, 0, 1)_I$ configuration. Right: $(\frac{1}{2}, -\frac{1}{2}, -\frac{3}{2})_R$ configuration.

Finally, let us discuss the equations of motion to be used in the simulations of charged particle trajectories under the knotted electromagnetic field configurations.

For simplicity, we will only consider basis field configurations of up to spin-1. The trajectories are governed by the relativistic Lorentz equation

$$\frac{d\vec{p}}{dt} = q \left(\vec{E}_\ell + \vec{v} \times \vec{B}_\ell \right), \quad (5.95)$$

where q is the charge of the test particle, $\vec{p} = \tilde{\gamma} m \vec{v}$ is its relativistic three-momentum, \vec{v} its three-velocity, m its mass, $\tilde{\gamma} = (1 - \vec{v}^2)^{-\frac{1}{2}}$ its Lorentz factor, and \vec{E}_ℓ and \vec{B}_ℓ are the dimensionful electric and magnetic fields, respectively, which carry the ℓ factor of the map from the cylinder over the three-sphere to the Minkowski space. It is worth noticing here that we will neglect effects of backreaction of the electromagnetic fields generated by the charged particle's acceleration. This choice will be justified later for a family of scenarios.

It is straightforward to rewrite the equation of motion above directly in terms of the derivative of the three-velocity [41]. Specifically, if E_p is the energy of the particle, we use

$$E_p = \tilde{\gamma} m \quad \text{and} \quad \frac{dE_p}{dt} = q(\vec{v} \cdot \vec{E}_\ell) \quad (5.96)$$

to rewrite (5.95) as

$$\frac{d\vec{v}}{dt} = \frac{q}{\tilde{\gamma} m} \left(\vec{E}_\ell + \vec{v} \times \vec{B}_\ell - (\vec{v} \cdot \vec{E}_\ell) \vec{v} \right), \quad (5.97)$$

which is an equivalent equation of motion, only differing by the position of the non-linearity on the three-velocity, which proved to be more efficient for simulations. Moreover, before proceeding with the numerics, it will be useful to use the length scale ℓ to once more rewrite the equation of motion, now only in terms of dimensionless quantities. Defining

$$T := \frac{t}{\ell}, \quad \vec{X} := \frac{\vec{x}}{\ell}, \quad \vec{V} := \frac{d\vec{X}}{dT} = \vec{v}, \quad \vec{E} := \ell^2 \vec{E}_\ell, \quad \text{and} \quad \vec{B} := \ell^2 \vec{B}_\ell, \quad (5.98)$$

we rewrite (5.95) as

$$\frac{d(\tilde{\gamma} \vec{V})}{dT} = \kappa \left(\vec{E} + \vec{V} \times \vec{B} \right) \quad (5.99)$$

and (5.97) as

$$\frac{d\vec{V}}{dT} = \frac{\kappa}{\tilde{\gamma}} \left(\vec{E} + \vec{V} \times \vec{B} - (\vec{V} \cdot \vec{E}) \vec{V} \right), \quad (5.100)$$

where $\kappa = \frac{q\ell^3\lambda}{m}$ is a dimensionless parameter and λ is a numerical constant that can be factored from the $\Lambda_{j;m,n}$ coefficients. The numerical parameter κ may be used to justify neglecting the backreaction, since we can tune the other parameters on the definition of κ to keep its value fixed while making the charge as small as needed, then justifying this approximation to whichever precision is required. The description of the dynamics in terms of dimensionless quantities from equations (5.99) and (5.100) is more suitable for numerical simulations.

Before proceeding to the results, we need to specify the initial conditions to be used, for which we separated the main scenarios in

- (1) N identical particles with $\vec{V}_0 := \vec{V}(T = 0) = 0$ and initial positions located symmetrically with respect to the origin, or
- (2) N identical particles with $\vec{X}_0 := \vec{X}(T = 0) = 0$ and initial velocities directed radially outward symmetrically with respect to the origin.

Each of those will be presented in three different settings, namely

- (A) Non-zero initial conditions distributed along a line, or
- (B) on a circle of radius r , or
- (C) on a sphere of radius r .

For scenario (2), we separate the particle's initial speed in three different cases, namely

- (i) non-relativistic (here defined as $|\vec{V}_0| < 0.1$),
- (ii) relativistic ($0.1 < |\vec{V}_0| < 0.99$),
- (iii) ultra-relativistic ($0.99 < |\vec{V}_0|$).

In [33], we show more results for each setting and we further explain the thought process for the details in each simulation, including for the values of κ and for the initial conditions in terms of R_{\max} and E_{\max} , trying to maximise the effect of the electromagnetic fields on the particle trajectories. In the rest of this section, we will only briefly discuss two of the features we observed in the simulations, namely the possibility of acceleration from rest up to ultra-relativistic speeds and, for some configurations, the focusing of multi-particle trajectories with varied initial conditions into certain numbers of beams in small solid-angle regions of spacetime.

The two aforementioned features have to do with the fact that, with higher values of κ , it is possible to make the initial conditions increasingly irrelevant for the trajectories. Despite the fields decreasing with powers of both space and time coordinates, in most field configurations, we could observe particles being accelerated from rest to ultra-relativistic speeds, as illustrated in Figure 5.6. Furthermore, for higher-spin configurations, the number of vectors \vec{x} such that $|\vec{x}| = R_{\max}$ generally grow and the energy density gets localised in an increasing number of small solid-angle regions. Particles located near those regions are usually accelerated to ultra-relativistic speeds. Moreover, this effect may also cause the trajectories to get split and localised into a certain number of solid-angle regions of spacetime, as we see exemplified in Figure 5.7. The number of such regions for fixed j change with m and n , but the maximum number of regions observed grows with j , as expected from the complexity of the field lines.

In summary, both papers [32] and [33] are part of an effort to deepen our knowledge on the new electromagnetic knots generated from the method first described in [29]. The former focus on explicit comparison with fields constructed with other methods in the literature and on analytical results for Noether charges, which help not only in the comparison but also on categorising and better understanding the physical properties of such electromagnetic fields, both individually and on how they change with the parameters of the construction. The latter focus on a numerical investigation aiming at enabling a future discussion on possible experimental applications of such electromagnetic knots, similar to what is discussed in [39], by performing a first investigation on the variety of effects of such fields on charged particles in different relevant cases and the physical effects that would be relevant in such setups.

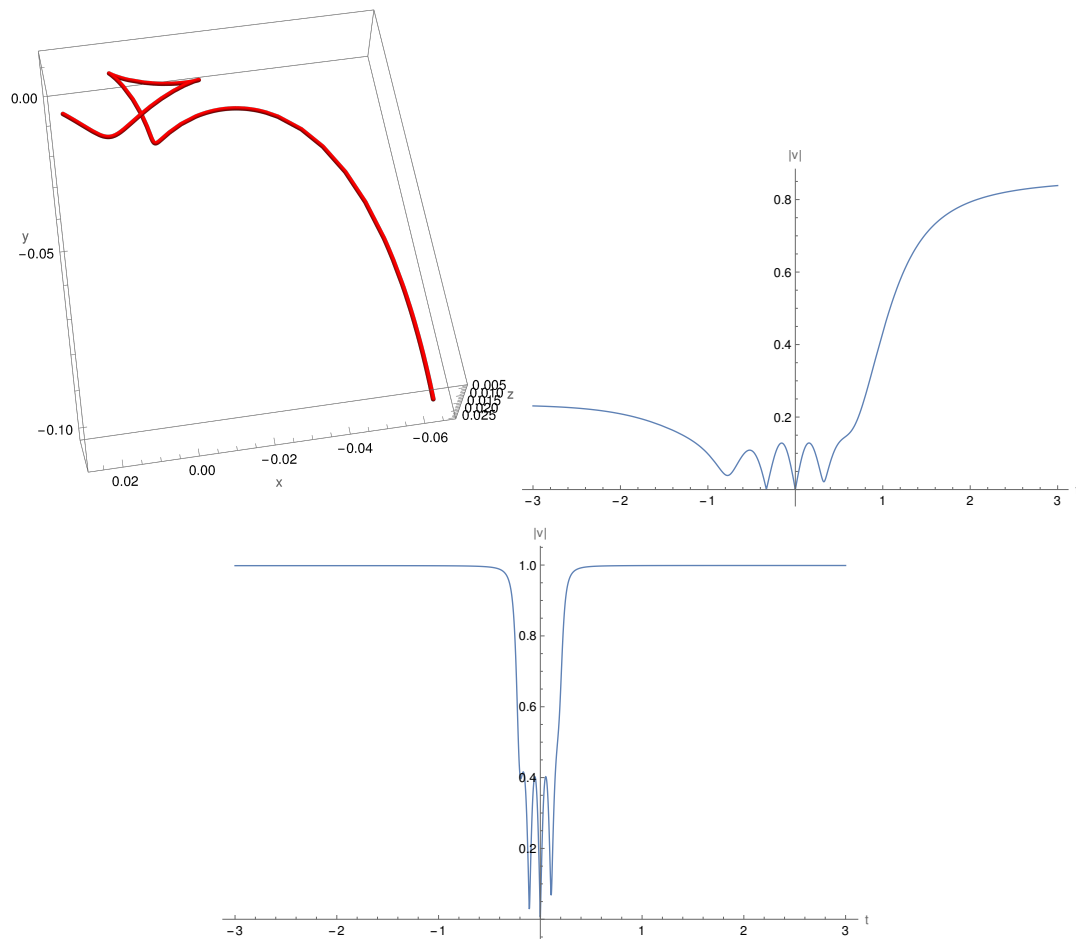


FIGURE 5.6: Trajectory of a charged particle for the $(\frac{1}{2}; -\frac{1}{2}, -\frac{3}{2})_R$ field configuration with initial conditions $\mathbf{X}_0=(0.01, 0.01, 0.01)$ and $\mathbf{V}_0=0$ simulated for $T \in [-1, 1]$. Upper left: Particle trajectory for $\kappa=10$. Upper right: absolute velocity profile for $\kappa=10$. Bottom: absolute velocity profile for $\kappa=100$.

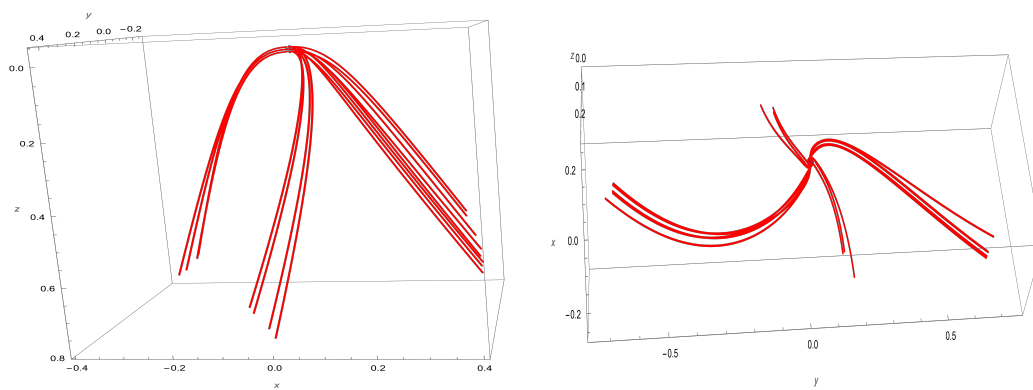


FIGURE 5.7: Simulation of $N=18$ particles in scenario (1C) with $r=0.01$ and $T \in [0, 3]$. Left: $(1, -1, -2)_R$ configuration with $\kappa=500$. Right: $(1, -1, -1)_R$ configuration with $\kappa=10$.

Chapter 6

The non-abelian case I: non-compact gauge groups

In the previous chapter, we explored the consequences of the reduction of a $SU(2)$ Yang–Mills theory on a cylinder over a three-sphere to a specific $U(1)$ subgroup, which is later conformally mapped into the Minkowski space. In this chapter, we will mostly work with the non-Abelian theory itself. Motivated by the results obtained with the deSitter method, we will investigate what kind of new Yang–Mills fields we can obtain in different settings; more specifically, for different gauge groups, spacetimes, and foliations. Section 6.1 is on a $SO(1,3)$ gauge theory while Section 6.2 is on a family of $SU(1,1)$ gauge theories, the two of which will be discussed in both specific foliations and on the Minkowski space.

It may be striking that both the aforementioned cases have non-compact gauge groups, which is unusual in particle physics. Regarding that, three observations are in order. Firstly, we can still reduce such non-abelian fields to particular abelian subgroups and generate new electromagnetic fields with their own applications, as we illustrate in the end of Section 6.2, where we reproduce recently discovered magnetic vortex solutions, with many other possibilities still open to be investigated. Secondly, non-Abelian gauge fields are relevant beyond the realm of standard particle physics, and so is our need to understand such theories. The immediate example is on the formulation of gravity as a gauge theory, however, they also appear, for example, in Condensed Matter physics [42]. Thirdly, despite initial methods of analysis pointing otherwise, gauge theories with non-compact gauge groups can indeed lead to particle theories with an unitary S -matrix [43] with indications of being renormalisable [44]. That said, in this thesis we only work with the classical Yang–Mills solutions, such that those issues are out of the scope of our work.

6.1 $SO(1,3)$ gauge theory on Minkowski space

In this section, we will work on foliations of parts of Minkowski space using the action of the Lorentz group. Explicitly, after choosing an origin, the interior of the lightcone \mathcal{T} (with \mathcal{T}_\pm representing its future and past halves) will be foliated by cosets $SO(1,3)/SO(3) \equiv H^3$, the exterior of the lightcone \mathcal{S} will be foliated by cosets $SO(1,3)/SO(1,2) \equiv dS_3$, and the future and past lightcone surfaces \mathcal{L}_\pm will be mapped on $SO(1,3)/ISO(2)$. Gauge fields will be constructed in those three spaces, then we will discuss whether they can be glued together after pulling them back to Minkowski space.

6.1.1 General setting

The procedure we will follow is to choose a “base” vector x_0 in the region to be foliated and obtain the coset structure to be used in the foliation from the orbit-stabiliser theorem. From a G -action on the manifold, the sheet will be the orbit Orb_{x_0} , which is bijectively mapped onto G/Stab_{x_0} , according to Theorem 3. The subgroup Stab_{x_0} will be generally referred to as H , and will be clear from the context. Hence, a foliation $\mathbb{R} \times G/H$ will be constructed, where $u \in \mathbb{R}$ will be the foliation parameter. In all cases, we will be working on symmetric spaces, so the split of the algebra and the commutation relations will follow (2.28) and (2.29), with $f_{ab}^c = 0$. Hence, we may work with the one-forms as in 2.4, with $\{e^a\}$ on the coset space and $\{e^i\}$ on the stabiliser subgroup.

Finally, we will use the one-forms $\{e^a\}$ and $e^u := du$ to build a Yang–Mills theory on the foliation $\mathbb{R} \times G/H$. The gauge field \mathcal{A} and its curvature \mathcal{F} are decomposed as

$$\mathcal{A} = \mathcal{A}_u e^u + \mathcal{A}_a e^a \quad \text{and} \quad \mathcal{F} = \mathcal{F}_{ua} e^u \wedge e^a + \frac{1}{2} \mathcal{F}_{ab} e^a \wedge e^b. \quad (6.1)$$

The temporal gauge and the decomposition on the Lie-algebra elements read

$$\mathcal{A}_u = 0 \quad \text{and} \quad \mathcal{A}_a = \mathcal{A}_a^i T_i + \mathcal{A}_a^b T_b, \quad (6.2)$$

respectively. The equivariant Ansatz for the symmetric-space coset structure [4] then implies

$$\mathcal{A}_a^i = \chi_a^i \quad \text{and} \quad \mathcal{A}_b^a = \mathcal{A}_b^a(u) = \phi(u) \delta_b^a, \quad (6.3)$$

reducing the dynamics to that of a single real function $\phi(u)$. In summary, the gauge field reduces to

$$\mathcal{A} = T_i e^i + \phi(u) T_a e^a \quad (6.4)$$

and the field strength to

$$\mathcal{F}_{ua} = \dot{\phi} T_a \quad \text{and} \quad \mathcal{F}_{ab} = (\phi^2 - 1) f_{ab}^i T_i, \quad \text{with} \quad \dot{\phi} := \partial_u \phi. \quad (6.5)$$

Notice that the colour-electric field $\mathcal{E}_a = \mathcal{F}_{au}$ is valued in \mathfrak{m} while the colour-magnetic one $\mathcal{B}_a = \frac{1}{2} \varepsilon_{abc} \mathcal{F}_{bc}$ is valued in \mathfrak{h} . This implies that, for four-dimensional spacetimes foliated as symmetric spaces, the equivariant Ansatz cannot provide (anti-)self-dual solutions.

After the restriction of \mathcal{F} due to the equivariant Ansatz, we should in principle reduce the equation of motion to that of the scalar degree of freedom directly from the Yang–Mills equation $*D*\mathcal{F} = 0$, since the introduction of the reduced \mathcal{F} directly in the Yang–Mills action before extremising it could introduce spurious solutions. However, as G is semi-simple and analytic, the principle of symmetric criticality [45] guarantees that the two routes are indeed equivalent. Hence, we can simply reduce the action (4.62) with the explicit expression (6.5) for \mathcal{F} and extremise the reduced action in terms of $\phi(u)$.

6.1.2 Interior of the lightcone \mathcal{T}

For the foliation of the two halves \mathcal{T}_\pm of the interior of the lightcone, we will take the natural action of $\text{SO}(1,3)$ on $\mathbb{R}^{1,3}$. For simplicity, let us choose the base vector as $x_{\mathcal{T}} = (1,0,0,0)$. The stabiliser subgroup is $H = \text{SO}(3)$ and the sheets will be halves of the two-sheeted unit hyperboloid H^3 embedded in $\mathbb{R}^{1,3} \ni y$, with

$$y \cdot y = \eta_{\mu\nu} y^\mu y^\nu = -1. \quad (6.6)$$

The identification between H^3 and the coset $\text{SO}(1,3)/\text{SO}(3)$ for \mathcal{T}_+ is made explicit through

$$\begin{aligned} \alpha_{\mathcal{T}} : \text{SO}(1,3)/\text{SO}(3) &\rightarrow H^3, & [\Lambda_{\mathcal{T}}] &\mapsto y^\mu = (\Lambda_{\mathcal{T}})^\mu{}_\nu x_{\mathcal{T}}^\nu, \\ \alpha_{\mathcal{T}}^{-1} : H^3 &\rightarrow \text{SO}(1,3)/\text{SO}(3), & y^\mu &\mapsto [\Lambda_{\mathcal{T}}], \end{aligned} \quad (6.7)$$

where $[\Lambda_{\mathcal{T}}] = \{\Lambda \in \text{SO}(1,3) : \Lambda \sim \Lambda_{\mathcal{T}}\}$ is the equivalence class under right $H = \text{SO}(3)$ -multiplication. Notice that the map from the equivalence classes into H^3 is only well-defined because H is the stabiliser subgroup of $x_{\mathcal{T}}$. The foliation of \mathcal{T}_+ is then performed with

$$\begin{aligned} \varphi_{\mathcal{T}} : \mathbb{R} \times H^3 &\rightarrow \mathcal{T}, & (u, y^\mu) &\mapsto x^\mu := e^u y^\mu, \\ \varphi_{\mathcal{T}}^{-1} : \mathcal{T} &\rightarrow \mathbb{R} \times H^3, & x^\mu &\mapsto (u, y^\mu) := \left(\ln \sqrt{|x \cdot x|}, \frac{x^\mu}{\sqrt{|x \cdot x|}} \right). \end{aligned} \quad (6.8)$$

If one employs $-x_{\mathcal{T}}$ as the base vector, \mathcal{T}_- will be obtained instead, in an analogous fashion.

With this setting, the Minkowskian metric on the interior of the lightcone is conformal to that of the Lorentzian cylinder over H^3 :

$$ds_{\mathcal{T}}^2 = e^{2u} (-du^2 + ds_{H^3}^2). \quad (6.9)$$

Moreover, the standard generators of $\mathfrak{so}(1,3)$,

$$\begin{aligned} K_1 &= \begin{pmatrix} 0 & 1 & 0 & 0 \\ 1 & 0 & 0 & 0 \\ 0 & 0 & 0 & 0 \\ 0 & 0 & 0 & 0 \end{pmatrix}, & K_2 &= \begin{pmatrix} 0 & 0 & 1 & 0 \\ 0 & 0 & 0 & 0 \\ 1 & 0 & 0 & 0 \\ 0 & 0 & 0 & 0 \end{pmatrix}, & K_3 &= \begin{pmatrix} 0 & 0 & 0 & 1 \\ 0 & 0 & 0 & 0 \\ 0 & 0 & 0 & 0 \\ 1 & 0 & 0 & 0 \end{pmatrix}, \\ J_1 &= \begin{pmatrix} 0 & 0 & 0 & 0 \\ 0 & 0 & 0 & 0 \\ 0 & 0 & 0 & -1 \\ 0 & 0 & 1 & 0 \end{pmatrix}, & J_2 &= \begin{pmatrix} 0 & 0 & 0 & 0 \\ 0 & 0 & 0 & 1 \\ 0 & 0 & 0 & 0 \\ 0 & -1 & 0 & 0 \end{pmatrix}, & J_3 &= \begin{pmatrix} 0 & 0 & 0 & 0 \\ 0 & 0 & -1 & 0 \\ 0 & 1 & 0 & 0 \\ 0 & 0 & 0 & 0 \end{pmatrix}, \end{aligned} \quad (6.10)$$

are split according to (2.28) as $T_i = J_i$ and $T_a = K_a$, with structure constants

$$f_{ij}{}^k = \varepsilon_{ijk}, \quad f_{ia}{}^b = \varepsilon_{iab}, \quad \text{and} \quad f_{ab}{}^i = -\varepsilon_{abi} \quad (6.11)$$

and indefinite Cartan–Killing metric

$$\begin{aligned} g_{ij} &= f_{ik}{}^l f_{lj}{}^k + f_{ia}{}^b f_{bj}{}^a = 4\delta_{ij}, \\ g_{ab} &= 2f_{ac}{}^i f_{ib}{}^c = -4\delta_{ab}, \quad \text{and} \quad g_{ia} = 0. \end{aligned} \quad (6.12)$$

Finally, using the coset map (6.7), we can obtain the Maurer–Cartan one-forms from

$$\Lambda_{\mathcal{T}}^{-1} d\Lambda_{\mathcal{T}} = e^a T_a + e^i T_i, \quad (6.13)$$

resulting in

$$e^a = \left(\delta^{ab} - \frac{y^a y^b}{y^0(1+y^0)} \right) dy^b \quad \text{and} \quad e^i = \varepsilon_{iab} \frac{y^a}{1+y^0} dy^b, \quad (6.14)$$

where

$$ds_{H^3}^2 = \delta_{ab} e^a \otimes e^b \quad \text{and} \quad e^i = \chi_a^i e^a, \quad \text{with} \quad \chi_a^i = \varepsilon_{aib} \frac{y^b}{1+y^0}. \quad (6.15)$$

The reduced action then reads

$$S_{\text{red}} = 6 \int_{\mathbb{R} \times H^3} \text{dvol} \left(\frac{1}{2} \dot{\phi}^2 - V(\phi) \right), \quad (6.16)$$

where $\text{dvol} = \frac{1}{3!} \varepsilon_{abc} \text{d}u \wedge e^a \wedge e^b \wedge e^c$ is the volume form and

$$V(\phi) = -\frac{1}{2}(\phi^2 - 1)^2. \quad (6.17)$$

This is the action of a Newtonian particle subjected to a potential $V(\phi)$. Hence, the equation of motion for the scalar degree of freedom ϕ is

$$\ddot{\phi} = -\frac{\partial V}{\partial \phi} = 2\phi(\phi^2 - 1). \quad (6.18)$$

The solutions for this equation can be parametrised in terms of the “initial time” u_0 and the mechanical energy $E = \frac{1}{2} \dot{\phi}^2 + V(\phi)$. If $E \in [-\frac{1}{2}, 0]$, the bounded solutions can be written in terms of the Jacobi sine function as

$$\phi_{E,u_0}(u) = f_-(E) \text{sn}(f_+(E)(u-u_0), k), \quad (6.19)$$

where

$$f_{\pm}(E) = \sqrt{1 \pm \sqrt{-2E}} \quad \text{and} \quad k^2 = \frac{f_-(E)}{f_+(E)}. \quad (6.20)$$

Limiting cases for $E \in \{-\frac{1}{2}, 0\}$ are

$$\phi = \begin{cases} 0 & \text{for } E = -\frac{1}{2}, \\ \tanh(u-u_0) & \text{for } E = 0, \\ \pm 1 & \text{for } E = 0. \end{cases} \quad (6.21)$$

Scattering solutions can be found for both positive and negative E . For $E > 0$, we have

$$\phi_{E,u_0}(u) = \frac{1}{\sqrt{2k^2-1}} \frac{1 + \text{cn}\left(\frac{2}{\sqrt{2k^2-1}}(u-u_0), k\right)}{\text{sn}\left(\frac{2}{\sqrt{2k^2-1}}(u-u_0), k\right)}, \quad \text{with} \quad E = -\frac{2k^2(k^2-1)}{(2k^2-1)^2}, \quad (6.22)$$

while, for $E < 0$,

$$\phi_{E,u_0}(u) = \sqrt{\frac{2k^2}{2k^2-1}} \text{cn}\left(\sqrt{\frac{2}{1-2k^2}}(u-u_0), k\right), \quad \text{with} \quad E = -\frac{1}{2(2k^2-1)^2}. \quad (6.23)$$

For any solution ϕ , we can use (6.8) to pull the gauge field back to the Minkowski space. The one-forms in both spaces are related according to

$$e^u = \frac{t \text{d}t - r \text{d}r}{t^2 - r^2} \quad \text{and} \quad e^a = \frac{1}{|x|} \left(\text{d}x^a - \frac{x^a}{|x|} \text{d}t + \frac{x^a}{|x|(|x|+t)} r \text{d}r \right), \quad (6.24)$$

where

$$r := \sqrt{\vec{x} \cdot \vec{x}} \quad \text{and} \quad |x| := \sqrt{|x \cdot x|} = \sqrt{|t^2 - r^2|}. \quad (6.25)$$

Hence, using the abbreviation $\phi(x) := \phi_{E,\mu_0}(u(x))$, the gauge field A on Minkowski space reads

$$A = \frac{1}{|x|} \left\{ \frac{\varepsilon_{ab}^k x^a}{|x|+t} dx^b T_k + \phi(x) \left(dx^a - \frac{x^a}{|x|} dt + \frac{x^a}{|x|(|x|+t)} r dr \right) T_a \right\} \quad (6.26)$$

and the field-strength tensor $F = F_{\mu\nu} dx^\mu \wedge dx^\nu$ can be written in terms of the colour-electric and -magnetic fields

$$\begin{aligned} E_a &= \frac{1}{|x|^3} \left\{ (\phi^2 - 1) \varepsilon_{ab}^i x^b T_i - \phi \left(t \delta^{ab} - \frac{x^a x^b}{|x|+t} \right) T_b \right\}, \quad \text{and} \\ B_a &= -\frac{1}{|x|^3} \left\{ (\phi^2 - 1) \left(t \delta^{ai} - \frac{x^a x^i}{|x|+t} \right) T_i + \phi \varepsilon_{ab}^c x^b T_c \right\}. \end{aligned} \quad (6.27)$$

Finally, the stress-energy tensor

$$T_{\mu\nu} = -\text{tr}_{\text{ad}} \left(F_{\mu\alpha} F_{\nu\beta} \eta^{\alpha\beta} - \frac{1}{4} \eta_{\mu\nu} F^2 \right), \quad \text{with} \quad F^2 = F_{\mu\nu} F^{\mu\nu}, \quad (6.28)$$

reads, explicitly,

$$T = \frac{E}{(r^2 - t^2)^3} \begin{pmatrix} 3t^2 + r^2 & -4tx & -4ty & -4tz \\ -4tx & t^2 + 4x^2 - r^2 & 4xy & 4xz \\ -4ty & 4xy & t^2 + 4y^2 - r^2 & 4yz \\ -4tz & 4xz & 4yz & t^2 + 4z^2 - r^2 \end{pmatrix}. \quad (6.29)$$

The gauge field, the field-strength tensor, and the stress-energy tensor are all singular on the lightcone $t = \pm r$. However, for now, the fields are only defined within the lightcone. This will be addressed later when we try to extend such fields to the entirety of the Minkowski space. Now, let us consider the same procedure outside the lightcone.

6.1.3 Exterior of the lightcone \mathcal{S}

The procedure to build a foliation, employ the equivariant Ansatz, and obtain the gauge fields in the corresponding part of the Minkowski space is very similar on the outside of the lightcone, here denoted as \mathcal{S} . Here, the chosen base vector is $x_{\mathcal{S}} = (0, 0, 0, 1)$ and its stabiliser subgroup is $H = \text{SO}(1, 2)$. The foliation will then be constructed from sheets of the three-dimensional de Sitter space $d\mathcal{S}_3$ embedded in $\mathbb{R}^{1,3} \ni y$ with

$$y \cdot y = \eta_{\mu\nu} y^\mu y^\nu = 1. \quad (6.30)$$

Once more, the identification with the coset is made explicit through

$$\begin{aligned} \alpha_{\mathcal{S}} : \text{SO}(1, 3) / \text{SO}(1, 2) &\rightarrow d\mathcal{S}_3, \quad [\Lambda_{\mathcal{S}}] \mapsto y^\mu = (\Lambda_{\mathcal{S}})^\mu{}_\nu x_{\mathcal{S}}^\nu, \\ \alpha_{\mathcal{S}}^{-1} : d\mathcal{S}_3 &\rightarrow \text{SO}(1, 3) / \text{SO}(1, 2), \quad y^\mu \mapsto [\Lambda_{\mathcal{S}}], \end{aligned} \quad (6.31)$$

where $[\Lambda_S] = \{\Lambda \in \text{SO}(1,3) : \Lambda \sim \Lambda_S\}$ is the equivalence class under right $\text{SO}(1,2)$ -multiplication. Once more, the map from the equivalence class is only well-defined since $\text{SO}(1,2)$ is the stabiliser of x_S . The foliation of \mathcal{S} is then performed with the map

$$\begin{aligned} \varphi_S : \mathbb{R} \times dS_3 &\rightarrow \mathcal{S}, & (u, y^\mu) &\mapsto x^\mu := e^\mu y^\mu, \\ \varphi_S^{-1} : \mathcal{S} &\rightarrow \mathbb{R} \times dS_3, & x^\mu &\mapsto (u, y^\mu) := \left(\ln \sqrt{|x \cdot x|}, \frac{x^\mu}{\sqrt{|x \cdot x|}} \right). \end{aligned} \quad (6.32)$$

The metric of the cylinder over the deSitter space will also be conformal to that of the Minkowski space. However, in this case, the generators of $\mathfrak{so}(1,3)$ will be split according to

$$T_i \in \{K_1, K_2, J_3\} \quad \text{and} \quad T_a \in \{J_1, J_2, K_3\}. \quad (6.33)$$

It is straightforward to get the structure constants from (2.28) in terms of such a split and to compute the Cartan–Killing metric and the new splitted one-forms. They read

$$e^a = dy^{3-a} - \frac{y^{3-a}}{1+y^3} dy^3 \quad \text{and} \quad e^i = -\varepsilon_{iab} \frac{y^{3-a}}{1+y^3} dy^{3-b} \quad (6.34)$$

and are related through

$$e^i = \chi_a^i e^a, \quad \text{with} \quad \chi_a^i = \varepsilon_{iab} \frac{y^{3-b}}{1+y^3}. \quad (6.35)$$

In this case, the dS_3 metric is already Lorentzian. If $\tilde{\eta}_{ab} = \text{diag}(-1, 1, 1)$,

$$ds_{dS_3}^2 = \tilde{\eta}_{ab} e^a \otimes e^b, \quad (6.36)$$

and the cylinder $\mathbb{R} \times dS_3$ is an Euclidean foliation, with metric

$$ds^2 = e^\mu \otimes e^\mu + \tilde{\eta}_{ab} e^a \otimes e^b. \quad (6.37)$$

Up to the volume form in terms of Minkowski components, the reduced action in this case is identical to the one obtained in the interior of the lightcone (6.16), with the same potential $V(\phi) = -\frac{1}{2}(\phi^2 - 1)^2$. Hence, the reduced equation of motion for the scalar degree of freedom will be the same 6.18, as will be its solutions (6.19, 6.21, 6.22, 6.23).

Pulling the one-forms back to the Minkowski space with (6.32), we obtain

$$\begin{aligned} e^\mu := du &= \frac{r dr - t dt}{r^2 - t^2} \quad \text{and} \\ e^a &= \frac{1}{|x|} \left(dx^{3-a} - \frac{x^{3-a}}{|x|} dz - \frac{\eta_{bc} x^{3-a} x^{b-1}}{|x|(|x| + z)} dx^{c-1} \right). \end{aligned} \quad (6.38)$$

Then, the gauge potential in Minkowski coordinates reads

$$\begin{aligned} A &= \frac{1}{|x|} \left\{ \frac{\varepsilon_{cb}^i x^{3-b}}{|x| + z} dx^{3-c} T_i + \right. \\ &\quad \left. \phi(x) \left(dx^{3-a} - \frac{x^{3-a}}{|x|} dz - \frac{\eta_{bc} x^{3-a} x^{b-1}}{|x|(|x| + z)} dx^{c-1} \right) T_a \right\} \end{aligned} \quad (6.39)$$

and the colour-electric E_i and -magnetic B_i fields read

$$\begin{aligned}
E_1 &= \frac{1}{|x|^3} \left[\dot{\phi} (T_2 t + T_3 x) + (\phi^2 - 1) \left\{ -\frac{y}{|x|+z} (T_6 t - T_5 x - T_4 y) + T_4 z \right\} \right], \\
E_2 &= \frac{1}{|x|^3} \left[\dot{\phi} (T_1 t + T_3 y) + (\phi^2 - 1) \left\{ \frac{x}{|x|+z} (T_6 t - T_5 x - T_4 y) - T_5 z \right\} \right], \\
E_3 &= \frac{1}{|x|^3} \left[\dot{\phi} \left\{ -\frac{t}{|x|+z} (T_3 t + T_1 y + T_2 x) + T_3 z \right\} - (\phi^2 - 1) (T_4 x - T_5 y) \right], \\
B_1 &= \frac{1}{|x|^3} \left[-\dot{\phi} \left\{ \frac{y}{|x|+z} (T_3 t + T_1 y + T_2 x) + T_1 z \right\} + (\phi^2 - 1) (T_5 t - T_6 x) \right], \\
B_2 &= \frac{1}{|x|^3} \left[\dot{\phi} \left\{ \frac{x}{|x|+z} (T_3 t + T_1 y + T_2 x) + T_2 z \right\} - (\phi^2 - 1) (T_6 y - T_4 t) \right], \\
B_3 &= \frac{1}{|x|^3} \left[\dot{\phi} (T_1 x - T_2 y) + (\phi^2 - 1) \left\{ \frac{t}{|x|+z} (T_6 t - T_5 x - T_4 y) - T_6 z \right\} \right],
\end{aligned} \tag{6.40}$$

where here the two sets $\{T_a\}$ and $\{T_i\}$ are mixed, so we denoted the generators T_a with numerical labels 4, 5, and 6 to avoid confusion.

The stress-energy tensor of such fields in terms of the Minkowski coordinates comes out as identical to the previous one (6.29), from the interior of the lightcone \mathcal{T} , which, disregarding the divergent behaviour in the lightcone surface, seems to favour that the two sets of fields can be considered together for a field defined in the whole space. Before we discuss this relation further, let us complete the picture by looking into the lightcone surface.

6.1.4 Lightcone surface \mathcal{L}

This case differs from the previous two in the fact that the lightcone surface is not an open set of the Minkowski space, but a hypersurface. This already indicates that a foliation by orbits of $\text{SO}(1,3)$ will not be possible. In our construction, that means that there would be no dynamical variable u , implying that a field we construct in the lightcone using the equivariant Ansatz should be trivial. Let us confirm such observation.

The stabiliser subgroup of a vector in the lightcone can be easily computed using the double cover of the Lorentz group, $\text{SL}(2, \mathbb{C})$, and its action on the vector space of 2×2 Hermitian matrices, isomorphic to $\mathbb{R}^{1,3}$. In this case, $H = \text{E}(2) = \text{ISO}(2)$, the Euclidean group, which is generated by two translations and one rotation. Choosing as base vector $x_{\mathcal{L}} = (1, 0, 0, 1)$, the subalgebra \mathfrak{h} of the stabiliser subgroup is generated by $\{P_3, P_4, J_3\}$, with

$$P_3 := K_1 - J_2 = \begin{pmatrix} 0 & 1 & 0 & 0 \\ 1 & 0 & 0 & -1 \\ 0 & 0 & 0 & 0 \\ 0 & 1 & 0 & 0 \end{pmatrix} \quad \text{and} \quad P_4 := K_2 + J_1 = \begin{pmatrix} 0 & 0 & 1 & 0 \\ 0 & 0 & 0 & 0 \\ 1 & 0 & 0 & -1 \\ 0 & 0 & 1 & 0 \end{pmatrix} \tag{6.41}$$

acting as generators of translations. The translations are orthogonal to themselves with respect to the Cartan–Killing metric of \mathfrak{g} and there is no orthogonal complement to \mathfrak{h} . However, we can still define \mathfrak{m} spanned by $\{P_1, P_2, K_3\}$, with

$$P_1 := K_1 + J_2 = \begin{pmatrix} 0 & 1 & 0 & 0 \\ 1 & 0 & 0 & 1 \\ 0 & 0 & 0 & 0 \\ 0 & -1 & 0 & 0 \end{pmatrix} \quad \text{and} \quad P_2 := K_2 - J_1 = \begin{pmatrix} 0 & 0 & 1 & 0 \\ 0 & 0 & 0 & 0 \\ 1 & 0 & 0 & 1 \\ 0 & 0 & -1 & 0 \end{pmatrix}, \tag{6.42}$$

such that \mathfrak{m} respects $\mathfrak{g} = \mathfrak{h} \oplus \mathfrak{m}$ and will generate the coset G/H . Notice that the generated space is not symmetric or even reductive, as in the previous cases. In fact, here \mathfrak{m} forms a subalgebra classified as type-V in Bianchi's classification of 3-dimensional real Lie algebras [46], generated by two translations and one dilation.

Using the base vector $x_{\mathcal{L}_+}$, we can explicitly construct the map between the coset $\text{SO}(1,3)/\text{ISO}(2)$ and the future-half of the lightcone surface, \mathcal{L}_+ , as in the previous cases. It reads

$$\begin{aligned} \alpha_{\mathcal{L}_+} : \text{SO}(1,3)/\text{ISO}(2) \supset \exp(\mathfrak{m}) &\rightarrow \mathcal{L}_+, & [\Lambda_{\mathcal{L}_+}] &\mapsto y^\mu = (\Lambda_{\mathcal{L}_+})^\mu{}_\nu x_{\mathcal{L}_+}^\nu, \\ \alpha_{\mathcal{L}_+}^{-1} : \mathcal{L}_+ &\rightarrow \text{SO}(1,3)/\text{ISO}(2), & y^\mu &\mapsto [\Lambda_{\mathcal{L}_+}], \end{aligned} \quad (6.43)$$

where $[\Lambda_{\mathcal{L}_+}] = \{\Lambda \in \text{SO}(1,3) : \Lambda \sim \Lambda_{\mathcal{L}_+}\}$ is the equivalence class of the representative $\Lambda_{\mathcal{L}_+}$ under right $\text{ISO}(2)$ -multiplication.

If one chooses $(-1, 0, 0, 1)$ as base vector, the same construction could be employed for the past-half of the lightcone surface, with the only difference being that the splitting between \mathfrak{h} and \mathfrak{m} would be realised by

$$T_i \in \{P_1, P_2, J_3\} \quad \text{and} \quad T_a \in \{P_3, P_4, K_3\}. \quad (6.44)$$

Moreover, contrary to the previous cases, no scaling of the base vector can be used in a tentative foliation. Indeed, such a dilation is generated by K_3 , as

$$e^{uK_3} \cdot \begin{pmatrix} 1 \\ 0 \\ 0 \\ 1 \end{pmatrix} = \begin{pmatrix} e^u \\ 0 \\ 0 \\ e^u \end{pmatrix}. \quad (6.45)$$

One can still construct the Maurer–Cartan form $\Lambda_{\mathcal{L}_+}^{-1} d\Lambda_{\mathcal{L}_+} = e^a T_a$ and obtain, in spherical coordinates (t, r, θ, φ) for the lightcone surface ($|t| = r$),

$$\begin{aligned} e^1 &= \frac{r}{2} (\cos \varphi d\theta - \sin \theta \sin \varphi d\varphi), \\ e^2 &= \frac{r}{2} (\sin \varphi d\theta + \sin \theta \cos \varphi d\varphi), \quad \text{and} \\ e^3 &= \frac{1}{r} dr - \tan \frac{\theta}{2} d\theta, \end{aligned} \quad (6.46)$$

which form a local orthonormal frame on \mathcal{L}_+ with

$$ds_{\mathbb{R}^{1,3}}^2|_{\mathcal{L}_+} = 4e^1 \otimes e^1 + 4e^2 \otimes e^2. \quad (6.47)$$

The metric in this case is degenerate, as expected for the lightcone surface. One can use such one-forms to construct a non-zero Yang–Mills field \mathcal{A} on the lightcone surface, however, it will always be pure gauge, with $\mathcal{F} = 0$, as previously discussed.

6.1.5 Energy-momentum tensor

Using the conformal equivariance of the Yang–Mills theory in four dimensions and foliations of the Minkowski spacetime with cosets of the Lorentz group, we employed the equivariant Ansatz to construct gauge fields inside, outside, and on the lightcone surface. On the lightcone, the procedure results in pure-gauge Yang–Mills fields. On the other hand, the energy-momentum tensors (6.29) obtained on

both \mathcal{T} and \mathcal{S} were non-trivial and identical in Minkowski coordinates, reading

$$T_{\mu\nu} = \epsilon \frac{4x_\mu x_\nu - \eta_{\mu\nu} x \cdot x}{(x \cdot x)^3}. \quad (6.48)$$

On the lightcone surface, it diverges as $|x \cdot x|^{-3/2}$. Furthermore, we can show that this energy-momentum tensor is of a pure ‘‘improvement’’ form

$$T_{\mu\nu} = \partial^\rho S_{\rho\mu\nu}, \quad \text{with} \quad S_{\rho\mu\nu} = \epsilon \frac{x_\rho \eta_{\mu\nu} - x_\mu \eta_{\rho\nu}}{(x \cdot x)^2}, \quad (6.49)$$

suggesting that the total energy and momentum may not diverge, but vanish on any given spatial slice, given that it has an adequate fall-off at spatial infinity. However, the singularity on the lightcone has to be considered, hence, energy and momentum integrals reduce to a divergent boundary term on the lightcone. A matching of solutions in \mathcal{T} and \mathcal{S} then require an adequate regularisation across the lightcone, where all densities change sign due to the denominator of (6.48). It is worth noticing that the standard principal-value prescription is not sufficient since the pole is of third order, but a fine-tuned prescription can remove all poles. Alternatively, additional degrees of freedom localised on the lightcone may provide a source which compensates for the singularity, which was left to be explored in possible follow-up works.

6.2 SU(1, 1) gauge theory on AdS₄

In chapter 5, we discussed how the geometric structure of a cylinder over the three-sphere S^3 , which is a foliation of the deSitter space dS_4 , can be explored in order to straightforwardly construct gauge fields on it. We then discussed the abelian case, which, using a conformal map to Minkowski space, gave rise to the basis of electromagnetic knots. In chapter 7, we will discuss a cosmological application of the non-abelian version of this construction. In this section, we will explore whether the hyperbolic version of this construction gives rise to physically relevant results, discussing both the abelian and the non-abelian versions, and exploring a conformal map to the Minkowski space.

Even in the classical theory, it is relevant to address the viability of constructing a physical gauge theory on AdS₄ or foliations thereof due to the presence of closed timelike curves and the lack of global hyperbolicity. For the former, one can simply work in the universal covering space $\widetilde{\text{AdS}}_4$, with an ‘‘unwrapped’’ timelike coordinate. For the latter, we point out that the timelike boundary at spatial infinity can be dealt with by using special boundary conditions and constructing an ‘‘effective’’ Cauchy surface, as discussed in details in [47]. That said, let us proceed to the explicit construction.

6.2.1 AdS₄, coframe, and map to Minkowski

The geometry of the anti-deSitter space has already been discussed in Section 3.4 where we showed that AdS₄ can be written as a warped Euclidean cylinder over AdS₃ according to (3.48),

$$ds_{\text{AdS}_4}^2 = \ell^2 [dz^2 + \cosh(z)^2 d\Omega_{1,2}^2], \quad (6.50)$$

or, up to a conformal factor, as a straight cylinder, according to (3.50),

$$ds_{\text{AdS}_4}^2 = \frac{\ell^2}{\cos(Z)^2} [dZ^2 + d\Omega_{1,2}^2], \quad (6.51)$$

where ℓ is the anti-deSitter radius and $Z \in \mathcal{I}_Z := (-\frac{\pi}{2}, +\frac{\pi}{2})$. Here, the AdS_3 will be parametrised as the three-dimensional version of (3.45), that is,

$$d\Omega_{1,2}^2 = d\rho^2 - \cosh(\rho)^2 d\tau^2 + \sinh(\rho)^2 d\phi^2, \quad (6.52)$$

with

$$\tau \in \mathcal{I}_\tau := [-\pi, \pi], \quad \rho \in \mathbb{R}_+, \quad \text{and} \quad \theta \in [0, 2\pi]. \quad (6.53)$$

This foliation allows us to make use of the fact that

$$\text{AdS}_3 \simeq \text{PSL}(2, \mathbb{R}) \simeq \text{SU}(1, 1) / \{\pm \text{Id}\} \quad (6.54)$$

is a group manifold in order to easily construct a coframe, in accordance with Section 2.4. The Lie algebra $\mathfrak{su}(1, 1) \simeq \mathfrak{sl}(2, \mathbb{R})$ is generated by

$$T_0 = \begin{pmatrix} -i & 0 \\ 0 & i \end{pmatrix}, \quad T_1 = \begin{pmatrix} 0 & 1 \\ 1 & 0 \end{pmatrix}, \quad T_2 = \begin{pmatrix} 0 & -i \\ i & 0 \end{pmatrix}, \quad (6.55)$$

where

$$[T_\alpha, T_\beta] = 2f_{\alpha\beta}^\gamma T_\gamma \quad \text{and} \quad \text{tr}(T_\alpha T_\beta) = 2\eta_{\alpha\beta}, \quad (6.56)$$

with $[\eta_{\alpha\beta}] = \text{diag}(-1, 1, 1)$ and the non-zero structure constants being

$$f_{01}^2 = f_{20}^1 = 1 = -f_{12}^0. \quad (6.57)$$

Hence, we can use the identification

$$g : \text{AdS}_3 \rightarrow \text{SU}(1, 1) \\ (\alpha^1, \alpha^2, \alpha^3, \alpha^4) \mapsto \begin{pmatrix} \alpha^1 - i\alpha^2 & \alpha^3 - i\alpha^4 \\ \alpha^3 + i\alpha^4 & \alpha^1 + i\alpha^2 \end{pmatrix} \quad (6.58)$$

to construct the $\text{SU}(1, 1)$ left-invariant one-forms $\{e^\alpha\}$. They read

$$\begin{aligned} e^0 &= \cosh^2 \rho \, d\tau + \sinh^2 \rho \, d\phi, \\ e^1 &= \cos(\tau - \phi) \, d\rho + \sinh \rho \, \cosh \rho \, \sin(\tau - \phi) \, d(\tau + \phi), \\ e^2 &= -\sin(\tau - \phi) \, d\rho + \sinh \rho \, \cosh \rho \, \cos(\tau - \phi) \, d(\tau + \phi), \end{aligned} \quad (6.59)$$

such that the metric on AdS_4 is conformal to

$$ds_{\text{cyl}}^2 = \eta_{\alpha\beta} e^\alpha e^\beta + dZ^2 = -(e^0)^2 + (e^1)^2 + (e^2)^2 + (e^3)^2, \quad (6.60)$$

with $e^3 := e^Z$.

Before we start working with the Yang–Mills theory in this setting, let us discuss the map from the foliation of AdS_4 to Minkowski space, which will be used later. We

will break it in two steps. First, we fix τ and ϕ and consider

$$\begin{aligned} g_1 : \mathcal{I}_Z \times \text{AdS}_3 &\rightarrow \mathcal{I}_\tau \times S_+^3 \\ (\tau, \rho, Z, \phi) &\mapsto (\tau, \lambda, \theta, \phi), \end{aligned} \quad (6.61)$$

with $(\lambda, \theta) \in \mathbb{R}_+ \times [0, \pi]$, such that

$$\tanh \rho = \sin \theta \tanh \lambda \quad \text{and} \quad \tan Z = -\cos \theta \sinh \lambda. \quad (6.62)$$

The metric then reads

$$\frac{ds_{\text{AdS}_4}^2}{\ell^2} = -\cosh^2 \lambda d\tau^2 + d\lambda^2 + \sinh^2 \lambda d\Omega_2^2, \quad \text{with} \quad d\Omega_2^2 = d\theta^2 + \sin^2 \theta d\phi^2, \quad (6.63)$$

expliciting that the constant- τ leaves are hyperbolic spaces H^3 . Equivalently, we could have taken this first step with a compactified radial coordinate χ . Choose

$$\sinh \lambda = \tan \chi, \quad \text{where} \quad \lambda \in \mathbb{R}_+ \implies \chi \in \left[0, \frac{\pi}{2}\right). \quad (6.64)$$

Then, (6.63) would instead read

$$ds_{\text{AdS}_4}^2 = \frac{\ell^2}{\cos^2 \chi} (-d\tau^2 + d\chi^2 + \sin^2 \chi d\Omega_2^2) = \frac{\ell^2}{\cos^2 \chi} (-d\tau^2 + d\Omega_{3+}^2), \quad (6.65)$$

which is a foliation where the leaves are the upper hemisphere S_+^3 of $S^3 = S_+^3 \cup S^2 \cup S_-^3$. Those two maps show that $\text{AdS}_4 \simeq S^1 \times H^3 \simeq S^1 \times S_+^3$.

In Section 5.2, we discussed a conformal map from a Lorentzian cylinder over S^3 to Minkowski space in terms of both its cartesian (t, x, y, z) and polar (t, r, θ, ϕ) coordinates. We can compose the same map (5.56) with the $\mathcal{I}_\tau \times S_+^3$ foliation, however, the foliations above would only cover the half of the Minkowski space that correspond to S_+^3 . Hence, let us insert a parameter $\varepsilon = \pm 1$ and take a second copy, with $\varepsilon = -1$, of the AdS_4 foliation in order to cover the other half of $\mathbb{R}^{1,3}$, with

$$\begin{cases} \tanh \rho = \sin \theta \tanh \lambda = \varepsilon \sin \theta \sin \chi \\ \tan Z = -\varepsilon \cos \theta \sinh \lambda = -\varepsilon \cos \theta \tan \chi \end{cases}. \quad (6.66)$$

Each one of the maps, with $\varepsilon = \pm 1$, will cover each half of the Minkowski space. Explicitly, they correspond to

$$\begin{aligned} \varepsilon = +1 : \quad \rho, \lambda \in \mathbb{R}_+, \chi \in [0, \frac{\pi}{2}) &\Leftrightarrow \text{northern hemisphere } S_+^3 \\ \varepsilon = -1 : \quad \rho, \lambda \in \mathbb{R}_-, \chi \in (\frac{\pi}{2}, \pi] &\Leftrightarrow \text{southern hemisphere } S_-^3. \end{aligned} \quad (6.67)$$

Hence, using the exact same description as in (5.51-5.56), the metric will then read

$$\begin{aligned} ds^2 &= \frac{4\ell^4}{(r^2 - t^2 - \ell^2)^2} (-dt^2 + dx^2 + dy^2 + dz^2) \\ &= \frac{4\ell^4}{(r^2 - t^2 - \ell^2)^2} (-dt^2 + dr^2 + r^2 d\Omega_2^2) \end{aligned} \quad (6.68)$$

and we cover the entire Minkowski space with the exception of the three-dimensional hypersurface $\chi = \pi/2$, in which $r^2 - t^2 = \ell^2$, such that the conformal factor diverges. This issue will be considered separately later. The $\varepsilon = +1$ map covers the

spatial exterior of the hyperboloid $r^2 - t^2 = \ell^2$, while the $\varepsilon = -1$ one covers its interior. From the relations

$$\cos \tau = \frac{\gamma}{2\ell^2} (r^2 - t^2 + \ell^2), \quad \cos \chi = \frac{\gamma}{2\ell^2} (r^2 - t^2 - \ell^2), \quad (6.69)$$

and (5.52), respectively, we can consider the boundary of the χ -interval and assume $t \neq 0$ to conclude that the north pole $\chi = 0$ is mapped into spatial infinity $r = +\infty$ of the Minkowski space while the south pole $\chi = \pi$ is mapped into $r = 0$. Figure 6.1 illustrates the two glued AdS_4 covering the Minkowski space in a Penrose diagram. For more details on the boundary between the two copies on the different parametrisations, we refer the reader to [48].

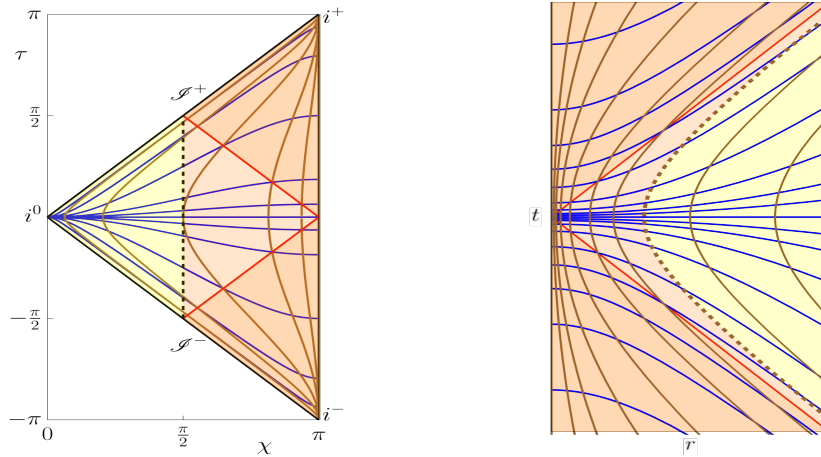


FIGURE 6.1: Illustration of two copies of AdS_4 covering the Minkowski space.

Left: Penrose diagram in (χ, τ) . Lightcone in red, constant- t lines in blue, constant- r lines in brown, and hyperboloid separating the two copies of AdS_4 in dashed black.

Right: (t, r) diagram of Minkowski space. Lightcone in red, constant- τ lines in blue, constant- χ lines in brown, and hyperboloid separating the two copies of AdS_4 in dashed brown.

With the conformal maps from AdS_4 to the cylinder over S^3_{\pm} then to $\mathbb{R}^{1,3}$, we straightforwardly pull the one-forms back from the anti-deSitter space. On the cylinder, they read

$$\begin{aligned} e^0 &= \frac{(d\tau + \sin^2\chi \sin^2\theta d\phi)}{1 - \sin^2\chi \sin^2\theta}, \\ e^1 &= \frac{\varepsilon [\cos(\tau - \phi)(\cos\chi \sin\theta d\chi + \sin\chi \cos\theta d\theta) + \sin\chi \sin\theta \sin(\tau - \phi)d(\tau + \phi)]}{1 - \sin^2\chi \sin^2\theta}, \\ e^2 &= \frac{-\varepsilon [\sin(\tau - \phi)(\cos\chi \sin\theta d\chi + \sin\chi \cos\theta d\theta) - \sin\chi \sin\theta \cos(\tau - \phi)d(\tau + \phi)]}{1 - \sin^2\chi \sin^2\theta}, \\ e^3 &= \frac{-\varepsilon(\cos\theta d\chi - \sin\chi \cos\chi \sin\theta d\theta)}{1 - \sin^2\chi \sin^2\theta}. \end{aligned} \quad (6.70)$$

Defining, for simplicity, ε^α such that $\varepsilon^0 := 1$ and $\varepsilon^1 = \varepsilon^2 := \varepsilon$, the one-forms in cartesian Minkowski coordinates read

$$\begin{aligned} e^\alpha &= \frac{\ell \varepsilon^\alpha}{\kappa^2 + 4\ell^2 z^2} (2(\kappa + 2\ell^2) dx^\alpha - 4x^\alpha x \cdot dx - 4\ell f_{\beta\gamma}^\alpha x^\beta dx^\gamma), \\ e^Z &= \frac{\ell \varepsilon}{\kappa^2 + 4\ell^2 z^2} (-2\kappa dz + 4z x \cdot dx), \end{aligned} \quad (6.71)$$

where $\kappa := r^2 - t^2 - \ell^2 = x^2 + y^2 + z^2 - t^2 - \ell^2$.

Even though the conformal factor in (6.68) diverges on the three-dimensional hyperboloid $\kappa = 0$, the one-forms surprisingly only diverge on the two-dimensional hyperboloid defined by $\kappa = z = 0$, or, in terms of the cylinder over S^3 , $\chi = \theta = \pi/2$. Consequently, we will see that the field strength is well-defined along $\kappa = 0$ as long as $z \neq 0$, which already allows us to extend the Minkowski solutions beyond the original domain of validity of the conformal map.

6.2.2 Equivariant Yang–Mills fields

With the left-invariant one-forms on foliations of AdS_4 and on $\mathbb{R}^{1,3}$ in hand, we can construct gauge fields in such foliations and, once more exploring the conformal invariance of the four-dimensional Yang–Mills theory, map them into the Minkowski space. Consider the $\mathfrak{su}(1,1)$ -valued gauge field \mathcal{A} and its field strength \mathcal{F} on $\mathcal{I} \times \text{AdS}_3$:

$$\mathcal{A} = \mathcal{A}_3 e^3 + \mathcal{A}_\alpha e^\alpha \quad \Longrightarrow \quad \mathcal{F} = \mathcal{F}_{3\alpha} e^3 \wedge e^\alpha + \frac{1}{2} \mathcal{F}_{\beta\gamma} e^\beta \wedge e^\gamma. \quad (6.72)$$

The $\text{SU}(1,1)$ symmetry suggests a “temporal” gauge $\mathcal{A}_3 = 0$. Taking the equivariant Ansatz, the $\mathfrak{su}(1,1)$ components of the gauge field may only depend on the foliation parameter Z :

$$\mathcal{A} = X_\alpha(Z) e^\alpha \quad \Longrightarrow \quad \mathcal{F} = X'_\alpha e^3 \wedge e^\alpha + \frac{1}{2} (-2f_{\beta\gamma}^\alpha X_\alpha + [X_\beta, X_\gamma]) e^\beta \wedge e^\gamma, \quad (6.73)$$

where $X'_\alpha := \frac{dX_\alpha}{dZ}$. Then, the Yang–Mills Lagrangian reduces to

$$\begin{aligned} \mathcal{L} &= \frac{1}{4} \text{tr} \mathcal{F}_{3\alpha} \mathcal{F}^{3\alpha} + \frac{1}{8} \text{tr} \mathcal{F}_{\beta\gamma} \mathcal{F}^{\beta\gamma} = \text{tr} \left\{ \frac{1}{4} ((X'_1)^2 + (X'_2)^2 - (X'_0)^2) + \right. \\ &\quad \left. - (X_1 - \frac{1}{2}[X_2, X_0])^2 - (X_2 - \frac{1}{2}[X_0, X_1])^2 + (X_0 + \frac{1}{2}[X_1, X_2])^2 \right\}. \end{aligned} \quad (6.74)$$

From (6.74), we will investigate two different Ansätze to simplify and allow us to solve the dynamics of the gauge fields: the non-abelian equivariant Ansatz and an abelian reduction. From now on, let us set $\ell = 1$ for simplicity, since it can always be reinstated from dimensional analysis.

The equivariant Ansatz imposes $\mathcal{A} \propto T_\alpha e^\alpha$. Hence, we will choose the proportionality factor as

$$X_\alpha = \frac{1}{2} (1 + \Phi(Z)) T_\alpha, \quad (6.75)$$

for convenience. The equivariant gauge field then reads

$$\mathcal{A} = \frac{1}{2} (1 + \Phi(Z)) T_\alpha e^\alpha \quad (6.76)$$

and, its field strength,

$$\mathcal{F} = \frac{1}{2} \Phi'(Z) T_\alpha e^3 \wedge e^\alpha - \frac{1}{4} (1 - \Phi(Z)^2) T_\alpha f_{\beta\gamma}^\alpha e^\beta \wedge e^\gamma. \quad (6.77)$$

With such field strength, the Lagrangian (6.74) further reduces to that of a Newtonian particle subjected to a straight quartic potential,

$$\mathcal{L} = \frac{3}{4} \left\{ \frac{1}{2} (\Phi')^2 - \frac{1}{2} (1 - \Phi^2)^2 \right\}, \quad (6.78)$$

with $V(\Phi) = \frac{1}{2} (\Phi^2 - 1)^2$. This potential is inverted with respect to the one in (6.18). The equation of motion for the scalar degree of freedom is

$$\Phi'' = 2\Phi(1 - \Phi^2) = -\frac{\partial V}{\partial \Phi}. \quad (6.79)$$

In this case, all solutions are bounded, and can once more be expressed in terms of Jacobi elliptic functions. Conservation of energy implies that

$$\frac{1}{2} \dot{\Phi}^2 + V(\Phi) = E = \text{const}, \quad (6.80)$$

such that the solutions will be periodic with period $T(E)$, up to a few exceptions. Fixing E and employing time translation invariance to set $\Phi(0) = 0$, we determine the classical solutions $\Phi(Z)$ up to half-period translations. Defining k and ϵ such that

$$2\epsilon^2 = 2k^2 - 1 = 1/\sqrt{2E}, \quad \text{with } k = \frac{1}{\sqrt{2}}, 1, \infty \Leftrightarrow E = \infty, \frac{1}{2}, 0, \quad (6.81)$$

we can express the solutions as

$$\Phi(Z) = \begin{cases} \frac{k}{\epsilon} \text{cn}\left(\frac{Z}{\epsilon}, k\right) & \text{with } T = 4\epsilon K(k) & \text{for } \frac{1}{2} < E < \infty \\ 0 & \text{with } T = \infty & \text{for } E = \frac{1}{2} \\ \pm \sqrt{2} \text{sech}(\sqrt{2}Z) & \text{with } T = \infty & \text{for } E = \frac{1}{2} \\ \pm \frac{k}{\epsilon} \text{dn}\left(\frac{kZ}{\epsilon}, \frac{1}{k}\right) & \text{with } T = 2\frac{\epsilon}{k} K\left(\frac{1}{k}\right) & \text{for } 0 < E < \frac{1}{2} \\ \pm 1 & \text{with } T = \pi & \text{for } E = 0 \end{cases}, \quad (6.82)$$

where cn and dn denote Jacobi elliptic functions and K is the complete elliptic integral of the first kind. It is worth noticing that the action of such field configurations is infinite, since the AdS_3 slices have an infinite volume. Finally, the energy-momentum tensor is computed through

$$\begin{cases} \mathcal{T}_{\alpha\beta} = -\frac{1}{2} \text{tr} \{ \mathcal{F}_{\alpha 3} \mathcal{F}_{\beta 3} + \mathcal{F}_{\alpha\gamma} \mathcal{F}_{\beta\delta} \eta^{\gamma\delta} - \frac{1}{4} \eta_{\alpha\beta} \mathcal{F}^2 \} \\ \mathcal{T}_{33} = -\frac{1}{2} \text{tr} \{ \mathcal{F}_{3\gamma} \mathcal{F}_{3\delta} \eta^{\gamma\delta} - \frac{1}{4} \mathcal{F}^2 \} \end{cases}, \quad (6.83)$$

with $\mathcal{F}^2 \equiv 2\mathcal{F}_{3\delta} \mathcal{F}^{3\delta} + \mathcal{F}_{\gamma\delta} \mathcal{F}^{\gamma\delta}$ and $\mathcal{T}_{\alpha 3} = 0$. Explicitly,

$$\begin{pmatrix} \mathcal{T}_{\alpha\beta} & \mathcal{T}_{\alpha 3} \\ \mathcal{T}_{3\beta} & \mathcal{T}_{33} \end{pmatrix} = \frac{1}{2} \begin{pmatrix} \rho & 0 & 0 & 0 \\ 0 & -\rho & 0 & 0 \\ 0 & 0 & -\rho & 0 \\ 0 & 0 & 0 & 3\rho \end{pmatrix}, \quad (6.84)$$

with the energy density ρ reading

$$\rho = -\frac{1}{2}\text{tr}(\mathcal{E}_\alpha\mathcal{E}_\alpha + \mathcal{B}_\alpha\mathcal{B}_\alpha) = -\frac{1}{4}((\Phi')^2 + (1-\Phi^2)^2). \quad (6.85)$$

Since ρ is negative, we can see that the contribution from the non-compact generators dominate the energy density on the anti-deSitter space.

After completely obtaining the Yang–Mills fields on AdS_4 , it is straightforward to explore the conformal invariance of the theory to compute the corresponding solutions on the Minkowski space from the one-forms (6.71). For simplicity, we can combine the colour-electric and -magnetic fields on Minkowski space in terms of the Riemann-Silberstein vector $\vec{S} = \vec{E} + i\vec{B}$, then

$$\begin{aligned} (E+iB)_x &= -C \left\{ 2[ty+ix(z+i)]T_0 + 2\varepsilon[xy+it(z+i)]T_1 + \varepsilon[t^2-x^2+y^2+(z+i)^2]T_2 \right\} \\ (E+iB)_y &= C \left\{ 2[tx-iy(z+i)]T_0 + \varepsilon[t^2+x^2-y^2+(z+i)^2]T_1 + 2\varepsilon[xy-it(z+i)]T_2 \right\}, \quad (6.86) \\ (E+iB)_z &= C \left\{ i[t^2+x^2+y^2-(z+i)^2]T_0 + 2\varepsilon[itx-y(z+i)]T_1 + 2\varepsilon[ity+x(z+i)]T_2 \right\} \end{aligned}$$

where all the dependence on $\Phi(Z(t, x, y, z))$ is in the pre-factor C , with

$$C = \frac{2(i\varepsilon\Phi' + \Phi^2 - 1)}{(\kappa - 2iz)(\kappa + 2iz)^2}. \quad (6.87)$$

The energy-momentum tensor does not depend on ε and its expression is valid throughout the Minkowski space, with the exception of the $\kappa = z = 0$ two-dimensional hyperboloid. It reads

$$[T_{\mu\nu}] = \frac{8\rho}{(\kappa^2 + 4z^2)^3} \begin{pmatrix} \mathfrak{t}_{\alpha\beta} & \mathfrak{t}_{\alpha 3} \\ \mathfrak{t}_{3\alpha} & \mathfrak{t}_{33} \end{pmatrix}, \quad (6.88)$$

where

$$\begin{aligned} \mathfrak{t}_{\alpha\beta} &= -\eta_{\alpha\beta}(\kappa^2 + 4z^2) + 16x_\alpha x_\beta z^2, \\ \mathfrak{t}_{3\alpha} &= \mathfrak{t}_{\alpha 3} = -8x_\alpha z(\kappa - 3z^2), \quad \text{and} \\ \mathfrak{t}_{33} &= 3\kappa^2 - 4z^2(1 + 4\kappa - 4z^2). \end{aligned} \quad (6.89)$$

Once more, the dependence on the specific solution $\Phi(Z(t, x, y, z))$ is only found in ρ , which carries a non-trivial dependence on the cartesian coordinates. The energy density in the Minkowski space is illustrated in Figures 6.2 and 6.3. Physical applications for such non-abelian gauge fields are still open for future investigations. Let us now discuss the abelian reduction of the theory.

6.2.3 Abelian reduction

Let us go back to equations (6.73-6.74), before we chose to employ the equivariant Ansatz. At this stage, the simplest way of reducing the theory to that of an abelian gauge field is to single out a single generator as the only one with non-trivial contribution, then we would derive physical electromagnetic fields on Minkowski space. Let us choose to keep, for example, the contribution of the T_0 generator, with

$$X_0 = h(Z) T_0 \quad \text{and} \quad X_1 = X_2 = 0. \quad (6.90)$$

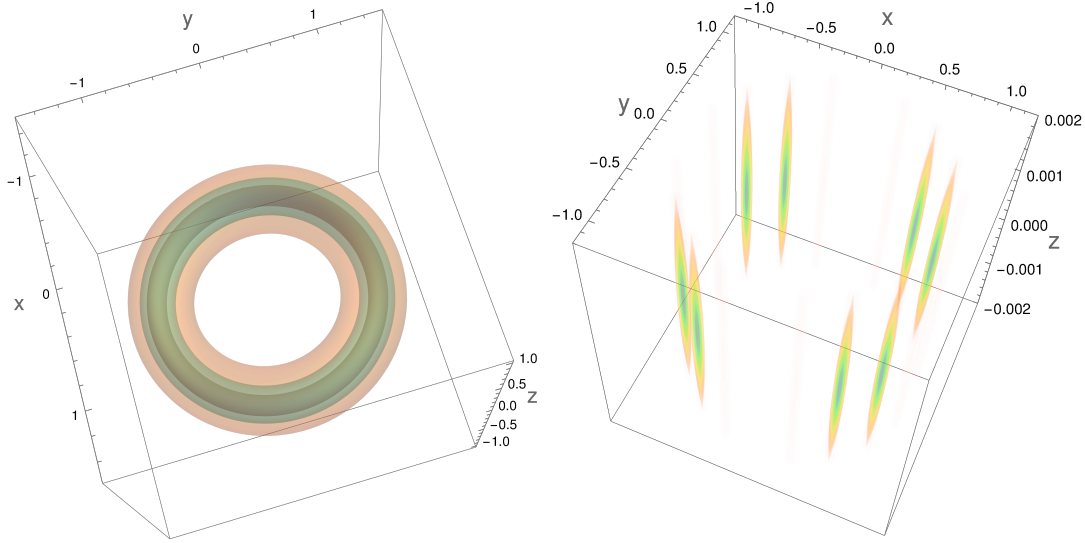


FIGURE 6.2: Energy density of the equivariant $SU(1,1)$ gauge field mapped into Minkowski space. Left: Level sets for the values 10 (orange), 100 (cyan), and 1000 (brown). Right: Density plot emphasizing the maxima.

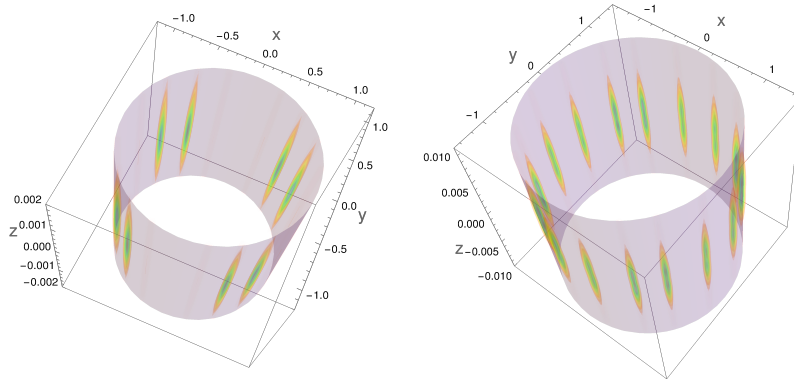


FIGURE 6.3: Illustration on the Minkowskian energy density largely concentrated on the hyperboloid $\kappa=0$ (gray) at two distinct values of time: $t=0$ (left) and $t=1$ (right).

The Ansatz (6.90) reduces (6.73) to

$$\mathcal{A} = h(Z) e^0 T_0 \quad \text{and} \quad \mathcal{F} = h'(Z) e^3 \wedge e^0 + 2h(Z) e^1 \wedge e^2, \quad (6.91)$$

that is, only the 0-th components of $[\mathcal{E}_\alpha]$ and $[\mathcal{B}_\alpha]$ will be non-zero. Furthermore, the Lagrangian (6.74) now reads

$$\mathcal{L} = \frac{1}{2} (h')^2 - 2h^2, \quad (6.92)$$

where $h' = dh/dZ$. This is simply the Lagrangian of a harmonic oscillator with angular frequency 2. It is worth noting that one could have equivalently chosen another generator to single out, or could have taken $X_1 = X_2 = X_0 = h(Z)T_0$, and (6.74) would be reduced to the same Lagrangian as in (6.92), but multiplied by a global factor of 3, which holds no physical relevance.

The equation of motion for the harmonic oscillator Lagrangian in h is

$$h'' = -4h, \quad (6.93)$$

which is solved in terms of Z by the general solution

$$h(Z) = -\frac{1}{2} f \cos 2(Z - Z_0) \quad (6.94)$$

in terms of the two parameters f and Z_0 . The energy-momentum tensor of such electromagnetic configuration is given by

$$[T_{\mu\nu}] = \begin{pmatrix} \tilde{\mathcal{T}}_{\alpha\beta} & \tilde{\mathcal{T}}_{\alpha 3} \\ \tilde{\mathcal{T}}_{3\beta} & \tilde{\mathcal{T}}_3 \end{pmatrix} = \frac{1}{2} \begin{pmatrix} \tilde{\rho} & 0 & 0 & 0 \\ 0 & \tilde{\rho} & 0 & 0 \\ 0 & 0 & \tilde{\rho} & 0 \\ 0 & 0 & 0 & -\tilde{\rho} \end{pmatrix}, \quad (6.95)$$

with energy density $\tilde{\rho} = (h')^2 + 4h^2 = f^2$. It is worth noticing that this is a non-null electrovacuum configuration on $\mathcal{I}_Z \times \text{AdS}_3$. Since Maxwell's theory is linear, let us set $f = 1$ from now on.

To find the corresponding electromagnetic fields on Minkowski space, we once more use the one-forms (6.71). Denoting x as the four-vector (t, x, y, z) , let us conveniently place an extra $\varepsilon = \pm 1$ to differentiate the arguments of the harmonic oscillators inside and outside the hyperboloid $\kappa = 0$ with

$$h(Z) = -\frac{1}{2} \cos 2(Z(\tilde{x}) + \varepsilon Z_0). \quad (6.96)$$

It is useful to define

$$\begin{aligned} h_1(x) &:= \cos 2(Z(x) + \varepsilon Z_0) = \frac{1}{\kappa^2 + 4z^2} (4z\kappa \sin 2Z_0 + (\kappa^2 - 4z^2) \cos 2Z_0), \\ h_2(x) &:= \sin 2(Z(x) + \varepsilon Z_0) = \frac{-\varepsilon}{\kappa^2 + 4z^2} (4z\kappa \cos 2Z_0 - (\kappa^2 - 4z^2) \sin 2Z_0). \end{aligned} \quad (6.97)$$

Hence, we can write the components of the electric and magnetic fields on Minkowski space as

$$\begin{aligned} E_1 &= h_1(x) q_1(x) + \varepsilon h_2(x) p_1(x), & B_1 &= -h_1(x) p_1(x) + \varepsilon h_2(x) q_1(x), \\ E_2 &= h_1(x) q_2(x) + \varepsilon h_2(x) p_2(x), & B_2 &= -h_1(x) p_2(x) + \varepsilon h_2(x) q_2(x), \\ E_3 &= h_1(x) q_3(x) + \varepsilon h_2(x) p_3(x), & B_3 &= -h_1(x) p_3(x) + \varepsilon h_2(x) q_3(x), \end{aligned} \quad (6.98)$$

where the functions $p_1(x), \dots, q_3(x)$ are given by

$$\begin{aligned} q_1(x) &= 2\tilde{C}(2xz^2 - \kappa(x - ty)), & p_1(x) &= -2\tilde{C}(\kappa xz + 2z(x - ty)), \\ q_2(x) &= 2\tilde{C}(2yz^2 - \kappa(y + tx)), & p_2(x) &= -2\tilde{C}(\kappa yz + 2z(y + tx)), \\ q_3(x) &= -4\tilde{C}(z(x^2 + y^2)), & p_3(x) &= -\tilde{C}(\kappa^2 - 2\kappa(x^2 + y^2) + 4z^2), \end{aligned} \quad (6.99)$$

with pre-factor $\tilde{C} = 4(\kappa^2 + 4z^2)^{-2}$. The electromagnetic duality $E_i \rightarrow B_i \rightarrow -E_i$ is clear from (6.98) via $h_1 \rightarrow \varepsilon h_2 \rightarrow -h_1$ and $h_2 \rightarrow -\varepsilon h_1 \rightarrow -h_2$. For illustration purposes, some examples of electric and magnetic field lines for such abelian fields can be seen in Figure 6.4. Once again, the Riemann-Silberstein vector $\vec{S} := \vec{E} + i\vec{B}$

takes a more compact form given by

$$\vec{S} = \frac{4e^{2iZ_0}}{(\kappa+2iz)^3} \begin{pmatrix} -2(ty + ix(z+i)) \\ 2(tx - iy(z+i)) \\ i(t^2 + x^2 + y^2 - (z+i)^2) \end{pmatrix}. \quad (6.100)$$

This expression explicitates that the only role of the parameter Z_0 is to enact a mixing between the oscillating electric and the magnetic fields.

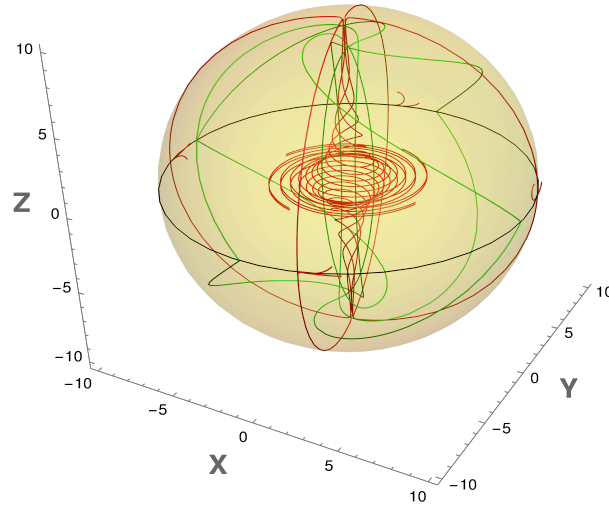


FIGURE 6.4: Illustration of the electric (red) and magnetic (green) field lines for the abelian reduction (6.100) on Minkowski space, with $t=10$, $Z_0=\frac{\pi}{2}$, and inside the boundary sphere $r=\sqrt{10}$. The fields diverge at the equatorial circle (black), the intersection of the boundary sphere with the $z=0$ plane.

Let us investigate a special case of this solution. Fixing $Z_0 = 0$, on the $z = 0$ plane, the Riemann-Silberstein vector (6.100) reduces to

$$\frac{4}{(x^2+y^2-t^2-1)^3} \begin{pmatrix} 2(x-ty) \\ 2(y+tx) \\ i(t^2+x^2+y^2+1) \end{pmatrix}. \quad (6.101)$$

The structure of such a Riemann-Silberstein vector, with the x - and y -components being purely electric and the z -component being purely magnetic, strongly resembles a 2+1-dimensional electromagnetic theory. Indeed, (6.101) exactly reproduces the magnetic vortex solution recently constructed in [49, eq. (5.15)] after the identification

$$x^0 = -t, \quad x^1 = -y \quad \text{and} \quad x^2 = x. \quad (6.102)$$

Such a solution is constructed on AdS_3 viewed in terms of a circle fibration $U(1) \rightarrow SU(1,1) \rightarrow H^2$, from a pair (Ψ, A) of spinor and $U(1)$ gauge field satisfying a gauged Dirac equation and a hyperbolic vortex equation, which together play the role of a Lorentzian 2+1-dimensional version of the Seiberg-Witten equations. In addition to

(6.101) being obtained from a ($z=0$) slice of a particular case ($Z_0=0$) of the higher-dimensional (6.100), the former is also only defined inside the $\kappa|_{z=0} = 0$ hyperboloid, while the latter is defined both inside and outside the hyperboloid.

Going back to the more general expression (6.100), we can compute the energy density of the abelian fields as

$$\frac{1}{2}\vec{S}^\dagger\vec{S} = \frac{1}{2}(E_iE_i + B_iB_i) = \frac{8}{(\kappa^2+4z^2)^3}(\kappa^2 + 8(1+t^2)(x^2+y^2) + 4z^2), \quad (6.103)$$

which has its behaviour illustrated in Figure 6.5. For completeness, even though

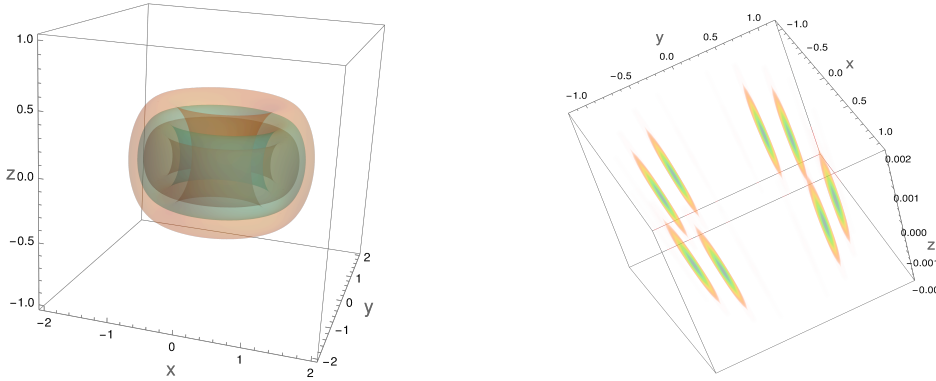


FIGURE 6.5: Energy density $\frac{1}{2}\vec{S}^\dagger\vec{S}(t=0)$ of the abelian reduction on Minkowski space. Left: Level sets for the values 10 (orange), 100 (cyan), and 1000 (brown). Right: Density plot emphasizing the maxima.

the energy-momentum tensor $T_{\mu\nu}$ does not simplify much, its components can be explicitly written as

$$\begin{aligned} T_{00} &= \bar{C}(\kappa^2+8(1+t^2)(x^2+y^2)+4z^2), & T_{01} &= -4\bar{C}((tx+y)(\kappa+2+2t^2)-2txz^2), \\ T_{02} &= 4\bar{C}((x-ty)(\kappa+2+2t^2)+2tyz^2), & T_{03} &= -8\bar{C}tz(x^2+y^2), \\ T_{11} &= \bar{C}(\kappa^2+8x^2(t^2-z^2)+8y(y+2tx)+4z^2), & T_{12} &= 8\bar{C}(-xy(z^2-t^2+1)+t(y^2-x^2)), \\ T_{13} &= 4\bar{C}(xz(\kappa-2z^2)+2tz(y+tx)), & T_{22} &= \bar{C}(\kappa^2+8y^2(t^2-z^2)+8x(x-2ty)+4z^2), \\ T_{23} &= 4\bar{C}(yz(\kappa-2z^2)-2tz(x-ty)), & T_{33} &= -\bar{C}(\kappa^2-4z^2(2x^2+2y^2-1)), \end{aligned} \quad (6.104)$$

where the pre-factor $\bar{C} = 4(\kappa^2 + 4z^2)^{-3}$.

The abelian solution discussed above represents a very simple instance of the kinds of fields that can be constructed from the geometric methods here employed. It can be regarded as the hyperbolic version of the Rañada-Hopf knot, which is indeed the equivalent (and simplest) case of the algorithmic construction of the infinite basis of electromagnetic knots using the deSitter space dS_4 and the group structure of its foliation [29]. The similarities with the compact case do not stop in the simplest scenario, though. When working on the cylinder $\mathcal{I}_Z \times \text{AdS}_3$, instead of disregarding the AdS_3 coordinates, one can consider the (continuum) basis of eigenfunctions of the Laplace operator in it. Similarly to the $\mathcal{I} \times S^3$ scenario from Chapter 5, the Maxwell equations could then be rewritten in terms of relations between those eigenfunctions, such that this system's solution would consist in a continuum-indexed set of "hyperbolic knots" in Minkowski space. This scenario is going to be investigated

as the next step in this research direction, and is currently beyond the scope of this thesis.

Chapter 7

The non-abelian case II: cosmic Yang–Mills fields

In previous chapters, we have worked on stationary spacetimes and just used their background metrics in order to investigate how the conformal invariance of the vacuum Maxwell and Yang–Mills theories in four dimensions can be used to construct new gauge fields from conformal mappings between spacetimes or cosets thereof. In this chapter, we will investigate the joint dynamics of the spacetimes with the gauge theory on them. Such investigations are relevant for both sub-areas of Cosmology, such as theories of gauge-flation, and also areas with high intersection with Cosmology, such as particle physics in the early universe. Specifically, we will consider Friedmann–Lemaître–Robertson–Walker (FLRW) universes, which are dynamical maximally symmetric Lorentzian spacetimes and are one of the basis for the *Lambda cold dark matter* (Λ CDM) model, also known as the standard model of Cosmology. We will then investigate the coupled dynamics described by the Einstein–Yang–Mills system of equations in different scenarios.

This chapter is divided in two sections. Section 7.1 is dedicated to a more systematic investigation on the use of the equivariant Ansatz in the construction of Yang–Mills theories in foliations of FLRW universes by coset spaces. This procedure is an example of *coset space dimensional reduction* (CSDR), referring to the reduction of degrees of freedom of the gauge fields. The results shown in this section will encompass some of the previous ones and extend the analysis to cases not considered before, including other foliations, spacetime dimensions other than four, and non-trivial warping of cylinders. On the other hand, Section 7.2 treats of a very specific highly-symmetric Yang–Mills field on the closed four-dimensional maximally symmetric spacetime dS_4 . More specifically, we will consider a model proposed by Friedan [6] to describe particle cosmology in the electroweak epoch, where the gauge field drives the stability of the Higgs potential pre-electroweak symmetry breaking. Using representation theory and dynamical system analyses, we will expand on the discussion on this scenario by considering the stability of the Yang–Mills field with respect to perturbations beyond its initial $SO(4)$ symmetry.

7.1 Coset space dimensional reduction of the Yang–Mills theory and its coupling to general relativity

Friedmann-Lemaître-Robertson-Walker universes are dynamical Lorentzian universes in which the manifold is maximally symmetric. Therefore, according to Section 3.1, the metric assumes the form (3.5), with its dynamics encoded in a single scalar degree of freedom, the so-called *scale factor* $a(t)$. The Einstein equation reduces to two

(non-linear) ordinary differential equations for the scale factor in terms of the universe's geometry (3.6,3.10) and its matter content (3.11), the Friedmann equations (3.12).

Alternatively, in terms of the conformal time (3.7), the metric reads (3.8) instead, in which the scale factor $a(\tau(t))$ appears only as a conformal factor on an otherwise stationary metric. In four dimensions, due to the conformal invariance, this implies that the dynamics of a gauge field will be independent from that of the scale factor, but the converse is not true due to the energy density of the gauge field contributing to the first Friedmann equation, in (3.12). Therefore, the system will be triangular, which greatly facilitates its resolution. In dimensions other than four, the Yang–Mills theory is no longer conformally invariant and the joint dynamics is mutually dependent.

In this section, we will consider the CSDR approach to construct Yang–Mills fields on both straight or warped cylinders over symmetric spaces, respectively $\mathbb{R} \times G/H$ or $\mathbb{R} \times_a G/H$, representing foliations of maximally symmetric spacetimes. The gauge fields will be coupled to the dynamics of the spacetime through the scale factor and their joint dynamics will be discussed, following [50].

7.1.1 CSDR on cylinders over symmetric spaces

Let us start from a more general approach, considering any symmetric space $\tilde{M} := G/H$ of a Lie group G and a Lie subgroup $H \subset G$, with index conventions following (2.28). Normalise the Killing form on \mathfrak{g} according to

$$K(T_A, T_B) = \varepsilon_K \mathcal{D}_n \tilde{\eta}_{AB}, \quad (7.1)$$

where ε_K can be used to adjust the global sign of the Killing form, \mathcal{D}_n is, for the rest of this section, a normalisation depending on the dimension $n := \dim(\mathfrak{m})$ of the coset, and

$$\tilde{\eta}_{AB} := \frac{\text{tr}_{\text{adj}}(T_A T_B)}{|\text{tr}_{\text{adj}}(T_A T_B)|} = \tilde{\eta}_{ij} \oplus \tilde{\eta}_{ab}. \quad (7.2)$$

Take $\{\tilde{e}^A\}$ a coframe on G . By its definition, the Cartan–Killing form on G reads

$$g_G = \tilde{\eta}_{AB} \tilde{e}^A \otimes \tilde{e}^B. \quad (7.3)$$

From any section $\sigma : G/H \rightarrow G$, we define the pulled-back one-forms $e^A := \sigma^* \tilde{e}^A$ on \tilde{M} , which will be split in $\{e^a\}$ and $\{e^i\}$ according to Section 2.4, with coefficients χ such that $e^i = \chi^i_a e^a$. Hence, the metric $g_{\tilde{M}}$ on the coset is

$$g_{\tilde{M}} = \tilde{\eta}_{ab} e^a \otimes e^b. \quad (7.4)$$

For now, let us restrict ourselves to straight cylinders. Then, the target spacetime M can be foliated as $M \simeq \mathbb{R} \times G/H$ (or an interval in \mathbb{R}) and its metric will be written in terms of a product metric

$$g := \varepsilon_g \tilde{g}_{\mu\nu} e^\mu \otimes e^\nu = \varepsilon_g \left(\tilde{g}_{00} e^0 \otimes e^0 + \tilde{\eta}_{ab} e^a \otimes e^b \right), \quad (7.5)$$

where $e^0 \equiv e^\mu := du$, for $u \in \mathbb{R}$ being the foliation parameter, $\varepsilon_g = \pm 1$ adjusts the global sign of the metric to fit our conventions, and $\tilde{g}_{00} = \pm 1$ is chosen depending on the signature of $\tilde{\eta}_{ab}$, such that M is Lorentzian.

As discussed in Section 6.1, a gauge theory on a cylinder over a symmetric space respecting the equivariant Ansatz has greatly simplified expressions for both the gauge field (6.4) and its field strength components (6.5), repeated below:

$$\begin{aligned} \mathcal{A} &= T_i e^i + \phi(u) T_a e^a, \\ \mathcal{F}_{ua} &= \dot{\phi} T_a \quad \text{and} \quad \mathcal{F}_{ab} = (\phi^2 - 1) f_{ab}^i T_i, \end{aligned} \quad (7.6)$$

with $\dot{\phi} := \partial_u \phi$. Moreover, the principle of symmetric criticality allows us to simply substitute (7.6) into the action and extremise the reduced action,

$$\begin{aligned} S[\mathcal{F}] &= -\frac{1}{4\alpha} \int_M K(\mathcal{F} \wedge * \mathcal{F}) = -\frac{1}{8\alpha} \int_{\mathbb{R}} \int_{G/H} K(\mathcal{F}_{\mu\nu}, \mathcal{F}^{\mu\nu}) d\text{Vol} \Rightarrow \\ S[\phi] &= -\text{Vol}(G/H) \int_{\mathbb{R}} \underbrace{\frac{1}{8\alpha} K(\mathcal{F}_{\mu\nu}, \mathcal{F}^{\mu\nu})}_{\mathcal{L}(\phi, \dot{\phi})} du, \end{aligned} \quad (7.7)$$

where α is the gauge coupling, which had to be recovered in this chapter since we will couple the gauge field to other fields. In the last line, we used that the only dependence on the coset coordinates is on the volume form. Combining the explicit expression for \mathcal{F} in terms of ϕ with the definition of the Killing form (7.1) and the metric g on the cylinder (7.5), it is straightforward to compute the Lagrangian $\mathcal{L}(\phi, \dot{\phi})$ as

$$\mathcal{L}(\phi, \dot{\phi}) = \frac{1}{8\alpha} K(\mathcal{F}_{\mu\nu}, \mathcal{F}^{\mu\nu}) = \frac{1}{2\alpha} n \mathcal{D}_n \varepsilon_K \tilde{g}^{00} \left(\frac{1}{2} \dot{\phi}^2 + \frac{\tilde{g}^{00}}{4n} \mathcal{S}_n (\phi^2 - 1)^2 \right), \quad (7.8)$$

where we defined the combinatorial factor

$$\mathcal{S}_n := \tilde{\eta}([I_a, I_b], [I_a, I_b]) \tilde{\eta}^{aa} \tilde{\eta}^{bb} = \sum_{I, J \in \mathfrak{m}} \|[I, J]\|_{\tilde{\eta}}^2 \|[I]\|_{\tilde{\eta}}^2 \|[J]\|_{\tilde{\eta}}^2, \quad (7.9)$$

which depends on how many compact and non-compact generators are on \mathfrak{m} . Notice that, for all possible coset structures, the Lagrangian reduces to that of a Newtonian particle with position ϕ and time u , subjected to a quartic potential

$$V(\phi) = -\frac{\tilde{g}^{00}}{4n} \mathcal{S}_n (\phi^2 - 1)^2, \quad (7.10)$$

with equation of motion

$$\ddot{\phi} = -\frac{dV(\phi)}{d\phi}. \quad (7.11)$$

Regardless of the concavity of the quartic, such equation can be solved in terms of Jacobi elliptic functions, as discussed in Chapter 6. For foliations with straight cylinders, the dynamics of the Yang–Mills fields are not going to be dependent on the scale factor for all spacetime dimensions, only on the initial coset structure. Later, we will see how the introduction of a warping function will change this picture for $n \neq 3$.

Even though the scale factor does not influence the gauge field's dynamics in the straight case, the converse is not true. Moreover, to be able to solve the spacetime dynamics, we need to compute the energy-momentum tensor $T = T_{\mu\nu} e^\mu \otimes e^\nu$ of the

gauge field. Its components read

$$T_{\mu\nu} = \frac{1}{2\alpha} \left(K(\mathcal{F}_{\mu\sigma}, \mathcal{F}_{\nu\rho}) g^{\sigma\rho} - \frac{1}{4} g_{\mu\nu} K(\mathcal{F}_{\sigma\rho}, \mathcal{F}^{\sigma\rho}) \right). \quad (7.12)$$

The second term is proportional to the Lagrangian itself, which was already discussed. Hence, let us compute the components of the first term. Its 00-component reads

$$K(\mathcal{F}_{0\sigma}, \mathcal{F}_{0\rho}) g^{\sigma\rho} = n \mathcal{D}_n \varepsilon_K \varepsilon_g \dot{\phi}^2, \quad (7.13)$$

the mixed 0*a*-components will immediately vanish due to $K(\mathfrak{m}, \mathfrak{h}) = 0$, and the coset *ab*-components read

$$\begin{aligned} K(\mathcal{F}_{a\sigma}, \mathcal{F}_{b\rho}) g^{\sigma\rho} &= \varepsilon_g \tilde{g}^{00} K(\mathcal{F}_{a0}, \mathcal{F}_{b0}) + K(\mathcal{F}_{am}, \mathcal{F}_{bn}) g^{mn} \\ &= \varepsilon_g \tilde{g}^{00} \varepsilon_K \mathcal{D}_n \tilde{\eta}_{ab} \dot{\phi}^2 + (\phi^2 - 1)^2 \varepsilon_K \mathcal{D}_n \varepsilon_g \tilde{\eta}([I_a, I_m], [I_b, I_n]) \tilde{\eta}^{mn}. \end{aligned} \quad (7.14)$$

Once again, we encounter a combinatorial factor

$$\begin{aligned} \tilde{\eta}([I_a, I_m], [I_b, I_n]) \tilde{\eta}^{mn} &= \sum_{I \in \mathfrak{m}} \tilde{\eta}([I, I_a], [I, I_b]) \|I\|_{\tilde{\eta}}^2 \\ &= \sum_{I \in \mathfrak{m}} \| [I, I_a] \|_{\tilde{\eta}}^2 \|I\|_{\tilde{\eta}}^2 \delta_{ab} =: \mathcal{C}_a \delta_{ab}, \end{aligned} \quad (7.15)$$

which is easy to be computed for any specified coset structure. In the last line, we used that $[I, \cdot] : \{I_a\} \rightarrow \{I_i\}$ is injective for $I \in \mathfrak{m}$. In terms of \mathcal{C}_a , the coset components read

$$K(\mathcal{F}_{a\sigma}, \mathcal{F}_{b\rho}) g^{\sigma\rho} = \varepsilon_g \tilde{g}^{00} \varepsilon_K \mathcal{D}_n \tilde{\eta}_{ab} \dot{\phi}^2 + (\phi^2 - 1)^2 \varepsilon_K \mathcal{D}_n \varepsilon_g \mathcal{C}_a \delta_{ab}. \quad (7.16)$$

This has to be explicitly computed for any particular universe structure before we are able to solve the equation of motion for its scale factor.

7.1.2 Application to H^n , dS_n , and AdS_n sheets

Our goal is to construct Yang–Mills theories on Lorentzian maximally symmetric spacetimes. Hence, let us recall that we can foliate the positively-curved case, dS_{n+1} , as an Euclidean cylinder over dS_n or as a Lorentzian cylinder over S^n . Analogously, we can foliate the negatively-curved case, AdS_{n+1} , as an Euclidean cylinder over AdS_n or as a Lorentzian cylinder over H^n . All of the spaces used as sheets are symmetric spaces in terms of the cosets

$$S^n \cong \text{SO}(n+1)/\text{SO}(n), \quad (7.17)$$

$$H^n \cong \text{SO}(1, n)/\text{SO}(n), \quad (7.18)$$

$$dS_n \cong \text{SO}(1, n)/\text{SO}(1, n-1), \text{ and} \quad (7.19)$$

$$AdS_n \cong \text{SO}(2, n-1)/\text{SO}(1, n-1), \quad (7.20)$$

implying that the discussions in this section apply to the four cases. The discussion on the sphere is trivial, since it only contains compact generators. Therefore, we will only explicitly discuss the other three foliations. To obtain the Killing forms on each case, let us employ a relation between the adjoint and the defining representations.

For $\text{SO}(p, q)$ with $p + q \geq 3$ and $p, q \geq 1$, we have

$$\text{tr}_{\text{adj}}(XY) = (p + q - 2)\text{tr}_{\text{def}}(XY), \quad (7.21)$$

which allows us to compute, for the three cases,

$$H^n : \tilde{\eta}_{AB} = \tilde{\eta}_{ij} \oplus \tilde{\eta}_{ab} = -\text{Id}_{\binom{n}{2}} \oplus \text{Id}_n, \quad (7.22)$$

$$\text{dS}_n : \tilde{\eta}_{AB} = \tilde{\eta}_{ij} \oplus \tilde{\eta}_{ab} = \begin{pmatrix} \text{Id}_{n-1} & \\ & -\text{Id}_{\binom{n-1}{2}} \end{pmatrix} \oplus \begin{pmatrix} 1 & \\ & -\text{Id}_{n-1} \end{pmatrix}, \quad \text{and} \quad (7.23)$$

$$\text{AdS}_n : \tilde{\eta}_{AB} = \tilde{\eta}_{ij} \oplus \tilde{\eta}_{ab} = \begin{pmatrix} \text{Id}_{n-1} & \\ & -\text{Id}_{\binom{n-1}{2}} \end{pmatrix} \oplus \begin{pmatrix} \text{Id}_{n-1} & \\ & -1 \end{pmatrix}, \quad (7.24)$$

with Killing-normalisation $\mathcal{D}_n = 2(n-1)$ in all of them. Naturally, the split in the deSitter case is just a reordering of the one on the hyperbolic case since $G = \text{SO}(1, n)$ for both of them. To preserve the Lorentzian nature of M , we fix \tilde{g}_{00} as -1 for H^n and dS_n and as $+1$ for AdS_n . Moreover, we see that only in the deSitter case the metric on \tilde{M} has a mostly negative signature, then, we use the global factor $\varepsilon_g = -1$ to make the metric on M have a mostly positive signature. In the other cases, we take $\varepsilon_g = 1$. With the split of the generators, we can compute the combinatorial factors for the Lagrangian and the energy-momentum density. To account for the indefiniteness of the Killing forms, we have to consider all possible combinations of compact and non-compact generators in the norms and commutators. Let us refer to generators that $\tilde{\eta}$ -square to -1 as compact generators (C) and to ones that $\tilde{\eta}$ -square to $+1$ as non-compact generators (\neg C). From the $\mathfrak{so}(1, n)$ algebra,

$$\begin{aligned} [C, C] &= C & [-, -] &= - \\ [C, \neg C] &= \neg C & [-, +] &= +. \\ [\neg C, \neg C] &= C & [+, +] &= - \end{aligned} \quad (7.25)$$

Hence, for $I \neq J$, we have the possible combinations

$\ [I, J] \ _{\tilde{\eta}}^2$	$\ I \ _{\tilde{\eta}}^2$	$\ J \ _{\tilde{\eta}}^2$	Π
–	–	–	–
+	+	–	–
+	–	+	–
–	+	+	–

where $\Pi = \| [I, J] \|_{\tilde{\eta}}^2 \| I \|_{\tilde{\eta}}^2 \| J \|_{\tilde{\eta}}^2$ is the product in each case. As $\Pi = -1$ for all non-trivial ($I \neq J$) cases, the double sum on I and J becomes trivial, resulting in $\mathcal{S}_n = -2\binom{n}{2}$ for the hyperbolic and the deSitter cases. To write \mathcal{S}_n in terms of \mathcal{D}_n , we use the relation

$$\mathcal{S}_n = -2\frac{\binom{n}{2}}{4n} = -(n-1)/4 = -\mathcal{D}_n/8, \quad (7.26)$$

such that the potential for the H^n and the dS_n cases can be finally expressed as

$$V_{H^n}(\phi) = V_{\text{dS}_n}(\phi) = -\frac{1}{8}\mathcal{D}_n(\phi^2 - 1)^2, \quad (7.27)$$

where $\tilde{g}^{00} = -1$ was also used. For $n = 3$, this exactly matches the potential (6.17) found for cylinders over H^3 and dS_3 in Section 6.1 and in [51]. Lastly, for the AdS_n

case, it is also straightforward to obtain all non-trivial combinations as

$\ [I, J] \ _{\tilde{\eta}}^2$	$\ I \ _{\tilde{\eta}}^2$	$\ J \ _{\tilde{\eta}}^2$	Π
+	+	−	−
+	−	+	−
−	+	+	−

where there is no non-trivial case with I and J $\tilde{\eta}$ -squaring to -1 since there is only one compact generator. Once more, the double sum becomes trivial and the potential can be expressed as

$$V_{\text{AdS}_n}(\phi) = +\frac{1}{8}\mathcal{D}_n(\phi^2 - 1)^2, \quad (7.28)$$

where in this case $\tilde{g}^{00} = +1$. The analysis above trivially applies to the case of the n -dimensional sphere as $\text{SO}(n+1)/\text{SO}(n)$, which only contains compact generators. It would foliate the deSitter space dS_{n+1} as a Lorentzian cylinder, then we conclude that $\varepsilon_g = -1$, $\tilde{g}^{00} = +1$, and we obtain the potential

$$V_{S^n}(\phi) = +\frac{1}{8}\mathcal{D}_n(\phi^2 - 1)^2, \quad (7.29)$$

reproducing the results from [52]. Summarising, for all the four cases, the Lagrangian has the same form

$$\mathcal{L} = \frac{1}{\alpha}\varepsilon_K\tilde{g}^{00}\frac{n}{2}\mathcal{D}_n\left(\frac{1}{2}\dot{\phi}^2 - V(\phi)\right) \quad \text{with} \quad V(\phi) = \tilde{g}^{00}\frac{1}{8}\mathcal{D}_n(\phi^2 - 1)^2, \quad (7.30)$$

with the only difference between them being the sign \tilde{g}^{00} determining if the quartic potential is inverted or not.

Using a similar argument, we can compute the numerical factor from (7.15) which appear on the energy-momentum tensors for each case,

$$\mathcal{C}_a = \sum_{I \in \mathfrak{m}} \| [I, I_a] \|_{\tilde{\eta}}^2 \| I \|_{\tilde{\eta}}^2. \quad (7.31)$$

For that, we consider all combinations of signals,

$\ [I_a] \ _{\tilde{\eta}}^2$	$\ I \ _{\tilde{\eta}}^2$	$\ [I, I_a] \ _{\tilde{\eta}}^2$	$\ I \ _{\tilde{\eta}}^2 \ [I, I_a] \ _{\tilde{\eta}}^2$
+	+	−	−
+	−	+	−
−	+	+	+
−	−	−	+

Once more, we see that the argument of the sum is 0 if $I = I_a$ and, otherwise, it is always $+1$ or always -1 , depending only if I_a is a compact or non-compact generator. Hence,

$$\mathcal{C}_a = (n-1) \begin{cases} -1, & a \text{ is } \neg C \\ +1, & a \text{ is } C \end{cases}. \quad (7.32)$$

Combining the sign of \mathcal{C}_a with δ_{ab} , we can rewrite

$$\mathcal{C}_a\delta_{ab} = -(n-1)\tilde{\eta}_{ab} \quad (7.33)$$

which reduces expression (7.14) to

$$\begin{aligned} K(\mathcal{F}_{a\sigma}, \mathcal{F}_{b\rho})g^{\sigma\rho} &= \varepsilon_g \tilde{g}^{00} \varepsilon_K \mathcal{D}_n \tilde{\eta}_{ab} \dot{\phi}^2 - (\dot{\phi}^2 - 1)^2 \varepsilon_K \mathcal{D}_n \varepsilon_g (n-1) \tilde{\eta}_{ab} \\ &= \varepsilon_K \mathcal{D}_n g_{ab} \tilde{g}^{00} (\dot{\phi}^2 - 4V(\phi)) . \end{aligned} \quad (7.34)$$

This concludes the computation of the first term of the energy-momentum tensor (7.12). As previously mentioned, the second term is simply proportional to the Lagrangian, which has already been computed. Hence, we have the full energy-momentum tensor of the Yang–Mills field provided by the equivariant Ansatz on all straight cylinders over symmetric spaces:

$$\begin{aligned} T_{00} &= \frac{1}{2\alpha} \varepsilon_K \tilde{g}^{00} n \mathcal{D}_n E g_{00} , \\ T_{0a} &= 0 , \quad \text{and} \\ T_{ab} &= -\frac{1}{2\alpha} \varepsilon_K \tilde{g}^{00} \mathcal{D}_n \left(\left(\frac{n}{2} - 1 \right) \dot{\phi}^2 + (4-n)V(\phi) \right) g_{ab} , \end{aligned} \quad (7.35)$$

where E is the energy of the reduced mechanical degree of freedom ϕ ,

$$E := \frac{1}{2} \dot{\phi}^2 + V(\phi) . \quad (7.36)$$

For the Lorentzian cylinders over S^n and H^n , the 00-component of the energy-momentum tensor will encode the energy density of the Yang–Mills configuration, which will contribute to the Friedmann equations for the scale factor. The factor of ε_K from the overall sign of the Killing form allows us to make the energy density positive by choosing $\varepsilon_K = \tilde{g}^{00}$. Moreover, as the spacetime is maximally symmetric, the energy-momentum tensor will have the perfect fluid-form, for any n . For $n = 3$ in particular, we recover the conformal invariance of the Yang–Mills theory, which should render the energy-momentum tensor traceless. Indeed, we can check that (7.35) reduces to

$$T = \rho \left(g_{00} e^0 \otimes e^0 - \frac{1}{3} g_{ab} e^a \otimes e^b \right) , \quad \text{with} \quad \rho := \frac{6}{\alpha} \varepsilon_K \tilde{g}^{00} E . \quad (7.37)$$

All solutions for the Newtonian degree of freedom ϕ subjected to a (inverted or not) quartic potential were already discussed in this thesis. For the standard quartic potential, the conventions are set in (6.81) and the solutions are shown in (6.82). For the inverted quartic potential, the conventions are set in (6.20) and the solutions are discussed in (6.19, 6.21, 6.22, 6.23).

7.1.3 Effect of the Yang–Mills field on the spacetime dynamics

In FLRW universes, the dynamics of the spacetime metric reduces to the two Friedmann equations describing the evolution of the scale factor, which only depend on the matter content through its energy density ρ and pressure p , diagonal components of the matter energy-momentum tensor T . Having computed them in (7.35), we can now try to explicitly solve the dynamics of the scale factor. To fully solve an explicit example, let us consider $n=3$. Moreover, as the dynamics of closed FLRW universes foliated by $S^3 \simeq \text{SU}(2)$ are extensively discussed in the literature,

including in [53] to be discussed in the next section, let us consider the hyperbolic universe, foliated by H^3 sheets.

In general, FLRW universes are warped Lorentzian cylinders $M = \mathbb{R} \times_a \tilde{M}$ over a Riemannian space \tilde{M} , such that their general metric reads

$$g = -dt \otimes dt + a(t)^2 g_{\tilde{M}}, \quad (7.38)$$

with $a(t)$ being the scale factor. A warped cylinder can always be made conformally flat with the introduction of the conformal time τ according to

$$d\tau = \frac{1}{a} dt \Rightarrow \tau(t) = \int^t dt' \frac{1}{a(t')}, \quad (7.39)$$

such that

$$g = a(\tau)^2 (-d\tau \otimes d\tau + g_{\tilde{M}}). \quad (7.40)$$

If the foliation parameter u in the coset space dimensional reduction of the Yang–Mills field is identified with the conformal time, the energy-momentum tensor (7.37) transforms under rescaling to

$$T = \frac{\rho}{a^2} (-d\tau \otimes d\tau - \frac{1}{3} g_{\tilde{M}}). \quad (7.41)$$

Moreover, in terms of the conformal time τ , the Friedmann equations (3.12) in four dimensions transform, respectively, into

$$E_{\text{GR}} := \frac{1}{2} \dot{a}^2 + W(a) = \frac{\kappa T_{00}}{6} \quad \text{and} \quad (7.42)$$

$$\ddot{a} + W'(a) = 0, \quad (7.43)$$

where here we redefine $\dot{a} := \frac{da}{d\tau}$, and

$$W(a) = \frac{k}{2} a^2 - \frac{\Lambda}{6} a^4, \quad (7.44)$$

which is illustrated in Figure 7.1 for different universes, with different cosmological constants Λ and sectional curvatures k . Substituting T_{00} from our construction (7.37)

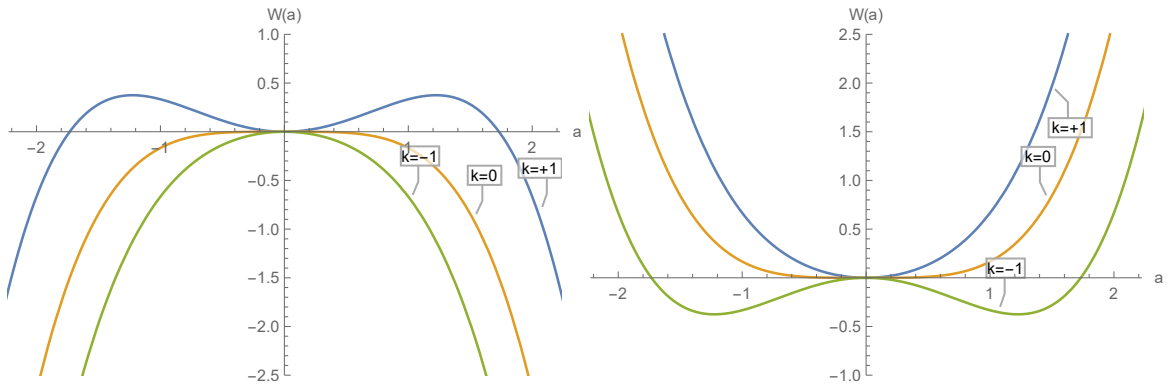


FIGURE 7.1: Cosmological potential $W(a)$ for different values of $k = \pm 1, 0$ and cosmological constant $\Lambda = +1$ (left), $\Lambda = -1$ (right).

in the first Friedmann equation (7.42), we get

$$E_{\text{GR}} = -\frac{\kappa}{\alpha}E \quad \Longrightarrow \quad E_{\text{GR}} + \frac{\kappa}{\alpha}E = 0, \quad (7.45)$$

which represents an energy balance between the Yang–Mills field and the scale factor. This relation is known as the Wheeler-DeWitt constraint.

Especially in four-dimensions, the second Friedmann equation (7.43) does not depend on the Yang–Mills field, since the trace of its energy-momentum tensor vanishes. In this case, the general solution for $a(\tau)$ can be obtained independently of the gauge sector. However, the dependency shows up when fixing the initial conditions to find any particular solutions, since the energies of the two fields are related through (7.45). For $n \neq 3$, the coupled differential equations for a and ϕ are in general not analytically solvable, as we will soon discuss for the gauge field in higher dimensions, hence requiring numerical methods for precise analyses beyond asymptotic or qualitative behaviour.

For the case of a hyperbolic cosmology of an open universe, let us take $k = -1$ and $\Lambda < 0$ on (7.44). Then, the function $W(a)$ is a standard double-well potential with, up to exceptions, only oscillatory solutions. The full set of solutions is the same as in (6.82) with conventions (6.81). However, we can still impose the physical restriction of $a(0) = 0$ such that $a(\tau)$ corresponds to a Big Bang solution, which guarantees $E_{\text{GR}} \geq 0$. If $E_{\text{GR}} = 0$, we would have the trivial solution $a(\tau) = 0$ and the bounce $a(\tau) \propto \text{sech}(C\tau)$ solution, for some constant C . In the latter case, the universe would expand monotonically, asymptotically approaching the supremum $a(+\infty) = \sqrt{\frac{3}{|\Lambda|}}$. On the other hand, if $E_{\text{GR}} > 0$, the periodic nature of the solutions guarantees that there would be a Big Crunch in finite time. Other possible scenarios of evolution and consequences of the coupling with the Yang–Mills field are described in [50, Section 3].

7.1.4 Effect of a general warping on the gauge field in arbitrary dimension

Lastly, let us briefly discuss the effect of a non-trivial warping function in the foliation on the dynamics of the Yang–Mills theory. Once more, we will consider a warped foliation with metric (7.38) and introduce the conformal time (7.39) such that the metric becomes

$$g = a(\tau)^2 \underbrace{(-d\tau \otimes d\tau + g_{\tilde{M}})}_{g_0}, \quad (7.46)$$

where g_0 is the metric of a straight cylinder over a symmetric space \tilde{M} , with foliation parameter τ . In the beginning of the section, we constructed the Yang–Mills fields that arose from the equivariant Ansatz on straight cylinders as g_0 . Hence, we may now use it to derive a corresponding solution on g through a conformal mapping, even if the gauge theory is not conformally invariant for $n \neq 3$. Indeed, under a conformal transformation

$$g \mapsto e^{2\sigma(\tau)}g, \quad (7.47)$$

the reduced action after employing the equivariant Ansatz on the cylinder over the symmetric space (7.7) transforms as

$$S[\phi] = \text{Vol}(G/H) \int_{\mathbb{R}} \mathcal{L} \, d\tau \mapsto \text{Vol}(G/H) \int_{\mathbb{R}} e^{(n-3)\sigma(\tau)} \mathcal{L} \, d\tau =: S^{(\sigma)}[\phi]. \quad (7.48)$$

Naturally, the conformal invariance in four spacetime dimensions is encoded in the $n - 3$ factor, which will be carried by any explicit dependence in σ on the new equation of motion for the gauge field. In fact, let us introduce the *conformal Hubble parameter* \mathcal{H} as

$$\mathcal{H}(u) := \frac{1}{e^{\sigma(u)}} \frac{d}{du} e^{\sigma(u)} = \dot{\sigma}(u). \quad (7.49)$$

Hence, the new reduced equation of motion for the scalar degree of freedom obtained from the extremisation of (7.48) now reads

$$\frac{\partial \mathcal{L}}{\partial \phi} - \frac{d}{du} \frac{\partial \mathcal{L}}{\partial \dot{\phi}} = (n-3) \mathcal{H}(u) \frac{\partial \mathcal{L}}{\partial \dot{\phi}}. \quad (7.50)$$

The new contribution on the right-hand side is similar to a cosmological Hubble friction term, but for the dynamics of the gauge field in conformal time. For the four foliations (7.17-7.20) worked out in the beginning of this section, the equation of motion reduces to

$$\ddot{\phi} + V'(\phi) - (n-3) \mathcal{H}(u) \dot{\phi} = 0. \quad (7.51)$$

This equation corresponds to a non-trivial gauge theory on any spacetime that is conformally equivalent to $\mathbb{R} \times \tilde{M}$, where $\tilde{M} \in \{H^n, S^n, \text{dS}_n, \text{AdS}_n\}$. The potential will still be a (inverted or not) double-well potential, however, there will be a new dissipative (for $n > 3$) term in the equation of motion for ϕ . Up to a set of measure zero of initial conditions in each case, the dynamics will necessarily evolve as follows:

- If $n=3$, the energy of the Yang–Mills field is conserved and we can solve its dynamics analytically, as discussed in the beginning of the chapter.
- If $n > 3$ and the double-well is not inverted, ϕ will lose energy up to the moment it freezes in one of the two minima of the potential.
- If $n > 3$ and the double-well is inverted, ϕ may freeze in the local minimum of the potential for a small range of initial conditions. Otherwise, it will blow up.
- If $n < 3$, regardless of the concavity of the potential, ϕ will blow up.

In four spacetime dimensions, the conformal invariance of the gauge theory allowed us to solve the full Einstein–Yang–Mills system analytically for a family of spacetimes. In any other spacetime dimension, the system cannot in general be analytically solved, but numerical computations can still probe the full system beyond asymptotic or qualitative behaviour. As an example of application of such results, it would be possible, in higher dimensions, to have a classical Yang–Mills field driving the growth of the scale factor in the very early universe, while eventually dying out to the Hubble friction-like effect, as to not contradict present observations. Further investigations in this direction are in order to study its viability, even though it would demand another mechanism to deal with the extra dimension(s).

7.2 Instability of cosmic Yang–Mills fields

In this last section, we will investigate a cosmological application of a Yang–Mills theory constructed using the equivariant Ansatz on a four-dimensional closed FLRW universe. The model, proposed by Friedan [6], considers an oscillating isotropic SU(2) gauge field stabilising the symmetric Higgs vacuum in the electroweak epoch of the evolution of such universe. The strength of the gauge solution is inversely proportional to that of the scale factor a , such that, when a reaches some critical a_{EW} value, the coupled system becomes unstable and the electroweak transition begins. It is worth noticing that Friedan considers thermodynamic stability, with the value of the average of the gauge contribution over its imaginary period determining the concavity of the Higgs potential around the critical point $h = 0$. Friedan’s work is restricted to the symmetric oscillations, while Hosotani had an earlier analysis on the singlet perturbation of such symmetric Yang–Mills fields on closed Friedmann universes [7]. Hence, a complete analysis of linear (non-symmetric) gauge-field perturbations was still in order. In [53], we showed that, except for the exactly solvable SO(4) singlet perturbation, which is marginally stable in the linear regime, all other “spin- j ” perturbations had modes growing exponentially due to resonance effects.

It is worth noting that, even beyond the cosmological relevance, investigating perturbations around classical Yang–Mills field configurations is of general interest for the quantum properties of the theory as well, as the leading quantum corrections to any saddle point in a semiclassical analysis of the path integral are given by the determinant of the second variation of the action.

7.2.1 Preliminaries

Let us start by briefly reducing the action of the Einstein–Yang–Mills–Higgs system in Friedan’s scenario. The full action reads

$$S = \int d^4x \sqrt{-g} \left\{ \frac{1}{2\kappa} R - \frac{1}{8\alpha} \text{tr} \mathcal{F}_{\mu\nu} \mathcal{F}^{\mu\nu} + D_\mu h^\dagger D^\mu h - U(h) \right\}, \quad (7.52)$$

where $h \in \mathbb{C}^2$ is the Higgs scalar field, $D^\mu h$ is its (metric and gauge) covariant derivative, and its potential is

$$U(h) = \frac{1}{2} \lambda^2 \left(h^\dagger h - \frac{1}{2} v^2 \right)^2. \quad (7.53)$$

The Higgs mass is λv and the cosmological constant comes from

$$\Lambda := \kappa U(0) = \frac{1}{8} \kappa \lambda^2 v^4. \quad (7.54)$$

The $\mathbb{R} \times S^3$ foliation was constructed in Section 3.3 with parametrisation (3.23), such that the FLRW metric reads (3.24) in terms of the coordinate time t , and, in terms of the conformal time τ (3.27), it reads (3.28). Exploring the $S^3 \simeq \text{SU}(2)$ relation, in Section 5.1, we used the group structure of SU(2) to construct the coframe on $\mathcal{I}_\tau \times S^3$, according to (5.8). If \mathcal{A} is the SU(2) gauge field on $\mathcal{I}_\tau \times S^3 \simeq \mathcal{I}_\tau \times \text{SU}(2) \ni (\tau, g)$, in the temporal gauge

$$\mathcal{A}_\tau(\tau, g) = 0, \quad (7.55)$$

the $\text{SO}(4)$ equivariance enforces

$$\mathcal{A}_a(\tau, g) = \frac{1}{2} (1 + \phi(\tau)) T_a. \quad (7.56)$$

Hence, the $\text{SO}(4)$ -invariant reduction of the action is given by

$$S[a, \phi, \Lambda] = 12\pi^2 \int_{\mathcal{I}_\tau} d\tau \left\{ \frac{1}{\kappa} \left(-\frac{1}{2} \dot{a}^2 + W(a) \right) + \frac{1}{2\alpha} \left(\frac{1}{2} \dot{\phi}^2 - V(\phi) \right) \right\}, \quad (7.57)$$

where $V(\phi)$ is the straight quartic potential

$$V(\phi) = \frac{1}{2} (\phi^2 - 1)^2. \quad (7.58)$$

The fact that the potential from the $\text{SO}(4)$ -invariant reduction of the $\text{SU}(2)$ gauge action matches the straight quartic potential (7.29) from the S^n foliation in Section 7.1 is not a coincidence, since, in that case, for $n = 3$, we were indeed working with the equivariant Ansatz on a $\text{SO}(4)$ gauge theory, with $\mathfrak{so}(4) \simeq \mathfrak{su}(2) \oplus \mathfrak{su}(2)$. Moreover, $W(a)$ is the inverted quartic potential of the scale factor (7.44) with $k = +1$. As discussed in 7.1, the potential for the scale factor does not get a contribution from ϕ , with their relation being given by the Wheeler-DeWitt constraint connecting their initial conditions. Hence, as the potentials are identical to the ones in last section, their solutions to the Newtonian reduced systems are also the same. See (6.81,6.82) for solutions of the straight quartic potential and (6.19-6.23) for solutions of the inverted quartic potential.

7.2.2 Linear fluctuations of Yang–Mills fields and their natural frequencies

Global stability is in general quite hard to assess in non-linear dynamics, and, in fact, we will only be able to probe it in the simplest perturbation, the singlet case. Hence, let us start by analysing local stability from the linearisation of the equations of motion around its solutions. Our goal is to diagonalise the fluctuation operator for the time-dependent Yang–Mills backgrounds. In our analysis, we will not consider fluctuations on the scale factor, or how the fluctuations of the Yang–Mills field impact its dynamics. This is due to the fact that the time scale of the gauge theory dynamics in the electroweak epoch is supposed to be many orders of magnitude shorter than that of the spacetime metric, such that these effects can be neglected.

From a solution \mathcal{A} to the Yang–Mills equation on $\mathcal{I}_\tau \times S^3 \ni (\tau, g)$, let us consider a fluctuation

$$\begin{aligned} \mathcal{A} + \Phi &= \mathcal{A}(\tau, g) + \sum_{p=1}^3 \Phi_0^p(\tau, g) T_p d\tau + \sum_{a=1}^3 \sum_{p=1}^3 \Phi_a^p(\tau, g) T_p e^a(g) \\ &= \mathcal{A}(\tau, g) + \sum_{\mu=0}^3 \sum_{p=1}^3 \Phi_\mu^p(\tau, g) T_p e^\mu(g), \end{aligned} \quad (7.59)$$

where, for simplicity, we define $e^0(g) := d\tau$, and here we will use indices p, q for the algebra elements instead of a, b or i, j to avoid confusion with the forms and the harmonics indices, respectively. Hence, we can use the hyperspherical harmonics to

decompose the dependence on the Φ_μ^p components as

$$\Phi_\mu^p(\tau, g) = \sum_{j,m,n} \Phi_{\mu|j;m,n}^p(\tau) Y_{j;m,n}(g). \quad (7.60)$$

From the group structure of $S^3 \simeq \text{SU}(2)$, recall the L_a operators (5.10) used to define the differential of any scalar function on S^3 according to (5.13). They also follow the $\mathfrak{su}(2)$ algebra (5.12). In terms of the basis of hyperspherical harmonics, its matrix elements are determined from (5.17, 5.20, 5.23). Hence, suppressing functional arguments, we have the following actions on the fluctuation:

$$\begin{aligned} (L_a \Phi_\mu^p)_{j;m,n} &= \Phi_{\mu|j;m',n}^p (L_a)^{m'}_m, & (T_a \Phi)_\mu^p &= -2\varepsilon_{apq} \Phi_\mu^q, \\ (S_a \Phi)_0^p &= 0, & \text{and } (S_a \Phi)_b^p &= -2\varepsilon_{abc} \Phi_c^p, \end{aligned} \quad (7.61)$$

where we introduce the S_a as components of the spin operator. Moreover, the background-covariant derivative of the fluctuation reads

$$D_\tau \Phi = \partial_\tau \Phi \quad \text{and} \quad D_a \Phi = L_a \Phi + [\mathcal{A}_a, \Phi], \quad (7.62)$$

which, using

$$\mathcal{A}_a = \frac{1}{2}(1 + \phi(\tau)) T_a \quad \text{and} \quad D_a e^b = L_a e^b - \varepsilon_{abc} e^c = \varepsilon_{abc} e^c, \quad (7.63)$$

is equivalent to

$$D_a \Phi_b^p = L_a \Phi_b^p - \varepsilon_{abc} \Phi_c^p + [\mathcal{A}_a, \Phi_b]^p. \quad (7.64)$$

In addition to the temporal gauge condition $\mathcal{A}_\tau = 0$, since we are dealing with vacuum solutions, we also impose the Coulomb gauge condition on top,

$$L_a \mathcal{A}_a = 0. \quad (7.65)$$

As the linearised fluctuation operator will mix the temporal and spatial components of Φ non-trivially, we impose on it the Lorenz gauge condition instead,

$$D^\mu \Phi_\mu^p = 0 \quad \Rightarrow \quad \partial_\tau \Phi_0^p - L_a \Phi_a^p - \frac{1}{2}(1 + \phi)(T_a \Phi_a)^p = 0. \quad (7.66)$$

Lastly, we linearise the Yang–Mills equation around the background solution \mathcal{A} and obtain

$$D^\nu D_\nu \Phi_\mu - R_{\mu\nu} \Phi^\nu + 2[\mathcal{F}_{\mu\nu}, \Phi^\nu] = 0, \quad (7.67)$$

where \mathcal{F} is the field strength of \mathcal{A} . The Ricci tensor of $\mathcal{I}_\tau \times S^3$ reads

$$R_{\mu 0} = 0 \quad \text{and} \quad R_{ab} = 2\delta_{ab}. \quad (7.68)$$

Hence, the equation for the fluctuation (7.67) can be separated in its $\mu = 0$ component,

$$[\partial_\tau^2 - L_b L_b + 2(1 + \phi)^2] \Phi_0^p - (1 + \phi) L_b (T_b \Phi_0)^p - \dot{\phi} (T_b \Phi_b)^p = 0, \quad (7.69)$$

and its $\mu = a$ spatial components,

$$\begin{aligned} & [\partial_\tau^2 - L_b L_b + 2(1+\phi)^2 + 4] \Phi_a^p - (1+\phi) L_b (T_b \Phi)_a^p - L_b (S_b \Phi)_a^p + \\ & - \frac{1}{2} (1+\phi) (2-\phi) (S_b T_b \Phi)_a^p - \dot{\phi} (T_a \Phi_0)^p = 0. \end{aligned} \quad (7.70)$$

Even though they act on different indices, it is convenient to combine the orbital, spin, isospin, and fluctuation triplets according to

$$\vec{L} = (L_a), \quad \vec{S} = (S_a), \quad \vec{T} = (T_a), \quad \vec{\Phi} = (\Phi_a), \quad (7.71)$$

where

$$\vec{S}^2 \vec{\Phi} = \vec{T}^2 \vec{\Phi} = -8 \vec{\Phi} \quad \text{and} \quad \vec{L}^2 \vec{\Phi}|_j = -4j(j+1) \vec{\Phi}|_j, \quad (7.72)$$

with $\vec{\Phi}|_j$ representing combinations of fluctuation triplets restricted to the same orbital spin j . As there is no operator coupling different j -sectors, we can treat them separately. In such notation, equations (7.66, 7.69, 7.70) can be written in a more compact form as, suppressing the colour index p ,

$$\partial_\tau \Phi_0 - \vec{L} \cdot \vec{\Phi} - \frac{1}{2} (1+\phi) \vec{T} \cdot \vec{\Phi} = 0, \quad (7.73)$$

$$[\partial_\tau^2 - \vec{L}^2 + 2(1+\phi)^2] \Phi_0 - (1+\phi) \vec{L} \cdot \vec{T} \Phi_0 - \dot{\phi} \vec{T} \cdot \vec{\Phi} = 0, \quad (7.74)$$

and

$$\begin{aligned} & [\partial_\tau^2 - \vec{L}^2 - \frac{1}{2} \vec{S}^2 + 2(1+\phi)^2] \Phi_a - (1+\phi) \vec{L} \cdot \vec{T} \Phi_a - \vec{L} \cdot (\vec{S} \Phi)_a \\ & - \frac{1}{2} (1+\phi) (2-\phi) \vec{T} \cdot (\vec{S} \Phi)_a - \dot{\phi} T_a \Phi_0 = 0, \end{aligned} \quad (7.75)$$

respectively. Notice that, if one takes $\Phi_a \leftrightarrow \Phi_0$ and sets $\vec{S} = 0$ in (7.75), since Φ_0 does not carry a spin index, (7.74) will be obtained. Moreover, the two equations can be rewritten, respectively, as

$$\left[\partial_\tau^2 - \frac{1-\phi}{2} \vec{L}^2 - \frac{1+\phi}{2} (\vec{L} + \vec{T})^2 - 2(1+\phi)(1-\phi) \right] \Phi_0 = \dot{\phi} \vec{T} \cdot \vec{\Phi} \quad (7.76)$$

and

$$\begin{aligned} & \left[\partial_\tau^2 - \frac{(1-\phi)(2+\phi)}{4} \vec{L}^2 - \frac{\phi(1+\phi)}{4} (\vec{L} + \vec{T})^2 + \frac{\phi(1-\phi)}{4} (\vec{L} + \vec{S})^2 \right. \\ & \left. - \frac{(1+\phi)(2-\phi)}{4} (\vec{L} + \vec{T} + \vec{S})^2 - 2(1+\phi)(1-\phi) \right] \vec{\Phi} = \dot{\phi} \vec{T} \Phi_0. \end{aligned} \quad (7.77)$$

This form highlights that they can be better treated as a problem of addition of angular momenta, with symmetry under

$$\phi \leftrightarrow -\phi, \quad \vec{L} \leftrightarrow \vec{L} + \vec{T} + \vec{S}, \quad \text{and} \quad \vec{L} + \vec{S} \leftrightarrow \vec{L} + \vec{T}, \quad (7.78)$$

where we used once more that $S_a \Phi_0 = 0$. Finally, we can see that, for a constant background, $\dot{\phi} = 0$, the temporal Φ_0 and the spatial Φ_a fluctuations decouple in (7.76) and (7.77) and Φ_0 may be gauged away, further simplifying the problem. However, the fluctuation operator in equation (7.77) only becomes easily diagonalisable when one of the coefficients of the spin-square operators vanishes, which happens for example for the two vacua, $\phi = \pm 1$, and for $\phi = 0$, the so-called *meron* or *spharelon*, previously analysed by Hosotani [7] and Volkov [54].

To enable the treatment with a generic background ϕ , let us decompose the fluctuations in finite-dimensional blocks for each fixed orbital spin $j \in \frac{1}{2}\mathbb{N}$. Hence, in conjunction with equation (7.72), the problem of addition of spins becomes more clear. Defining

$$\vec{U} := \vec{L} + \vec{T} \quad \text{then} \quad \vec{V} := \vec{U} + \vec{S} = (\vec{L} + \vec{T}) + \vec{S}, \quad (7.79)$$

it is immediate to see that \vec{U} acts on $\vec{\Phi}$ as a $j \otimes 1$ representation of $\mathfrak{su}(2)$ while \vec{V} acts as a $j \otimes 1 \otimes 1$ representation. If $\vec{\Phi}$ was decoupled from Φ_0 , its equation of motion would form a square system of order $3 \cdot 3 \cdot (2j + 1) = 9(2j + 1)$. Moreover, for Φ_0 , $\vec{S} = 0$ implies that $\vec{U} = \vec{V}$, and they act as a $j \otimes 1$ representation of $\mathfrak{su}(2)$. Its decoupled system would have $3(2j + 1)$ degrees of freedom. Therefore, for a fixed j , the equation of motion for the linear fluctuations Φ_μ^p can be written in terms of a $12(2j + 1) \times 12(2j + 1)$ fluctuation matrix $\Omega_{(j)}^2$ as

$$[\delta_{\mu\nu}^{pq} \partial_\tau^2 - (\Omega_{(j)}^2)_{\mu\nu}^{pq}] \Phi_\nu^q = 0. \quad (7.80)$$

There is a trivial extra redundancy on the n index of the hyperspherical harmonics $Y_{j;m,n}$ which is associated with the operators R_a from (5.15). We will disregard such index, as it never plays any role in our discussion. Furthermore, recall that we still need to use the gauge redundancy to reduce the number of degrees of freedom of the system. We saw that, for $\phi = 0$, the $3(2j + 1)$ degrees of freedom associated with Φ_0 could be gauged away, would be purely gauge modes. If $\phi \neq 0$, however, the Φ_0 and the Φ_a will get non-trivially mixed in the gauge modes, but they can still be computed for particular cases. Moreover, the Coulomb gauge-fixing condition (7.73) still has to be considered, which further fixes $3(2j + 1)$ degrees of freedom, leaving us with $6(2j + 1)$ physical degrees of freedom for $j \geq 2$.

Let us introduce a new basis $\{|uvm\rangle\}$ in terms of the reinterpretation as a problem of addition of angular momenta, with indexes as eigenvalues of \vec{U}^2 , \vec{V}^2 , and V_3 . More specifically,

$$\begin{aligned} \vec{U}^2 |uvm\rangle &= -4u(u+1) |uvm\rangle, \\ \vec{V}^2 |uvm\rangle &= -4v(v+1) |uvm\rangle, \text{ and} \\ V_3 |uvm\rangle &= m |uvm\rangle, \end{aligned} \quad (7.81)$$

for $m = -v, \dots, v$. It is then instructive to consider the fluctuation operator in the block form

$$\Omega_{(j)}^2 = \begin{pmatrix} \bar{N} & -\phi T^\top \\ -\phi T & N \end{pmatrix}, \quad (7.82)$$

where \bar{N} and N are respectively the left-hand sides of equations (7.76) and (7.77). Define, for clarity, $\bar{v} \in \{j - 1, j, j + 1\}$ for \bar{N} and $v \in \{j - 2, j - 1, j, j + 1, j + 2\}$ for N . Let us momentarily consider $\phi = 0$ to more easily analyse the fluctuation operator in terms of the new basis. In this case, $\Omega_{(j)}^2$ becomes block diagonal with blocks \bar{N} and N , and there is a trivial degeneracy in m in both blocks. Since $\vec{S} = 0$ in the Φ_0 sector, $u = \bar{v}$, such that u is a redundant index. Other than the trivial degeneracy in m , \bar{N} is irreducible in \bar{v} . On the other hand, on the N block, there is a non-diagonal $(\vec{L} + \vec{S})^2$ term such that $[\vec{U}, N] \neq 0$, showing that u is not the correct index to diagonalise N . Indeed, the non-diagonal term will couple different copies of the same v -spin representation to each other such that N is not simply reducible. We then have to introduce an extra index α to account for the multiplicity of the spin- v representations. In the end, the unperturbed ($\phi = 0$) fluctuation equations

for $\Phi_0 = \Phi_{(\bar{v})}$ and $\vec{\Phi} = \Phi_{(v,\alpha)}$ read, respectively,

$$\text{Id}_{(\bar{v})} [\partial_\tau^2 - \bar{\omega}_{(\bar{v})}^2] \Phi_{(\bar{v})} = 0, \quad \text{with } \bar{v} \in \{j-1, j, j+1\}, \quad (7.83)$$

and

$$\text{Id}_{(v)} [\partial_\tau^2 - \omega_{(v,\alpha)}^2] \Phi_{(v,\alpha)} = 0, \quad \text{with } v \in \{j-2, j-1, j, j+1, j+2\}, \quad (7.84)$$

where $\text{Id}_{(k)}$ denotes the identity matrix of dimension $2k + 1$. We refer the reader to [53] for a discussion with examples.

In terms of such indices, it is now easy to compute, in the unperturbed case, the frequency-squares for \bar{N} and N from equations (7.76) and (7.77), respectively. For \bar{N} , we have

$$\bar{\omega}_{(\bar{v})}^2 = 2(1-\phi)j(j+1) + 2(1+\phi)\bar{v}(\bar{v}+1) - 2(1+\phi)(1-\phi), \quad (7.85)$$

each with an extra multiplicity of $2\bar{v} + 1$ due to m . For the three values of \bar{v} , it reduces to

$$\begin{aligned} \bar{\omega}_{(j-1)}^2 &= 2\phi^2 - 4j\phi + 2(2j^2 - 1), \\ \bar{\omega}_{(j)}^2 &= 2\phi^2 + 2(2j^2 + 2j - 1), \quad \text{and} \\ \bar{\omega}_{(j+1)}^2 &= 2\phi^2 + 4(j+1)\phi + 2(2j^2 + 4j + 1). \end{aligned} \quad (7.86)$$

For N , other than the trivial $2v + 1$ multiplicity from m , the fluctuation operator is non-diagonal. To compute its eigenvalues λ , we need to find the roots of the characteristic polynomial $Q_{v(j)}(\lambda)$ for each case. Then, we obtain

$$\begin{aligned} \omega_{(j-2)}^2 &= \text{root of } Q_{j-2}(\lambda) = -2(2j-1)\phi + 2(2j^2 - 2j + 1), \\ \omega_{(j-1,\alpha)}^2 &= \text{two roots of } Q_{j-1}(\lambda), \\ \omega_{(j,\alpha)}^2 &= \text{three roots of } Q_j(\lambda), \\ \omega_{(j+1,\alpha)}^2 &= \text{two roots of } Q_{j+1}(\lambda), \\ \omega_{(j+2)}^2 &= \text{root of } Q_{j+2}(\lambda) = 2(2j+3)\phi + 2(2j^2 + 6j + 5), \end{aligned} \quad (7.87)$$

The degree of the characteristic polynomial Q_v determines the range of α for each value of v , going from 1 in the extrema $v = j \pm 2$ up to 3 when $v = j$. The explicit expressions for the Q_v have to be computed individually for each pair (j, v) and are in general not very enlightening. In case the reader is interested, all polynomials up to $j = 2$ are listed in [53, Appendix].

If we consider the complete fluctuation operator, with $\phi \neq 0$, the modes in \bar{N} and N will be mixed. However, the coupling term cannot change v , which guarantees that only sectors with $\bar{v} = v$ are related. Moreover, it is straightforward to show that the coupling term does not lift the degeneracy in m . As the \bar{N} and N sectors are mixed, the polynomials accounting for the number of copies of spin- v representations coupled to each other will become more complex, and we will use an index β in the complete case to play the role the α had in the simplest, unperturbed one. Summarising, for fixed j , we employed successive changes of basis

$$\{|\mu p m'\rangle\} \Rightarrow \{|\bar{v}m\rangle, |vum\rangle\} \Rightarrow \{|\bar{v}m\rangle, |v\alpha m\rangle\} \Rightarrow \{|\sigma\beta m\rangle\}, \quad (7.88)$$

with m' here being the index associated with L_3 , to avoid confusion with m from V_3 . Hence, we diagonalised the fluctuation operator to

$$[\partial_\tau^2 - \Omega_{(j,v,\beta)}^2] \Phi_{(v,\beta)} = 0, \quad \text{with } v \in \{j-2, j-1, j, j+1, j+2\}, \quad (7.89)$$

where $\Omega_{(j,v,\beta)}^2$ are the distinct roots of the characteristic polynomial of $\Omega_{(j)}^2$, in equation (7.82), and the number of roots for each pair (j, v) fixes the range of β . Checking each case, we can see that, for $j \geq 2$,

$$\begin{aligned} \Omega_{(j,j\pm 2)}^2 &= \omega_{(j\pm 2)}^2, & \Omega_{(j,j\pm 1,\beta)}^2 &= \text{three roots of polynomial } R_{j\pm 1}(\lambda), \\ & & \text{and } \Omega_{(j,j,\beta)}^2 &= \text{four roots of polynomial } R_j(\lambda), \end{aligned} \quad (7.90)$$

which fixes the multiplicities

$$\#\beta = 1, 3, 4, 3, 1 \quad \text{for } v \in \{j-2, j-1, j, j+1, j+2\}, \quad (7.91)$$

respectively, with $\#\beta$ denoting the number of different values β can take in each case. It is worth noticing that the reflexion symmetry (7.78) implies

$$\Omega_{(v,j,\cdot)}^2(\phi) = \Omega_{(j,v,\cdot)}^2(-\phi). \quad (7.92)$$

We treated the full fluctuation operator with the perturbation coupling \bar{N} and N , but now we have to deal with the fact that it is not clear anymore which modes are indeed physical and which are only gauge or unphysical modes. It turns out that, when turning on the perturbation, for $\dot{\phi} \neq 0$, we can compute the eigenmodes as a function of $\dot{\phi}(\tau)$ and continuously follow the ones that corresponded to the \bar{N} block when $\dot{\phi} = 0$. Keeping track of such modes allows us to remove them for $\dot{\phi} \neq 0$. Furthermore, we still have to remove the modes corresponding to the gauge fixing condition (7.73). For fixed j , such equation can be rewritten directly in terms of the final basis $|\bar{v}\beta\bar{m}\rangle$ as

$$\left[L_{\bar{v},\bar{m}}^{\bar{v}',\beta,\bar{m}'}(\phi) \partial_\tau - M_{\bar{v},\bar{m}}^{\bar{v}',\beta,\bar{m}'}(\phi) \right] \Phi_{(\bar{v}',\beta,\bar{m}')} = 0, \quad (7.93)$$

where L and M are $3(2j+1) \times 10(2j+1)$ matrix functions in ϕ , allowing us to further remove $3(2j+1)$ (or less, if $j < 2$) unphysical modes when solved.

The $j = 0$ case is simple enough to be solved by hand, which can be very useful to build intuition for higher values of j . For a detailed discussion on it, we refer the reader to [53].

Finally, let us recall that the fluctuation operators in this section are functions of the scalar degree of freedom $\phi(\tau)$ for the background solution, which is one of the functions in (6.82) with conventions (6.81). Therefore, the fluctuation operators are also parametrised by the energy E of the Newtonian system for ϕ , or, equivalently, by the moduli parameter k . In Figure 7.2, we illustrate the frequency-squares $\Omega_{(0,v,\beta)}^2$ as a function of τ of the four physical degrees of freedom with $j = 0$ and for different values of k^2 . The $j = 0$ case was explicitly solved in [53]. In Figure 7.3, the physical frequency-squares for the numerically-solved $j = 2$ scenario are illustrated. In such figures, we see that many of the physical modes have frequency-square dipping into negative values for a non-negligible fraction of the period $T(k)$. However, due to the complexity of the τ dependency on the natural frequencies, it is not easy to predict the long-term behaviour of the fluctuation modes. A more in-depth analysis will be needed.

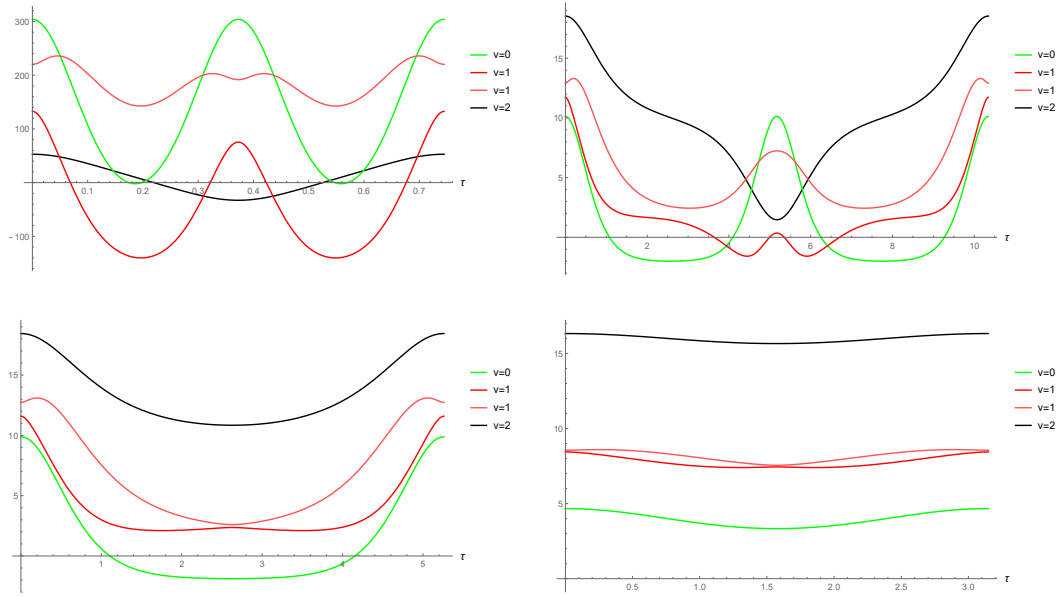


FIGURE 7.2: Frequency-squares $\Omega_{(0,v,\beta)}^2(\tau)$ over their respective periods, for different values of k^2 : 0.51 (top left), 0.99 (top right), 1.01 (bottom left) and 5 (bottom right).

7.2.3 Stability analysis with Floquet theory

For a more general treatment of the fluctuation modes, notice that their equation of motion (7.89) is of the form

$$[\partial_\tau^2 \Phi(\tau) - \Omega^2(\tau)] \Phi(\tau) = 0, \quad (7.94)$$

where $\Omega^2(\tau)$ is periodic, with the same period $T(k)$ (sometimes, half of it) as the background solution $\phi(\tau)$ with mechanical energy E corresponding to the parameter k in (6.81). Equation (7.94) is known as the Hill differential equation and many of its phenomena are known in the literature, for example the fact that its solutions may display parametric resonance in the limit of Mathieu's dynamics, generating stable solutions to otherwise unstable systems, or vice-versa.

In order to treat (7.94), let us switch to a Hamiltonian picture, using phase space coordinates. Then, Hill's equation can be conveniently rewritten as

$$\partial_\tau \begin{pmatrix} \Phi \\ \dot{\Phi} \end{pmatrix} = \begin{pmatrix} 0 & 1 \\ -\Omega^2(\tau) & 0 \end{pmatrix} \begin{pmatrix} \Phi \\ \dot{\Phi} \end{pmatrix} =: i\hat{\Omega}(\tau) \begin{pmatrix} \Phi \\ \dot{\Phi} \end{pmatrix}, \quad (7.95)$$

with formal solution

$$\begin{pmatrix} \Phi \\ \dot{\Phi} \end{pmatrix}(\tau) = \mathcal{T} \exp \left\{ \int_0^\tau d\tau' i\hat{\Omega}(\tau') \right\} \begin{pmatrix} \Phi \\ \dot{\Phi} \end{pmatrix}(0), \quad (7.96)$$

where \mathcal{T} denotes the time-ordering operator acting on the exponential. Since the

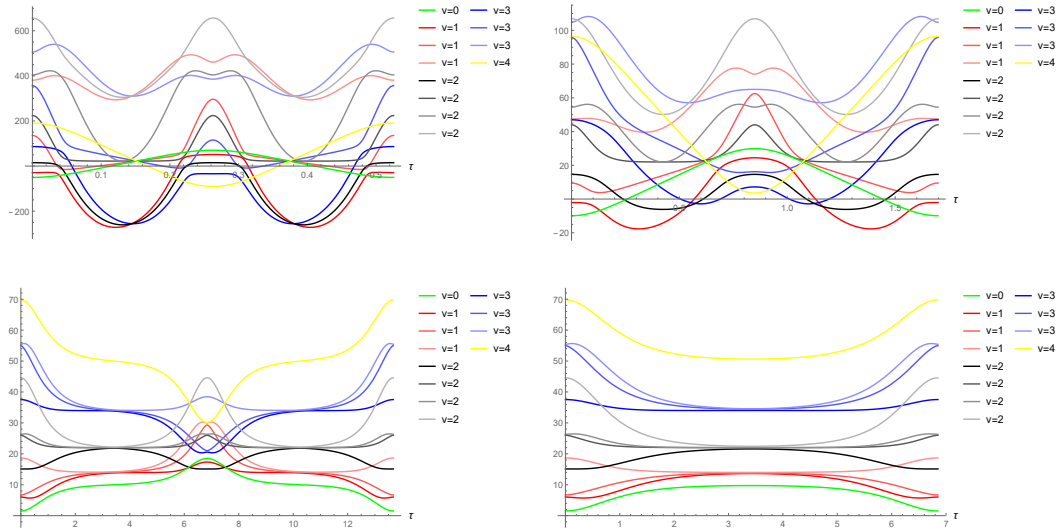


FIGURE 7.3: Frequency-squares $\Omega_{(2,v,\beta)}^2(\tau)$ over their respective periods, for different values of k^2 : 0.505 (top left), 0.550 (top right), 0.999 (bottom left) and 1.001 (bottom right).

time dependency of Ω is non-trivial, the time-evolution operator is not homogeneous and does not constitute a one-parameter group, except when restricting τ to multiples of its period T [55]. Let us define the stroboscopic map as

$$M := \mathcal{T} \exp \left\{ \int_0^T d\tau i \hat{\Omega}(\tau) \right\}, \quad (7.97)$$

hence, evolutions of multiple periods are simply given by the iteration of M , according to

$$\begin{pmatrix} \Phi \\ \dot{\Phi} \end{pmatrix} (nT) = M^n \begin{pmatrix} \Phi \\ \dot{\Phi} \end{pmatrix} (0). \quad (7.98)$$

The stroboscopic map as a functional of the background solution $\phi(\tau)$ has to be investigated as a function of its parameter E or k . The background solution is Lyapunov stable if and only if the trivial solution $\Phi = 0$ also is, which is computed from the eigenvalues μ_1 and μ_2 of M . Since the system is Hamiltonian, $\det M = 1$, hence,

$$\begin{aligned} |\operatorname{tr} M| > 2 &\Leftrightarrow \mu_i \in \mathbb{R} &\Leftrightarrow \text{hyperbolic/boost} &\Leftrightarrow \text{strongly unstable}, \\ |\operatorname{tr} M| = 2 &\Leftrightarrow \mu_i = \pm 1 &\Leftrightarrow \text{parabolic/translation} &\Leftrightarrow \text{marginally stable}, \\ |\operatorname{tr} M| < 2 &\Leftrightarrow \mu_i \in \mathbb{U}(1) &\Leftrightarrow \text{elliptic/rotation} &\Leftrightarrow \text{strongly stable}, \end{aligned} \quad (7.99)$$

such that the linear stability of the background is simply determined by $\operatorname{tr} M$.

The special form of the matrix $\hat{\Omega}$ can be used to simplify the nested integrations required for $\operatorname{tr} M$ at each order in Ω^2 . Even though it helps build intuition, it does not bring final results, hence, we once more just refer the reader to [53] and move on to the formal analysis with Floquet theory.

Let $\Phi(\tau)$ follow linear Hamiltonian dynamics determined by (7.95) with periodic coefficients in some period T . Hence, define the 2×2 matrix

$$\widehat{\Phi}(\tau) := \begin{pmatrix} \Phi_1 & \Phi_2 \\ \dot{\Phi}_1 & \dot{\Phi}_2 \end{pmatrix}(\tau). \quad (7.100)$$

If Φ_1 and Φ_2 are linearly-independent solutions to the original ODE, $\widehat{\Phi}(\tau)$ is said to be a **fundamental matrix solution** to the system. Moreover, if $\exists \tau_0$ such that $\widehat{\Phi}(\tau_0) = \text{Id}$, then $\widehat{\Phi}(\tau)$ is a **principal** fundamental matrix solution. The matrix variable $\widehat{\Phi}$ follows the same dynamics

$$\partial_\tau \widehat{\Phi}(\tau) = i\widehat{\Omega}(\tau) \widehat{\Phi}(\tau), \quad (7.101)$$

with $\widehat{\Omega}(\tau + T) = \widehat{\Omega}(\tau)$ and initial conditions given by $\widehat{\Phi}_0 := \widehat{\Phi}(0)$. For any pair of initial conditions $(\Phi \ \dot{\Phi})^T(0)$ to the original equation (7.95), the corresponding solution can be constructed from

$$\begin{pmatrix} \Phi \\ \dot{\Phi} \end{pmatrix}(\tau) = \left(\widehat{\Phi}(\tau) \widehat{\Phi}^{-1}(0) \right) \begin{pmatrix} \Phi \\ \dot{\Phi} \end{pmatrix}(0). \quad (7.102)$$

The Floquet theorem establishes that a fundamental matrix solution can always be represented in the so-called Floquet normal form:

$$\widehat{\Phi}(\tau) = Q(\tau) e^{\tau R} \quad \text{with} \quad Q(\tau + 2T) = Q(\tau), \quad (7.103)$$

where $Q(\tau)$ and R are real 2×2 matrices and R is constant. Recall that

$$\widehat{\Phi}(T) = M \widehat{\Phi}(0) \quad \text{and} \quad \widehat{\Phi}(2T) = M^2 \widehat{\Phi}(0), \quad (7.104)$$

where M is the stroboscopic map formally constructed in equation (7.97). From $\tau = 0, 2T$, some immediate consequences of the Floquet normal form (7.103) are

$$\widehat{\Phi}(0) = Q(0) \quad \text{and} \quad (7.105)$$

$$\widehat{\Phi}(2T) = Q(2T) e^{2TR} = Q(0) e^{2TR}, \quad (7.106)$$

which, when substituted in the second part of (7.104), give rise to

$$Q(0) e^{2TR} = M^2 Q(0) \quad \Rightarrow \quad M^2 = Q(0) e^{2TR} Q(0)^{-1}. \quad (7.107)$$

From a fundamental matrix solution $\widehat{\Phi}(\tau)$, one can always construct a principal fundamental matrix solution $\widetilde{\Phi}(\tau) := \widehat{\Phi}(\tau) \widehat{\Phi}(0)^{-1}$, in which case $Q(0) = \text{Id}$ and $M = e^{TR}$. The eigenvalues μ_i of the stroboscopic map M , the characteristic multipliers of the system, are written in terms of the eigenvalues ρ_i of R , the so-called Floquet exponents, as

$$\mu_i = e^{\rho_i T}, \quad \text{for } i = 1, 2. \quad (7.108)$$

The Lyapunov exponents of the system will simply be the real part of the Floquet exponents. As $\det M = 1$, $\mu_1 \mu_2 = 1$, implying $\rho_1 + \rho_2 = 0$. Hence, the system is linearly stable if and only if the Floquet exponents are zero or purely imaginary.

Even in terms of the Floquet theory, it will be generally impossible to find analytical solutions to the system. The exception here will be the singlet perturbation, for which there is a fully analytical solution available. The other modes are going to be treated numerically.

Let us now treat the singlet perturbation. In this case, the gauge field maintains its form as in (7.63). Therefore, the perturbation is simply a time-dependent shift in ϕ . Recall that the moduli space of solutions ϕ is parametrised by the initial time and by the energy scale of the solution. Consequently, one can expect that the two linearly independent perturbations may be directly related to such degrees of freedom. Indeed, the generator of a time-shift is simply a time derivative, and we can trivially check that $\dot{\phi}$ solves the fluctuation equation,

$$(\dot{\phi})'' = (\ddot{\phi})' = -(V'(\phi))' = -V''(\phi)\dot{\phi} = -(6\phi^2 - 2)\dot{\phi} = -\Omega_{(0,0)}^2(\tau)\dot{\phi}. \quad (7.109)$$

With an explicit solution, we can reduce the fluctuation equation to first-order and obtain a second solution. With a convenient normalisation, we define

$$\begin{aligned} \Phi_1(\tau) &= -\frac{\epsilon^3}{k}\dot{\phi}(\tau) \quad \text{and} \\ \Phi_2(\tau) &= \Phi_1(\tau) \int^\tau \frac{d\sigma}{\Phi_1(\sigma)^2} = -\frac{k}{\epsilon^3}\dot{\phi}(\tau) \int^\tau \frac{d\sigma}{\dot{\phi}^2(\sigma)}. \end{aligned} \quad (7.110)$$

From the Wronskian, we confirm that they are linearly independent:

$$W(\Phi_1, \Phi_2) \equiv \Phi_1\dot{\Phi}_2 - \Phi_2\dot{\Phi}_1 = 1. \quad (7.111)$$

As the relevant regime for the cosmological application is the high-energy one, let us restrict our analysis to $\frac{1}{2} < E < \infty$, which is equivalent to $\frac{1}{2} < k < 1$. Then,

$$\begin{aligned} \Phi_1(\tau) &= \epsilon \operatorname{sn}\left(\frac{\tau}{\epsilon}, k\right) \operatorname{dn}\left(\frac{\tau}{\epsilon}, k\right), \\ \Phi_2(\tau) &= \frac{1}{1-k^2} \operatorname{cn}\left(\frac{\tau}{\epsilon}, k\right) \left[(2k^2-1) \operatorname{dn}^2\left(\frac{\tau}{\epsilon}, k\right) - k^2 \right] + \\ &\quad \operatorname{sn}\left(\frac{\tau}{\epsilon}, k\right) \operatorname{dn}\left(\frac{\tau}{\epsilon}, k\right) \left[\frac{\tau}{\epsilon} + \frac{2k^2-1}{1-k^2} E(\operatorname{am}\left(\frac{\tau}{\epsilon}, k\right), k) \right], \end{aligned} \quad (7.112)$$

where $E(z, k)$ denotes the elliptic integral of the second kind and $\operatorname{am}(z, k)$ is the Jacobi amplitude. The two functions are illustrated in Figure 7.4. With the chosen

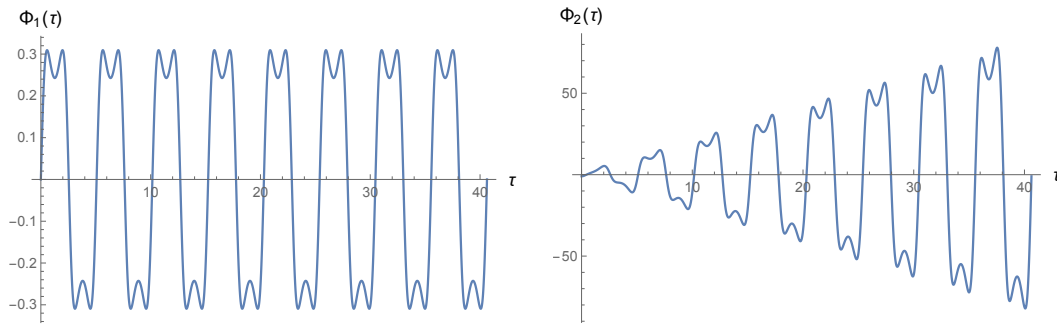


FIGURE 7.4: SO(4) singlet fluctuation modes Φ_1 (left) and Φ_2 (right) over eight periods, for $k^2=0.81$.

normalisation, the initial conditions read

$$\Phi_1(0) = 0, \quad \dot{\Phi}_1(0) = 1 \quad \text{and} \quad \Phi_2(0) = -1, \quad \dot{\Phi}_2(0) = 0. \quad (7.113)$$

Hence, the fundamental matrix solution is such that

$$\widehat{\Phi}(0) = \begin{pmatrix} 0 & -1 \\ 1 & 0 \end{pmatrix} \quad \text{and} \quad M = \widehat{\Phi}(T) \begin{pmatrix} 0 & 1 \\ -1 & 0 \end{pmatrix}. \quad (7.114)$$

In order to compute the stroboscopic map, note that Φ_1 is T -periodic but Φ_2 is not periodic at all. Indeed, from (7.112), we get

$$\Phi_2(\tau+T) = \Phi_2(\tau) + \gamma T \Phi_1(\tau), \quad (7.115)$$

where

$$\gamma = \frac{1}{\epsilon^2} \left[1 + \frac{2k^2-1}{1-k^2} \frac{E(k)}{K(k)} \right] \quad (7.116)$$

is the rate of growth of amplitude of Φ_2 per period of Φ_1 and is always positive (with minimum of ≈ 7.629). Hence, the stroboscopic map reads

$$M = \begin{pmatrix} -\Phi_2(T) & \Phi_1(T) \\ -\dot{\Phi}_2(T) & \dot{\Phi}_1(T) \end{pmatrix} = \begin{pmatrix} 1 & 0 \\ -\gamma T & 1 \end{pmatrix} = \exp \left\{ -\gamma T \begin{pmatrix} 0 & 0 \\ 1 & 0 \end{pmatrix} \right\}, \quad (7.117)$$

such that the Floquet representation is constructed with

$$R = \begin{pmatrix} 0 & \gamma \\ 0 & 0 \end{pmatrix} \quad \Rightarrow \quad e^{\tau R} = \begin{pmatrix} 1 & \gamma \tau \\ 0 & 1 \end{pmatrix} \quad (7.118)$$

and $Q(\tau) = \begin{pmatrix} \Phi_1 & \Phi_2 - \Phi_1 \gamma \tau \\ \dot{\Phi}_1 & \dot{\Phi}_2 - \dot{\Phi}_1 \gamma \tau \end{pmatrix}.$

As expected, there is no exponential growth and the singlet is marginally stable, with Φ_2 growing linearly in the linear regime of fluctuations. However, we never associated Φ_2 with a variation of energy on ϕ , as mentioned above. In fact, this association only becomes clear in the non-linear regime, where we can consider the full fluctuation $\eta(\tau)$ beyond the linear regime, to all orders. Then, we find the familiar beat wave behaviour illustrated in Figure 7.5, since the derivative of ϕ with respect to the moduli parameter k is essentially a difference between two oscillating functions with slightly different frequencies. Notice that the boundedness of η beyond the linear regime is a consequence of the boundedness of ϕ .

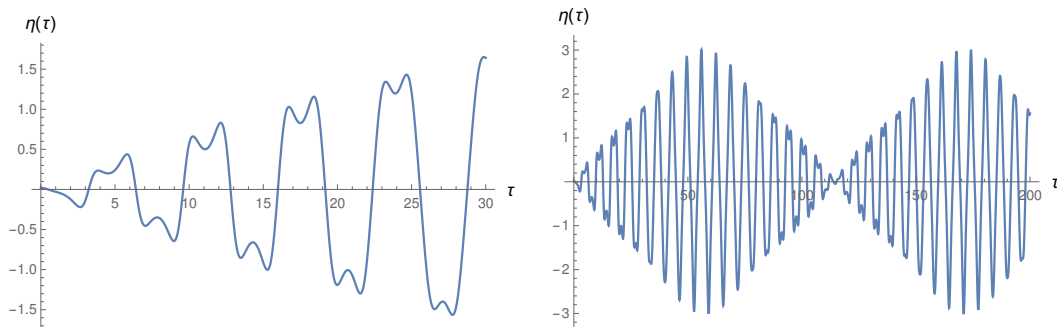


FIGURE 7.5: Exact perturbation $\eta(\tau)$ for $\eta(0)=0.02$ and $\dot{\eta}(0)=0$, illustrating marginally-stable initial behaviour (left) and long-time beat-wave behaviour (right) with beat ratio ~ 19 .

The non-singlet modes, on the other hand, are not so simple to analyse and will

in general not have closed analytical expressions. We can, however, treat them numerically and still obtain the trace of the stroboscopic map for any background field ϕ , in any energy scale E . However, before we discuss the numerical results, let us investigate the possibility of parametric resonance and try to predict at which energies E or moduli-parameter k they might occur. Let us simply model the periodic coefficient in terms of its average and frequency, as

$$\Omega^2(\tau) \approx \langle \Omega^2 \rangle (1 + h(\tau)), \quad (7.119)$$

where

$$\langle \Omega^2 \rangle = \frac{1}{T} \int_0^T d\tau \Omega^2(\tau), \quad h(\tau) \propto \cos(2\pi\tau/T), \quad (7.120)$$

and $T = 4\epsilon K(k)$ is the period of Ω^2 as a function of the background field $\phi_k(\tau)$. Then, the resonance condition reads [55]

$$\sqrt{\langle \Omega^2 \rangle} = \ell \frac{\pi}{T}, \quad (7.121)$$

which can be solved to get the values of k in which a resonance would occur in the simplified model,

$$k = k_\ell(j, v, \beta), \quad \text{for } \ell = 1, 2, 3, \dots \quad (7.122)$$

The resonances on the full system will of course not be found for those exact values of k , however, they are still expected to be close to the k_ℓ values. Indeed, our predictions were confirmed by numerical calculations on the full system, which are illustrated by Figures 7.6 and 7.7, respectively for $(j = 2, v = 0)$ and $(j = 2, v = 2)$.

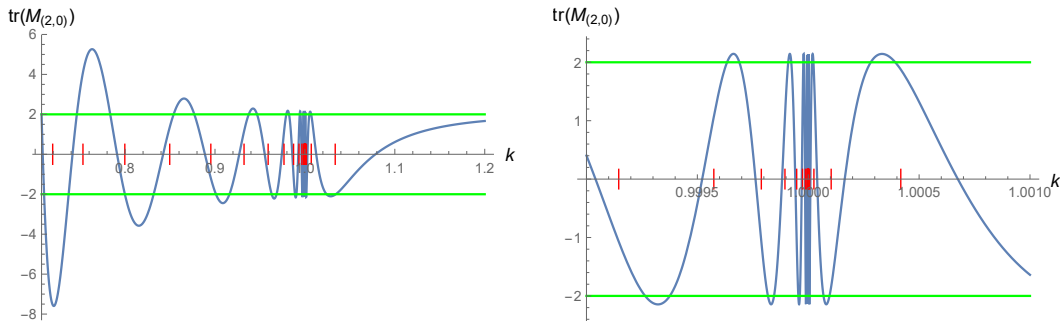


FIGURE 7.6: Plot of $\text{tr } M(k)$ for $(j, v) = (2, 0)$, with detail on the right. Resonances of the simplified model are marked in red.

Let us recall that the moduli-parameter value $k = 1$ corresponds to $E = \frac{1}{2}$, the local maximum of the quartic potential. Close to this value of energy, the solutions change from oscillating around one of the true vacua to oscillating around 0. Moreover, the period diverges when $E \rightarrow \frac{1}{2}$, from above or from below. Hence, the odd behaviour of the trace of the stroboscopic map is expected around $k = 1$. And, indeed, even for the parametric resonance predictions, the values of k_ℓ accumulate at 1 from both directions. Far from $k \neq 1$, it is clear to see that the predicted resonances, marked in red, are in one-to-one correspondence with regions where $|\text{tr } M| > 2$, in which the background becomes unstable.

For $k > 1$, meaning that the energy E is below the local maximum of the potential, we see that the system is rarely unstable. On the other hand, for $k < 1$, with energy E above the local maximum of the potential, the trace of M oscillates quickly and the amplitude of the oscillation increases with E . While bands of stability and

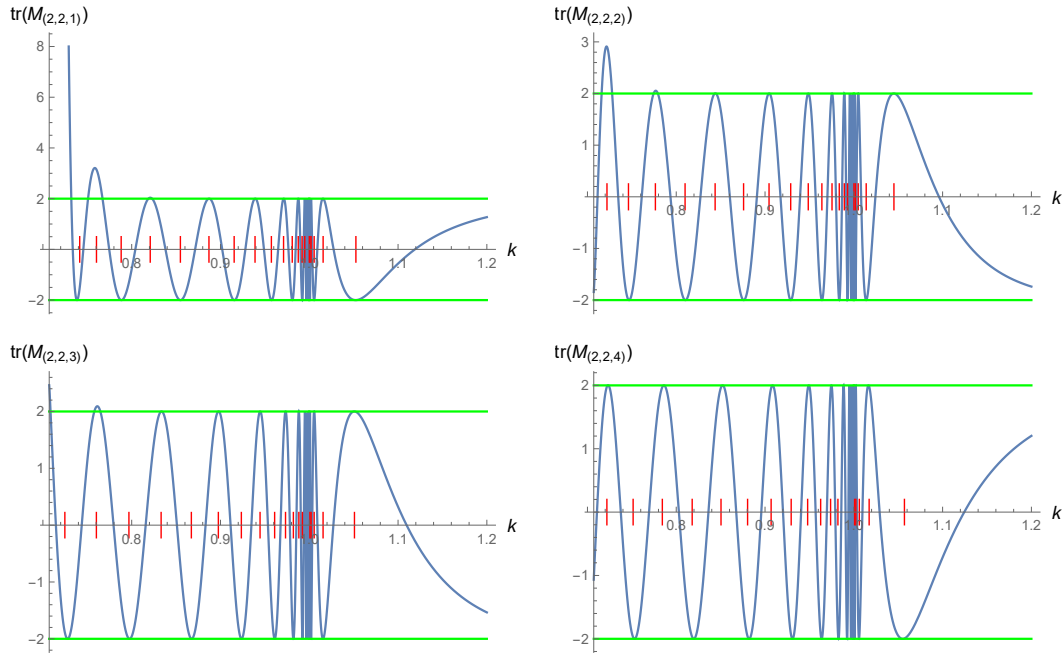


FIGURE 7.7: Plots of $\text{tr } M(k)$ for $(j, v) = (2, 2)$ and $\beta = 1, 2, 3, 4$. Resonances of the simplified model are marked in red.

instability alternate, this indicates that the likelihood of instability of the modes increases with the energy. For completeness, we explicitly confirmed the change of regime of fluctuations in many instances where $\text{tr } M$ crosses 2, from instability to stability or vice-versa, by performing long-term numerical integrations on both sides of the crossing. One of such results is illustrated in Figure 7.8.

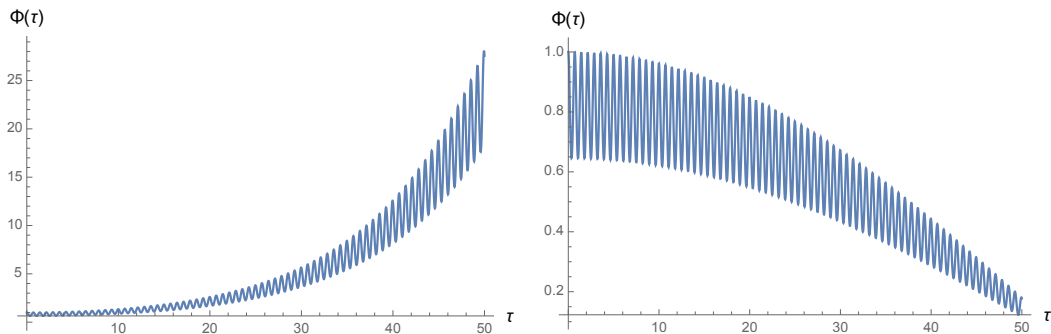


FIGURE 7.8: Long-term numerical integration of $\Phi(\tau)$ for $(j, v, \beta) = (2, 2, 1)$ and $k=0.73198$ (left) and $k=0.73199$ (right) illustrating the change in behaviour from unstable to stable.

Finally, let us address the scenario which is more relevant for the intended cosmological application, the regime in which $E \rightarrow +\infty$, corresponding to $k \rightarrow \frac{1}{\sqrt{2}}^+$. As in this limit the period collapses with $\epsilon = \sqrt{k^2 - 1/2}$, before we compute the eigenvalues of (7.89) we have to perform the following rescalings:

$$\frac{\tau}{\epsilon} = z \in [0, 4K(\frac{1}{2})], \quad \epsilon \phi = \tilde{\phi}, \quad \epsilon^2 \dot{\phi} = \partial_z \tilde{\phi}, \quad \epsilon^2 \Omega^2 = \tilde{\Omega}^2, \quad \epsilon^2 \lambda = \tilde{\lambda}, \quad (7.123)$$

allowing us to obtain finite results. After a lengthly but straightforward computation, we see that all the j -dependent terms are subleading and drop out in the limit

of $\epsilon \rightarrow 0$, such that there are four universal natural frequency-squares

$$\tilde{\Omega}_1^2 = 0, \quad \tilde{\Omega}_2^2 = 3\tilde{\phi}^2 - \sqrt{\tilde{\phi}^4 + 8(\partial_z \tilde{\phi})^2}, \quad (7.124)$$

$$\tilde{\Omega}_3^2 = 3\tilde{\phi}^2 + \sqrt{\tilde{\phi}^4 + 8(\partial_z \tilde{\phi})^2}, \quad \text{and} \quad \tilde{\Omega}_4^2 = 6\tilde{\phi}^2, \quad (7.125)$$

with the sorted frequencies for each v being given by

$$\begin{aligned} \tilde{\Omega}_{(j,j\pm 2)}^2 &= 0, \\ \tilde{\Omega}_{(j,j\pm 1,\beta)}^2 &\in \{\min(\tilde{\Omega}_1^2, \tilde{\Omega}_2^2), \max(\tilde{\Omega}_1^2, \tilde{\Omega}_2^2), \tilde{\Omega}_3^2\}, \\ \tilde{\Omega}_{(j,j,\beta)}^2 &\in \{\min(\tilde{\Omega}_1^2, \tilde{\Omega}_2^2), \max(\tilde{\Omega}_1^2, \tilde{\Omega}_2^2), \min(\tilde{\Omega}_3^2, \tilde{\Omega}_4^2), \max(\tilde{\Omega}_3^2, \tilde{\Omega}_4^2)\}, \end{aligned} \quad (7.126)$$

for $j \geq 2$. In Figure 7.9, we illustrate the universal frequencies for the most complex case, $v = j$.

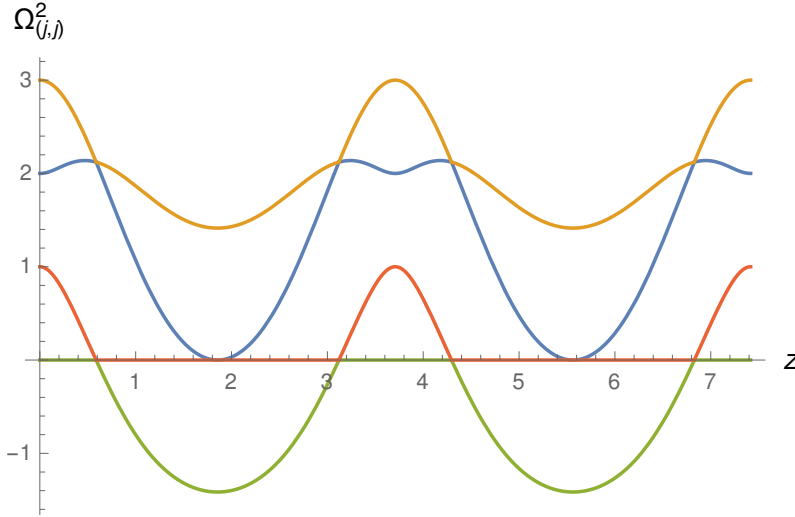


FIGURE 7.9: Universal limiting natural frequency-squares $\tilde{\Omega}_{(j,v,\beta)}^2$ over one period in Z for $v=j$ and $\beta = 1, 2, 3, 4$.

Finally, the traces of the stroboscopic map for each β are easily computed numerically, for all (j, v) . For $(0, 0)$, $\text{tr } M = 2$, as we already knew from the exact computation. For $(1, 0)$ or $(0, 1)$, $\text{tr } M \in \{56.769, -1.659\}$. For $j \geq 2$,

$$\begin{aligned} \text{tr } M_{(j,j\pm 2)}(E \rightarrow \infty) &= 2, \\ \text{tr } M_{(j,j\pm 1,\beta)}(E \rightarrow \infty) &\in \{\underline{306.704}, -1.842, -1.659\}, \\ \text{tr } M_{(j,j,\beta)}(E \rightarrow \infty) &\in \{\underline{306.704}, -1.842, \underline{2.462}, -1.067\}. \end{aligned} \quad (7.127)$$

Notice that, for $j \geq 2$, there are still $3(2j + 1)$ unphysical modes to be removed from the system from a gauge fixing condition. However, from (7.127), we see that there are always $4(2j + 1)$ unstable modes (underlined), such that a projection in physical modes cannot remove all instabilities. Beyond the already discussed singlet mode, similar arguments apply to $j < 2$, with the same conclusion.

We see that, for all j , there is at least one unstable physical mode in the limit $E \rightarrow +\infty$. Therefore, for sufficient high-energy E , the solution $\Phi = 0$ is always linearly unstable, and so is the corresponding Yang–Mills background.

Chapter 8

Conclusion and outlook

In this thesis, we reviewed how geometric methods can be used to construct non-trivial Maxwell and Yang–Mills fields in n -dimensional Lorentzian maximally symmetric spacetimes, namely, in the deSitter space dS_n , the anti-deSitter space AdS_n , and the Minkowski space $\mathbb{R}^{1,n-1}$. In each case, we discussed the properties of the solutions and possible applications of such theories.

In the first half of the thesis, we briefly discussed the theoretical framework which is needed for the following chapters. It started with an overview on differential geometric aspects of Lie algebras, Lie groups, and cosets thereof. Then, we reviewed the properties and description of Euclidean and Lorentzian maximally symmetric spacetimes. Lastly, we discussed principal bundles, connections on them, and the Yang–Mills theory.

The second half of the thesis consisted in an overview on different results in the context of geometrical construction of Maxwell and Yang–Mills theories in maximally symmetric spacetimes. It was divided in three parts, which we will review separately. The first one was on particular aspects of field configurations from a basis of electromagnetic knots in Minkowski space. The second, on vacuum non-abelian theories with non-compact gauge group, constructed from other maximally symmetric spacetimes. Finally, the third one considered the coupling of such solutions with gravity in FLRW universes, through the scale factor.

In Chapter 5, after reviewing the basis of electromagnetic knots from [29]. The discussions on new results in this direction were divided into the two Sections 5.3 and 5.4. In the former, we computed closed expressions for conserved quantities associated with the conformal invariance of such solutions in terms of their quantum numbers, which not only improved our understanding of their behaviour but also opened up a new way of comparing them with electromagnetic knots obtained from other construction methods. With it, we showed that our basis reproduces generalisations of the Rañada-Hopf knot, as the rotated Hopfions, and knots obtained from Bateman’s construction. Further relations can be explored in the future. In the latter section, we focused on possible experimental applications of the electromagnetic knots, as there are recent advances in experimental techniques to reproduce them. Therefore, we put forward numerical simulations in order to investigate the effects of such fields in charged particle trajectories, which are essential for e.g. their use in atomic particle traps. From the numerical results, in the thesis, we only highlighted a couple of interesting behaviours that can be explored in the future.

In Chapter 6, we explored non-abelian theories that could be obtained from similar construction methods in different spacetimes, with different gauge groups. The two sections of this chapter, 6.1 and 6.2, cover the results of our two research projects in this direction. The first section covers an investigation on the construction of $SO(1,3)$ gauge fields in the four-dimensional Minkowski space through its foliation by orbits of the Lorentz group. Separate computations were performed in each of

the three sectors of $\mathbb{R}^{1,3}$, inside, outside, and on the lightcone. The fields in the two halves of the space could be glued together, despite a divergence on the lightcone. For that, we described a regularisation prescription in the energy-momentum tensor, which turned out to be an improvement term. The second section covers the initial procedures for the hyperbolic equivalent of the aforementioned construction of a basis of electromagnetic knots in the Minkowski space. That is, we work with an $SU(1, 1)$ gauge theory on AdS_4 foliated with AdS_3 sheets, then we conformally map it into the Minkowski space. In this thesis, we only discussed the equivariant Ansatz for the non-abelian field and one abelian reduction, which turns out to be the hyperbolic equivalent of the Rañada-Hopf knot. Its electromagnetic fields, when projected onto a plane, are identical to the ones of a recently constructed magnetic vortex solution coming from the a solution of the Lorentzian (1+2)-dimensional version of the Seiberg-Witten equations. A direct follow-up of such work is to skip the equivariant Ansatz and instead use the eigenfunctions of the Laplace operator in the negatively-curved space to fully solve Maxwell's equations in this context. If successfully implemented, this procedure would generate a (continuum-indexed) basis of hyperbolic equivalents of the electromagnetic knots.

Finally, in Chapter 7, we considered the dynamics of Friedmann universes and how Yang–Mills fields would impact and be impacted by it. Even though the full Einstein–Yang–Mills–Higgs is greatly simplified in a FLRW universe and using the equivariant Ansatz for the gauge sector, the non-linearities and the coupling in both ways still make the system in general impossible to solve analytically. Even so, the simplifications allow us to investigate the system more in-depth and extract physically relevant results from it. In Section 7.1, we put forward a general treatment of Yang–Mills theories constructed on cylinders over symmetric spaces, showing that the equivariant Ansatz always reduce the dynamics to that of a Newtonian degree of freedom subjected to a (inverted or not) quartic potential. In particular, for non-flat Lorentzian maximally symmetric spacetimes, we explicitly compute the four cases, the Lorentzian and Euclidean foliations of the $(1+n)$ -dimensional deSitter and anti-deSitter spaces. Afterwards, we discuss how the energy density of the Yang–Mills fields affects the scale factor of the Friedmann universe, which is encoded in the Wheeler-DeWitt constraint. Then, we finalise by computing the effects on the Yang–Mills dynamics when $n \neq 3$ of both warped foliations of the spacetime foliation or, equivalently, of a scale factor, which translate to a Hubble friction-like term in conformal time in the gauge dynamics. For $n > 3$, this term may result in the freezing of the cosmic Yang–Mills field, which may have interesting consequences for cosmological applications. Lastly, in Section 7.2, we performed a complete stability analysis of a $SO(4)$ -invariant $SU(2)$ gauge field in a closed four-dimensional Friedmann universe. Using representation theory and Floquet theory, we analysed the singlet perturbation analytically, which turned out to be marginally stable, and further treated the non-singlet ones to enable a subsequent numerical analysis on the stability of the individual normal modes. For the cosmological application in the electroweak epoch, we investigate the very-high-energies limit, in which we showed that there are universal natural frequency-squares for the fluctuation modes. We computed the trace of the stroboscopic map for all possible cases, concluding that there is always at least one unstable physical mode, such that the classical background field itself is necessarily unstable. Those results depend on the assumption that the spacetime dynamics is frozen, which is physically motivated but not explicitly shown. A possible future analysis could also include dynamical gravity in a full stability study of the coupled system, which would be final in the classical setting and would be able to confirm the validity of the results here discussed.

Bibliography

- [1] C. N. Yang and R. L. Mills, “Conservation of isotopic spin and isotopic gauge invariance”, *Phys. Rev.* **96**, 191–195 (1954).
- [2] T. Skyrme, “A unified field theory of mesons and baryons”, *Nucl. Phys.* **31**, 556–569 (1962).
- [3] B. Berche and E. Medina, “Classical Yang–Mills theory in condensed matter physics”, *Eur. J. Phys.* **34**, 161 (2012).
- [4] D. Kapetanakis and G. Zoupanos, “Coset space dimensional reduction of gauge theories”, *Phys. Rep.* **219**, 4–76 (1992).
- [5] A. Maleknejad, M. M. Sheikh-Jabbari, and J. Soda, “Gauge fields and inflation”, *Phys. Rep.* **528**, 161–261 (2012).
- [6] D. Friedan, *Origin of cosmological temperature*, arXiv:2005.05349v1 [astro-ph.CO], 2020.
- [7] Y. Hosotani, “Exact solution to the Einstein–Yang–Mills equation”, *Phys. Lett. B* **147**, 44–46 (1984).
- [8] C. J. Isham, *Modern Differential Geometry for Physicists*, 2nd edition (World Scientific, 1999).
- [9] M. Nakahara, *Geometry, Topology and Physics*, 2nd edition (CRC Press, 2003).
- [10] B. C. Hall, *Lie Groups, Lie Algebras, and Representations, An Elementary Introduction*, 2nd edition, Graduate Texts in Mathematics (Springer Cham, 2015).
- [11] M. J. D. Hamilton, *Mathematical Gauge Theory, With Applications to the Standard Model of Particle Physics*, Universitext (Springer Cham, 2017).
- [12] K. Kumar, “Solutions of Yang–Mills theory in four-dimensional de Sitter space”, PhD thesis (Gottfried Wilhelm Leibniz Universität Hannover, 2022).
- [13] M. E. Peskin and D. V. Schroeder, *An Introduction to Quantum Field Theory* (Addison-Wesley, 1995).
- [14] S. Pokorski, *Gauge Field Theories* (Cambridge University Press, 2005).
- [15] R. M. Wald, *General Relativity* (Chicago University Press, 1984).
- [16] S. M. Carroll, *Spacetime and Geometry, An Introduction to General Relativity* (Cambridge University Press, 2019).
- [17] M. Burgess, *Classical Covariant Fields*, Cambridge Monographs on Mathematical Physics (Cambridge University Press, 2023).
- [18] D. Bleecker, *Gauge Theory and Variational Principles*, Global analysis, pure and applied (Addison-Wesley, 1981).
- [19] V. N. Romanov, A. S. Schwarz, and Y. S. Tyupkin, “On spherically symmetric fields in gauge theories”, *Nucl. Phys. B* **130**, 209–220 (1977).
- [20] R. Jackiw, “Gauge-covariant conformal transformations”, *Phys. Rev. Lett.* **41**, 1635 (1978).

- [21] P. G. Bergmann and E. J. Flaherty, "Symmetries in gauge theories", *J. Math. Phys.* **19**, 212–214 (1978).
- [22] P. Forgacs and N. S. Manton, "Space-time symmetries in gauge theories", *Commun. Math. Phys.* **72**, 15 (1980).
- [23] J. Harnad, S. Shnider, and L. Vinet, "Group actions on principal bundles and invariance conditions for gauge fields", *J. Math. Phys.* **21**, 2719–2724 (1980).
- [24] M. Molelekoa, "Symmetries of gauge fields", *J. Math. Phys.* **26**, 192–197 (1985).
- [25] J. M. Arms, "The structure of the solution set for the Yang–Mills equations", *Math. Proc. Camb. Philos. Soc.* **90**, 361–372 (1981).
- [26] M. Henneaux, "Remarks on space-time symmetries and nonabelian gauge fields", *J. Math. Phys.* **23**, 830–833 (1982).
- [27] M. Basler, "Yang–Mills fields invariant under subgroups of the Poincare group", *J. Phys. A* **18**, 3087–3100 (1985).
- [28] D. V. Galtsov and M. S. Volkov, "Yang–Mills cosmology: cold matter for a hot universe", *Phys. Lett. B* **256**, 17–21 (1991).
- [29] O. Lechtenfeld and G. Zhilin, "A new construction of rational electromagnetic knots", *Phys. Lett. A* **382**, 1528–1533 (2018).
- [30] A. F. Rañada, "A topological theory of the electromagnetic field", *Lett. Math. Phys.* **18**, 97–106 (1989).
- [31] M. Arrayás, D. Bouwmeester, and J. Trueba, "Knots in electromagnetism", *Phys. Rep.* **667**, *Knots in Electromagnetism*, 1–61 (2017).
- [32] L. Hantzko, K. Kumar, and G. Picanço Costa, "Conserved charges for rational electromagnetic knots", *Eur. Phys. J. Plus* **137** (2022).
- [33] K. Kumar, O. Lechtenfeld, and G. Picanço Costa, "Trajectories of charged particles in knotted electromagnetic fields", *J. Phys. A-Math* **55**, 315401 (2022).
- [34] A. Higuchi, "Symmetric tensor spherical harmonics on the N sphere and their application to the de Sitter group $SO(N,1)$ ", *J. Math. Phys.* **28**, 1553 (1987), erratum: *J. Math. Phys.* **43**, 6385 (2002).
- [35] L. Lindblom, N. W. Taylor, and F. Zhang, "Scalar, vector and tensor harmonics on the three-sphere", *Gen. Rel. Grav.* **49**, 139 (2017).
- [36] K. Kumar and O. Lechtenfeld, "On rational electromagnetic fields", *Phys. Lett. A* **384**, 126445 (2020).
- [37] M. Schottenloher, *A Mathematical Introduction to Conformal Field Theory*, Lecture Notes in Physics (Springer Berlin, Heidelberg, 2008).
- [38] C. Hoyos, N. Sircar, and J. Sonnenschein, "New knotted solutions of Maxwell's equations", *J. Phys. A-Math* **48**, 255204 (2015).
- [39] W. T. M. Irvine and D. Bouwmeester, "Linked and knotted beams of light", *Nat. Phys.* **4**, 716–720 (2008).
- [40] H. Larocque, D. Sugic, D. Mortimer, A. J. Taylor, R. Fickler, R. W. Boyd, M. R. Dennis, and E. Karimi, "Reconstructing the topology of optical polarization knots", *Nat. Phys.* **14**, 1079–1082 (2018).
- [41] L. Landau and E. Lifschitz, *The Classical Theory of Fields, Course of Theoretical Physics*, Vol. 2 (Elsevier Science, 1975), p. 52.
- [42] C. Bonati, A. Pelissetto, and E. Vicari, "Lattice abelian-Higgs model with non-compact gauge fields", *Phys. Rev. B* **103**, 085104 (2021).

- [43] A. E. Margolin and V. I. Strazhev, “Yang–Mills field quantization with non-compact gauge group”, *Mod. Phys. Lett. A* **7**, 2747–2752 (1992).
- [44] K. E. Cahill and S. Ozenli, “Unitary gauge theories of noncompact groups”, *Phys. Rev. D* **27**, 1396 (1983).
- [45] R. S. Palais, “The principle of symmetric criticality”, *Comm. Math. Phys.* **69**, 19–30 (1979).
- [46] A. Ballesteros, I. Gutierrez-Sagredo, and F. J. Herranz, “The noncommutative space of light-like worldlines”, *Phys. Lett. B*, 137120 (2022).
- [47] S. J. Avis, C. J. Isham, and D. Storey, “Quantum field theory in anti-de Sitter space-time”, *Phys. Rev. D* **18**, 3565–3576 (1978).
- [48] S. Hirpara, K. Kumar, O. Lechtenfeld, and G. Picanço Costa, *Exact gauge fields from anti-de Sitter space*, [arXiv:2301.03606v2 \[hep-th\]](https://arxiv.org/abs/2301.03606v2), 2023.
- [49] C. Ross and B. J. Schroers, “Hyperbolic vortices and Dirac fields in 2+1 dimensions”, *J. Phys. A-Math* **51**, 295202 (2018).
- [50] M. Ertürk and G. Picanço Costa, *Coset space dimensional reduction of Yang–Mills theory on non-compact symmetric spaces*, [arXiv:2304.13645v1 \[hep-th\]](https://arxiv.org/abs/2304.13645v1), 2023.
- [51] K. Kumar, O. Lechtenfeld, G. Picanço Costa, and J. Röhrig, “Yang–Mills solutions on Minkowski space via non-compact coset spaces”, *Phys. Lett. B* **835**, 137564 (2022).
- [52] O. Lechtenfeld and G. Ünal, “Yang–Mills solutions on de Sitter space of any dimension”, *Phys. Rev. D* **98**, 085008 (2018).
- [53] K. Kumar, O. Lechtenfeld, and G. Picanço Costa, “Instability of cosmic Yang–Mills fields”, *Nucl. Phys. B* **973**, 115583 (2021).
- [54] M. S. Volkov, “Computation of the winding number diffusion rate due to the cosmological sphaleron”, *Phys. Rev. D* **54**, 5014–5030 (1996).
- [55] V. I. Arnold, *Mathematical Methods of Classical Mechanics*, Lecture Notes in Physics (Springer Berlin, 1989).

Curriculum Vitae

PERSONAL INFORMATION

Name: Gabriel Picanço Costa
Date of birth: 12 April 1996
Place of birth: Fortaleza, Brazil
Nationality: Brazilian

EDUCATION

PhD in Theoretical Physics **Aug 2020 - Apr 2024**

ITP-LUH - Institut für Theoretische Physik - Leibniz Universität Hannover

- Supervisor: Olaf Lechtenfeld (ITP-LUH)
- Theme: Geometric construction of Yang-Mills fields on maximally symmetric spacetimes

Visiting Researcher **Nov 2022 - Dec 2022**

MPS-US - School of Mathematical and Physical Sciences - University of Sussex

- Supervisor: Daniel F. Litim (MPS-US)
- Theme: Non-perturbative ultraviolet fixed points of 4D supersymmetric Yang-Mills theory coupled to chiral superfields

MSc in Physics **Aug 2018 - Jul 2020**

CBPF - Brazilian Center for Research in Physics

- External Supervisor: Carlos Zarro (UFRJ)
- Internal Supervisor: Nami Svaiter (CBPF)
- Theme: Entanglement harvesting and degradation of pair of Unruh-DeWitt detectors in rotating frames
- GPA: 4.0/4.0

BSc in Physics **Mar 2015 - Jul 2018**

UFRJ - Federal University in Rio de Janeiro

- Magna cum Laude Diploma (GPA: 9.1/10.0)
- Bachelor project: Trans-series and Resurgence applied to non-perturbative effects in QFT
- Description: Resummation and treatment of divergent perturbative (asymptotic) expansions as a way to extract non-perturbative effects (instantons and quasi-zero modes) in QFT.
- Supervisor: Eduardo S. Fraga (UFRJ)

OTHER QUALIFICATIONS

Languages

- Portuguese - Native Speaker
- English - Advanced - C2
- German - Intermediate - B1

Computer Skills

Mathematica
Python
Labview

Hannover, 15.02.2024

Place and date

Gabriel Picanço Costa

Signature

List of Publications

Gabriel Picanço Costa

Feb 2024

Remark: Authors were ordered alphabetically in [1-6].

[1] **Coset space dimensional reduction of Yang–Mills theory on non-compact symmetric spaces**

Ertürk, M.; Picanço Costa, G.; submitted to *Phys. Lett. B* (2023) - arXiv:[2304.13645](#)

[2] **Exact gauge fields from anti-de Sitter space**

Hirpara, S.; Kumar, K.; Lechtenfeld, O.; Picanço Costa, G.; submitted to *J. Math. Phys.* (2023) - arXiv:[2301.03606](#)

[3] **Yang–Mills solutions on Minkowski space via non-compact coset spaces**

Kumar, K.; Lechtenfeld, O.; Picanço Costa, G.; *Phys. Lett. B* (2022) 137564 - arXiv:[2206.12009](#)

[4] **Trajectories of charged particles in knotted electromagnetic fields**

Kumar, K.; Lechtenfeld, O.; Picanço Costa, G.; *J. Phys. A: Math. Theor.* 55 (2022) 315401 - arXiv:[2202.00169](#)

[5] **Conserved charges for rational electromagnetic knots**

Hantzko, L.; Kumar, K.; Picanço Costa, G.; *Eur. Phys. J. Plus* 137 (2022) 407 - arXiv:[2106.05952](#)

[6] **Instability of cosmic Yang–Mills fields**

Kumar, K.; Lechtenfeld, O.; Picanço Costa, G.; *Nucl. Phys. B* 973 (2021) - arXiv:[2102.08401](#)

[7] **Radiative processes of entangled detectors in rotating frames**

Picanço Costa, G.; Svaiter, N.; Zarro, C.; *JHEP* 08 (2020) 025 - arXiv:[2002.06085](#)